

Electronic Theses and Dissertations, 2004-2019

2018

Development of Soil Compressibility Prediction Models

Scott Kirts
University of Central Florida

 Part of the [Civil Engineering Commons](#)
Find similar works at: <https://stars.library.ucf.edu/etd>
University of Central Florida Libraries <http://library.ucf.edu>

This Doctoral Dissertation (Open Access) is brought to you for free and open access by STARS. It has been accepted for inclusion in Electronic Theses and Dissertations, 2004-2019 by an authorized administrator of STARS. For more information, please contact STARS@ucf.edu.

STARS Citation

Kirts, Scott, "Development of Soil Compressibility Prediction Models" (2018). *Electronic Theses and Dissertations, 2004-2019*. 5954.
<https://stars.library.ucf.edu/etd/5954>

THE DEVELOPMENT OF SOIL COMPRESSIBILITY PREDICTION MODELS AND APPLICATION TO SITE SETTLEMENT

by

SCOTT KIRTS

B.S. University of Florida, 2009

M.S. University of Florida, 2012

A dissertation submitted in partial fulfillment of the requirements
for the degree of Doctor of Philosophy
in the Department of Civil, Environmental and Construction Engineering
in the College of Engineering and Computer Science
at the University of Central Florida
Orlando, Florida

Summer Term

2018

Major Professor: Boo Hyun Nam

© 2018 Scott Kirts

ABSTRACT

The magnitude of the overall settlement depends on several variables such as the Compression Index, C_c , and Recompression Index, C_r , which are determined by a consolidation test; however, the test is time consuming and labor intensive. Correlations have been developed to approximate these compressibility indexes. In this study, a data driven approach has been employed in order to estimate C_c and C_r . Support Vector Machines classification is used to determine the number of distinct models to be developed. The statistical models are built through a forward selection stepwise regression procedure. Ten variables were used, including the moisture content (w), initial void ratio (e_o), dry unit weight (γ_{dry}), wet unit weight (γ_{wet}), automatic hammer SPT blow count (N), overburden stress (σ), fines content (-200), liquid limit (LL), plasticity index (PI), and specific gravity (G_s). The results confirm the need for separate models for three out of four soil types, these being Coarse Grained, Fine Grained, and Organic Peat. The models for each classification have varying degrees of accuracy. The correlations were tested through a series of field tests, settlement analysis, and comparison to known site settlement. The first analysis incorporates developed correlations for C_r , and the second utilizes measured C_c and C_r for each soil layer. The predicted settlements from these two analyses were compared to the measured settlement taken in close proximity. Upon conclusion of the analyses, the results indicate that settlement predictions applying a rule of thumb equating C_c to C_r , accounting for elastic settlement, and using a conventional influence zone of settlement, compares more favorably to measured settlement than that of predictions using measured compressibility index(s). Accuracy of settlement predictions is contingent on a thorough field investigation.

This work is dedicated to my family and colleagues.
Without their support, this work would not have been possible.

ACKNOWLEDGMENTS

I would like to express my sincerest gratitude to my head advisor, Professor Boo Hyun Nam. His guidance through this process was instrumental. I would also like to extend my appreciation to the rest of my advisory board including Professor Manoj Chopra, Adjunct Professor Amr Sallam, and Professor Petros Xanthopoulos. The time and efforts they gave to make this possible is most appreciated. This work would not have been possible without their valuable contributions.

Very special thanks also goes to Professor Orestis Panagopoulos. His tireless efforts to contribute and make this a complete and thorough study have been invaluable. I sincerely appreciate his willingness to lend his expertise when called upon and his overall positive attitude. He has been an asset throughout this process.

Most importantly, my deepest gratitude goes to my wife Clary Kirts and my mother and father, Nancy Albertson and Chris Kirts. They have made me what I am and deserve all the credit for making this a possibility. Their unwavering support and timely “wind in my sails” gave me all the push that I needed to keep going. A very special thanks also goes to my sons, Jack and Jace, for learning to sleep on their own quickly so that I could wake up refreshed and ready to tackle the challenges from this study.

PREFACE

This dissertation is the result of a Ph.D. study carried out at the department of Civil, Environmental and Construction Engineering (CECE). This study led to a state funded project by the Florida Department of Transportation (FDOT). Professor Dr. BooHyun Nam and Professor Dr. Manoj Chopra acted as supervisors.

Journal manuscripts prepared during the course of this study include:

- Kirts, S, Panagopoulos, O, Xanthopoulos, P, and Nam, B (2017). “Soil-Compressibility Prediction Models Using Machine Learning”. *Journal of Computing in Civil Engineering*. 32(1).
- Kirts, S, Panagopoulos, O, and Nam, B. “Settlement Prediction using Machine Learning-Based Soil Compressibility Models”. Submitted to *Journal of Geotechnical and Geo-Environmental Engineering*.
- Scott Kirts, Orestis Panagopoulos, Petros Xanthopoulos, and BooHyun Nam, The Effect of Influential Parameters on Soil Compressibility Prediction Models (In preparation).

UNIT CONVERSION

To convert from	To	Multiply by
mm	cm	0.1
	m	0.01
	in.	0.03937
	ft.	0.003281
mg	g	0.001
	kg	$1e^{-6}$
	oz	0.000035
	lb	$2.2046e^{-6}$
ml	l	0.001
	cm ³	1
	m ³	$1e^{-6}$
	in. ³	0.061024
	ft. ³	0.000035
	gal	0.000264
	oz	0.033814
	Pa	0.01
Pa	hPa	0.01
	kPa	0.001
	MPa	$1e^{-6}$
	kgf/cm ²	0.00001
	psi	0.000145

TABLE OF CONTENTS

LIST OF FIGURES	xi
LIST OF TABLES	xiii
CHAPTER 1: INTRODUCTION	1
1.1 Problem Statement	1
1.2 Research Objectives	2
1.3 Research Methodology	3
1.4 Chapter Organization	4
CHAPTER 2: LITERATURE REVIEW	6
2.1 Introduction	6
2.2 Predicting Settlement with Consolidation Theory and Measured Compressibility Indexes	7
2.3 Predicting Settlement with Estimated Compressibility Indexes	15
2.4 Measuring Settlement with Settlement Plates	18
2.5 Florida’s Geological Formation	21
2.6 Model Development Approach	25
2.7 Summary	26
CHAPTER 3: DEVELOPMENT OF SOIL COMPRESSIBILITY PREDICTION MODELS - METHODOLOGY	28
3.1 Introduction	28
3.2 Data Collection	28
3.3 Methodology	32

3.3.1 Framework and Theoretical Background.....	32
3.3.2 Preprocessing	40
3.3.3 Classification.....	40
3.4 Summary	44
CHAPTER 4: DEVELOPMENT OF SOIL COMPRESSIBILITY PREDICTION MODELS - DATA	
ANALYSIS AND RESULTS	45
4.1 Introduction.....	45
4.2 Regression Models.....	45
4.3 Comparison of Existing Correlations.....	59
4.4 Identification of Influential Parameters	62
4.5 Discussions	74
4.6 Summary	80
CHAPTER 5: VERIFICATION OF SOIL COMPRESSIBILITY PREDICTION MODELS	
82	
5.1 Introduction.....	82
5.2 Site Description.....	83
5.3 Field Testing Program.....	85
5.3.1 Settlement Measurement and Monitoring.....	85
5.3.2 Site Characterization	88
5.4 Case Studies Comparing Predicted Settlement to Measured Settlement	96
5.4.1 Case Study 1: SPT Boring TB-6 Analysis	96
5.4.2 Case Study 2: SPT Boring TB-12 Analysis	107

5.5 Discussions	113
5.6 Summary and Conclusions.....	117
CHAPTER 6: CONCLUSIONS AND RECOMMENDATIONS	121
6.1 Conclusions.....	121
6.2 Limitations and Recommendations.....	124
APPENDIX: FIELD TESTING PICTURES	127
REFERENCES	132

LIST OF FIGURES

Figure 1: Embankment Loading Schematic.....	9
Figure 2: Consolidometer Schematic.....	11
Figure 3: Typical Consolidation Test Results.....	12
Figure 4: Determination of Maximum Past Stress.....	14
Figure 5: Settlement Plate Schematic	19
Figure 6: Typical Settlement Plate Measurement Plot	20
Figure 7: Geology of Florida	22
Figure 8: FDOT District Map	29
Figure 9: Hyperplane Generation for Coarse Grained and Organic Peat Classes	37
Figure 10: Hyperplane Generation for Organic Silt/Clay and Fine Grained Classes	37
Figure 11: Overall Predictive Modeling Framework for C_c and C_r	39
Figure 12: Predicted versus Measured Plot for C_c model of Coarse Grained.....	51
Figure 13: Residual by Predicted Plot for C_c Model of Coarse Grained	51
Figure 14: Predicted versus Measured Plot for C_r model of Coarse Grained.....	52
Figure 15: Residual by Predicted Plot for C_r Model of Coarse Grained	52
Figure 16: Predicted versus Measured Plot for C_c model of Fine Grained.....	53
Figure 17: Residual by Predicted Plot for C_c Model of Fine Grained	53
Figure 18: Predicted versus Measured Plot for C_r model of Fine Grained.....	54
Figure 19: Residual by Predicted Plot for C_r Model of Fine Grained	54
Figure 20: Predicted versus Measured Plot for C_c Model of Organic Peat	55
Figure 21: Residual by Predicted Plot for C_c Model of Organic Peat	55
Figure 22: Predicted versus Measured Plot for C_r Model of Organic Peat.....	56

Figure 23: Residual by Predicted Plot for C_r Model of Organic Peat.....	56
Figure 24: Site Plan.....	83
Figure 25: Sample SPT Borings	84
Figure 26: Surcharge Details	85
Figure 27: Measured Settlement and Surcharge History for S-12.....	87
Figure 28: Measured Settlement and Surcharge History for S-18.....	88
Figure 29: Additional Field Testing Locations.....	89
Figure 30: Geotechnical Profile at both SPT Locations	92
Figure 31: SPT Results and Lab Testing for Complete Soil Profiles	94
Figure 32: Consolidation Test Results.....	96
Figure 33: SPT Results and Lab Testing for Complete Soil Profiles	98
Figure 34: Settlement Plate Results for Location S-12 (TB-6 Location)	102
Figure 35: Settlement Plate Results for Location S-18 (TB-12 Location)	109

LIST OF TABLES

Table 1: Granular Soil Correlation from SPT Blow Count to Wet Unit Weight.....	10
Table 2: Cohesive Soil Correlation from SPT Blow Count to Wet Unit Weight.....	10
Table 3: Summary of Existing Correlations	16
Table 4: Confusion Matrix.....	42
Table 5: Statistical Strength of Developed Correlations.....	47
Table 6: Statistical Strength of Developed Correlations.....	49
Table 7: Statistical Strength of Existing Correlations.....	59
Table 8: Existing Delineational Models for Soil Compressibility.....	63
Table 9: Silts: Pearson’s Correlation Coefficient for C_c	65
Table 10: Silts: Pearson’s Correlation Coefficient for C_r	66
Table 11: Fine Grained: Pearson’s Correlation Coefficient for C_c	67
Table 12: Fine Grained: Pearson’s Correlation Coefficient for C_r	68
Table 13: Clays: Pearson’s Correlation Coefficient for C_c	69
Table 14: Clays: Pearson’s Correlation Coefficient for C_r	70
Table 15: Organics: Pearson’s Correlation Coefficient for C_c	71
Table 16: Organics: Pearson’s Correlation Coefficient for C_r	72
Table 17: Coarse Grained: Pearson’s Correlation Coefficient for C_c	73
Table 18: Coarse Grained: Pearson’s Correlation Coefficient for C_r	74
Table 19: Influential Parameter Breakdown by Soil Classification.....	75
Table 20: Pearson’s Correlation Coefficient of Parameters Included in Compressibility Correlations.....	78
Table 21: Settlement Plate Data.....	86

Table 22: Field Testing Locations	90
Table 23: Additional Index Parameters Needed to Complete Soil Profile	93
Table 24: Additional Laboratory Testing	95
Table 25: Predicted Settlement from Measured C_r , SPT Boring TB-6.....	99
Table 26: Predicted Settlement from Predicted C_r , SPT Boring TB-6	100
Table 27: C_c to C_r Ratio for Each Soil Type.....	101
Table 28: Total Settlement from Predicted Compressibility Index(s) using the C_c correlation to C_r	101
Table 29: Total Settlement from Predicted C_r using Azzouz's correlation ($C_r = 0.142(e - 0.009w + 0.006)$) for all soils.....	103
Table 30: Correlations for Modulus of Elasticity for Various Soil Types.....	104
Table 31: Elastic Settlement Parameters SPT Boring TB-6	104
Table 32: Elastic Settlement SPT Boring TB-6.....	105
Table 33: Total Settlement SPT Boring TB-6	105
Table 34: Total Settlement from Predicted Compressibility Index(s) using the C_c correlation to C_r using Conventional Influence Zone of Settlement.....	106
Table 35: Elastic Settlement Parameters SPT Boring TB-6 using Conventional Influence Zone of Settlement	106
Table 36: Elastic Settlement SPT Boring TB-6 using Conventional Influence Zone of Settlement	107
Table 37: Total Settlement SPT Boring TB-6 using Conventional Influence Zone of Settlement	107
Table 38: Predicted Settlement from Measured C_r	108

Table 39: Predicted Settlement from Predicted C_r , SPT Boring TB-12	108
Table 40: Total Settlement from Predicted Compressibility Index(s) using the C_c correlation to C_r	109
Table 41: Total Settlement from Predicted C_r using Azzouz's correlation ($C_r = 0.142(e - 0.009w + 0.006)$) for all soils.....	110
Table 42: Elastic Settlement Parameters SPT Boring TB-12	110
Table 43: Elastic Settlement SPT Boring TB-12.....	111
Table 44: Total Settlement SPT Boring TB-12	111
Table 45: Total Settlement from Predicted Compressibility Index(s) using the C_c correlation to C_r using Conventional Influence Zone of Settlement.....	112
Table 46: Elastic Settlement Parameters SPT Boring TB-12 using Conventional Influence Zone of Settlement	112
Table 47: Elastic Settlement SPT Boring TB-12 using Conventional Influence Zone of Settlement	112
Table 48: Total Settlement SPT Boring TB-12 using Conventional Influence Zone of Settlement	113
Table 49: Statistical Strength of Prediction Models	114
Table 50: Measured vs. Predicted Settlement Summary	116
Table 51: Measured vs. Predicted Settlement Summary, Considering Conventional Influence Zone of Settlement and Elastic Settlement Contribution.....	117
Table 52: Optimal Correlations for Field Use	119

CHAPTER 1: INTRODUCTION

1.1 Problem Statement

Ground settlement from compressible soils is a phenomena that is quite commonplace in the construction world. Florida, particularly, has vast amounts of organics, silts, and clays, whose soil skeleton has a tendency to collapse when exposed to moisture and loading conditions. As Florida is wet for the majority of the year and the construction industry is booming due to upgrading an aging infrastructure and meeting the demands of population increases, conditions are ripe soil settlement, if unmitigated. Soil settlement causes increased maintenance costs and a decreased lifespan for structures, roadways, and bridges.

The magnitude of settlement is dependent on many variables, but the most important factors for primary settlement are the compressibility indexes. The Compression Index, C_c , and Recompression Index, C_r , describe the soil's reaction when being loaded and the degree in which permanent deformation is anticipated. These factors can be measured in a laboratory or approximated via correlations to other, easier to obtain, soil descriptors. Direct measurement comes in the form of a consolidation test, which takes approximately two weeks to perform, is fraught with potential for human error, and is relatively costly (in the rage of \$500).

The compressibility indexes can also be estimated from soil correlations that have been developed and are widely used in academia and industry, alike. These correlations have been generated from soils all over the world, from Greece, to Brazil and Turkey, and even in the United States. The use of these correlations in application of settlement predictions of Florida soils poses two important questions:

- How well can the existing correlations predict the compressible nature of Florida soils?
- Can the existing correlations be improved upon to yield more reliable settlement predictions?

1.2 Research Objectives

The primary objective of this study is to answer the two questions stated above. There are, however, several other research goals that are stated below:

- The existing correlations assume that only certain soil descriptors will influence the compressibility indexes. These correlations will be tested to verify their predictive capabilities. In developed correlations from this study, additional descriptors will be added to determine if predictive capabilities can be enhanced.
- Existing correlations are abundant for silts and clays (fine grained materials). There is, however, a dearth of correlations for coarse grained materials and a precious few for organics. This study aims to examine these materials as well and determine if reliable correlations for these soil types can be generated.
- The Compression Index, C_c , has largely been studied and existing correlations are plentiful. However, there is a noticeable lack of existing correlations for the Recompression Index, C_r . As this parameter plays an important part in the potential settlement of a large portion of Florida's soils (discussed later in the study), it will need to be included in data analysis to determine if dependable models can be created.

1.3 Research Methodology

This study incorporates the following research approach to the development of soil compressibility prediction models and determination of applicability to site settlement:

- Data Collection
 - Gathering SPT borings and consolidation tests
 - Building a Microsoft Access database to house and sort all data
 - Gathering existing models of compressibility indexes and reviewing existing literature
- Data Analysis
 - Developing the soil classifications through Support Vector Machines
 - Creating regression models for each classification
 - Comparing to existing correlations
 - Identifying influential parameters for each regression model
- Model Verification
 - Identifying sites with consolidation data and measured settlement
 - Performing field/laboratory tests to complete the soil profile, as needed
 - Developing settlement predictions based on measured compressibility indexes
 - Performing settlement predictions based on developed compressibility models
 - Comparing settlement predictions from measured compressibility indexes to predicted compressibility indexes.

1.4 Chapter Organization

The chapters are organized similarly to the research methodology. Chapter 2, which follows this section, covers consolidation theory and background information about how settlement predictions are made. Existing compressibility index correlations are then covered. These correlations comprise both C_c and C_r , with notations for soil types that are applicable. A settlement plate discussion is also included in Chapter 2. Specifics will be discussed, such as how they are typically installed and what the settlement plots usually look like. A brief history of Florida's geology will follow, as this establishes stress history and other specifics about what to expect when encountering Florida soils. Lastly, the model development approach will be discussed.

Chapter 3 will house the development of soil compressibility prediction model methodology. This includes a discussion of data collection and a description of what is included in each data point. After that, the methodology of developing soil classifications will be outlined. This includes a framework of establishing assumed soil classes and testing them. Also included is data processing, and the subsequent creation of soil classifications. Afterwards, a summary of the process will be given, as well as preliminary results.

Chapter 4 will consist of the creation of regression models for each soil classification. After each regression model is derived, they will then be compared to existing correlations, to determine which models are the strongest and most applicable for Florida soils. Also included in this portion of the study is the identification of influential parameters for each soil class. Upon conclusion of these analyses, a brief summary will be given.

Chapter 5's contents will include the verification of the regression models generated. A site description will be given for SR 415. Then, the field testing program will be highlighted, which includes both field and laboratory testing for soil index parameters and consolidation. After the field/lab testing is completed, two case studies will be performed for two different locations at the SR 415 site. These case studies will include settlement predictions from measured compressibility indexes, as well as settlement predictions from predicted compressibility indexes. These predictions will then be compared to measured settlement for both locations. Afterwards, observations and conclusions will be discussed.

Chapter 6 will summarize the findings of the study and provide limitations and recommendations.

CHAPTER 2: LITERATURE REVIEW

2.1 Introduction

Estimating settlement is an essential component of any geotechnical design. As soil is subjected to a load from an overlying structure, it will begin to compress, or settle, immediately. This is called primary consolidation and is the main focus of this study. Primary consolidation occurs immediately upon being loaded from dead or live loads (Das, 2002). When subjected to a load, water escapes the pores of the soil skeleton. The voids created from the vacated water are highly unstable and susceptible to collapse. This continued displacement propagates its way to ground surface and settlement is observed. Over time, the soil will continue to compress, in which case it may take several years to extract its entirety. This is called secondary compression, and is not a component of this study.

Mitigation can be costly and time consuming. When settlement is expected, a surcharge can be placed at ground surface in an attempt to extract all structurally damaging settlement before construction begins. This practice can take several years, which is not conducive to efficient construction. The problematic soils, such as organics and clays, can also be excavated and replaced with clean, well-draining materials to prevent this phenomena from occurring. If the compressible soils are too thick or too deep, this may not be practical.

Mitigation can best be served with adequate settlement predictions. This starts with a strong understanding of consolidation theory.

2.2 Predicting Settlement with Consolidation Theory and Measured Compressibility Indexes

The magnitude of settlement is dependent on the soil's stress state, which can be either normally consolidated (NC) or over-consolidated (OC). Normally consolidated soils have never experienced a higher stress than the present stress; thus, are referred as “virgin” soils in their natural state. Over-consolidated soils have experienced a higher stress in the past than the present stress (Hough, 1957). The settlement of NC soils can be determined from Equation 1 and the settlement for OC soils can be determined from Equations 2 and 3 (Das, 2002).

$$S_c = \frac{C_c H_c}{1+e_o} \log \left(\frac{\sigma'_o + \Delta\sigma'}{\sigma'_o} \right) \quad (1)$$

Where S_c = settlement caused from loading condition, C_c = compression index in soil layer of interest, H_c = thickness of soil layer of interest, e_o = initial void ratio in soil layer of interest, σ'_o = initial vertical effective stress at midpoint of soil layer of interest, $\Delta\sigma'$ = change in vertical stress due to loading.

If a soil is over-consolidated, the computed settlement can be determined from one of two cases. If the initial stress, plus the change in stress from a load inducing agent, is less than the maximum past stress (σ'_c), the following settlement equation applies:

$$S_c = \frac{C_r H_c}{1+e_o} \log \left(\frac{\sigma'_o + \Delta\sigma'}{\sigma'_o} \right) \quad (2)$$

Where C_r = recompression index in soil layer of interest.

If the initial stress, plus the change in stress from a load inducing agent, is greater than the maximum past stress (σ'_c), the following settlement equation applies:

$$S_c = \frac{C_r H_c}{1+e_o} \log\left(\frac{\sigma'_c}{\sigma'_o}\right) + \frac{C_c H_c}{1+e_o} \log\left(\frac{\sigma'_o + \Delta\sigma'}{\sigma'_c}\right) \quad (3)$$

For this study, the stress change in the settlement analysis will come in the form of a surcharge. The encountered stress change of the soil layer will be determined by depth and spatial geometry in relation to embankment surcharge dimensions (Das, 2002) and governed by the following equation:

$$\Delta\sigma = \frac{q_o}{\pi} * \left[\frac{B_1+B_2}{B_2} * (\alpha_1 + \alpha_2) - \frac{B_1}{B_2} * \alpha_2 \right] \quad (4)$$

Where $\Delta\sigma$ = stress change in soil layer of interest, B_1 = horizontal distance from beginning of full height of surcharge to point of interest, B_2 = horizontal distance from toe of surcharge embankment to full height of surcharge, α_1 = angle from point of depth interest to horizontal point B_1 at ground surface (in radians), and α_2 = angle from point of depth interest to horizontal point B_2 at ground surface (in radians). The equations for α_1 and α_2 are defined below.

$$\alpha_1 = \tan^{-1}((B_1 + B_2)/z) - \tan^{-1}(B_1/z) \quad (5)$$

$$\alpha_2 = \tan^{-1}(B_1/z) \quad (6)$$

Where z = depth to point of interest (ft.).

$$q_o = \gamma H \quad (7)$$

Where γ = unit weight of embankment soil (pcf.), and H = height of embankment (ft.).

The following figure is used to further illustrate the meaning of these variables:

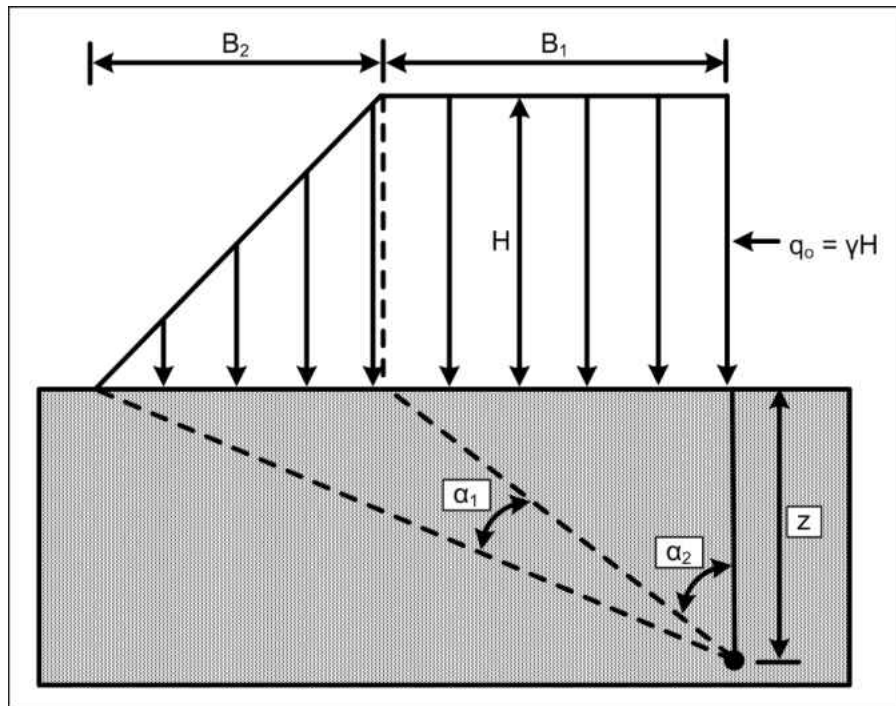


Figure 1: Embankment Loading Schematic

The initial vertical effective stress, σ'_o , will then need to be determined for each layer of interest. This can be accomplished by multiplying the height of the soil layer by its wet unit weight (accounting for water table depth and pore water pressure). This will need to be performed up to the depth of interest, and is governed by the equation below:

$$\sigma_o = H(\gamma_{wet} - u) \quad (8)$$

Where σ'_o = initial vertical effective stress (psf.), H = depth to point of interest (ft.), γ_{wet} = wet unit weight (pcf.), and u = pore water pressure (62.4 psf.). The vertical effective stress will increase with depth.

Correlations for determining wet unit weight from SPT blow counts can be used to simplify the process (Teng, 1962). The following tables provide an estimate for wet unit weight to SPT blow counts for granular and cohesive soils.

Table 1: Granular Soil Correlation from SPT Blow Count to Wet Unit Weight

SPT Blow Count (N)	Compactness	Wet Unit Weight (pcf)
0-4	Very Loose	Less than 100
5-10	Loose	101-110
11-30	Medium	111-130
31-50	Dense	131-140
Above 50	Very Dense	Greater than 140

Source: Teng, 1962

Table 2: Cohesive Soil Correlation from SPT Blow Count to Wet Unit Weight

SPT Blow Count (N)	Compactness	Wet Unit Weight (pcf)
0-2	Very Soft	Less than 100
3-4	Soft	101-110
5-8	Medium	111-120
9-16	Stiff	121-130
17-32	Very Stiff	131-140
Above 32	Hard	Greater than 140

Source: Teng, 1962

The compression indexes, C_c and C_r , can be measured via a consolidation test. A consolidation test consists of one dimensional compression where lateral movement and strains are restricted. The undisturbed sample of soil is prepared and loaded into a confining apparatus, called a consolidometer, such that soil strain and water flow are restricted to the vertical direction (Das, 2002).

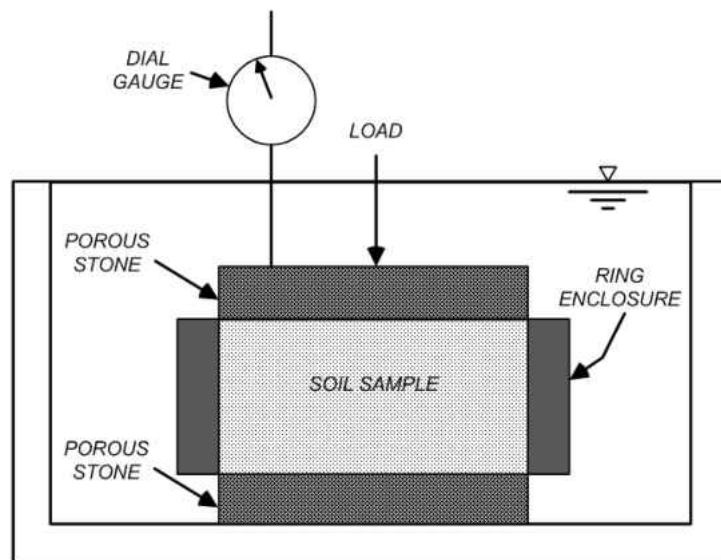


Figure 2: Consolidometer Schematic

The soil sample is then subjected to a series of incremental loads with the resulting deformations recorded with time. In a typical consolidation test, the incremental loads are applied at 24 hour intervals and will have a magnitude of twice the previously applied load. Deformation readings are usually noted throughout the 24 hour loading period at times such that the interval between readings approximately doubles (Das, 2002). A commonly used deformation reading schedule is 2, 4, 8, and 24 hours after the application of the load.

As soils encountered in the field have a tendency to be over-consolidated, where the soil has experienced a higher stress in its history than what is currently being experienced, a common practice in a consolidation test is to run an unload-reload cycle. This will capture the behavior of the soil as the subjected stress is reduced and the sample is allowed to recover. Unloading intervals are taken at decreasing installments similar to loading intervals, such that the next interval will be decreased by half of the existing. Since each loading and unloading cycle takes 24 hours, a typical consolidation test will have approximately a two week duration.

Consolidation test results are generally plotted in a graph that illustrates the sample's compressive behavior throughout the loading sequence. As the sample gets loaded, the air voids will slowly decrease and water will escape. The graph is typically plotted showing the variation of the void ratio, e , with the corresponding changes in applied pressure, in kips per square foot, on a semilogarithmic graph in which void ratio, e , is plotted on the arithmetic scale and pressure on the log scale.

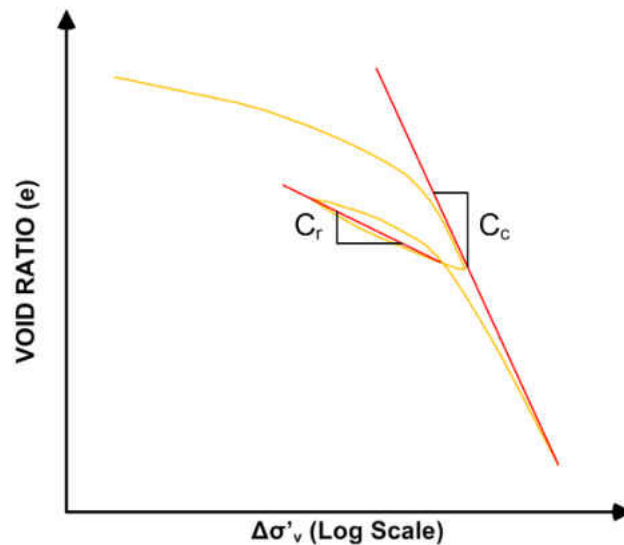


Figure 3: Typical Consolidation Test Results

Upon conclusion of the consolidation test, the engineer will usually note the compression indexes (C_c and C_r) and other descriptors of the sample such as the liquid and plastic limit of the soil, dry or moist density, moisture content, initial and final void ratios, USCS (Unified Soil Classification System) soil classification, location of undisturbed sample extraction (boring number and depth), sample description, and the maximum past pressure, σ'_c , that the soil has experienced.

The maximum past stress, σ'_c , also commonly referred to as the preconsolidation pressure, P_c , is normally interpreted from the void ratio to pressure relationship exhibited above. Consolidation tests performed on samples taken from the field generally show a change in slope at the preconsolidation pressure (Sabatini et al., 2002). Sampling disturbance will usually lower the overall e - $\log\sigma$ curve relative to that of actual field conditions in the soil's natural state. As a result, the preconsolidation pressure is often underestimated during routine testing. The Cassagrande Method is used to reconstruct the e - $\log\sigma$ field curve to account for any disturbance during sample extraction from its natural state and during preparation for testing (Sabatini et al., 2002).

There are four primary steps to determining this value from the consolidation test results. They are as follows (NAVFAC, 1982):

1. Select the point of maximum curvature
2. Draw a tangent line at the point of maximum curvature defined in Step 1
3. Draw a horizontal line at the point of maximum curvature defined in Step 1
4. Bisect the lines drawn in Steps 2 and 3

5. Draw an extension of the line virgin compression zone

The point of intersection between the bisector line in Step 4 and the extension line constructed, in Step 5, is the location of the preconsolidation pressure, as noted in the figure below:

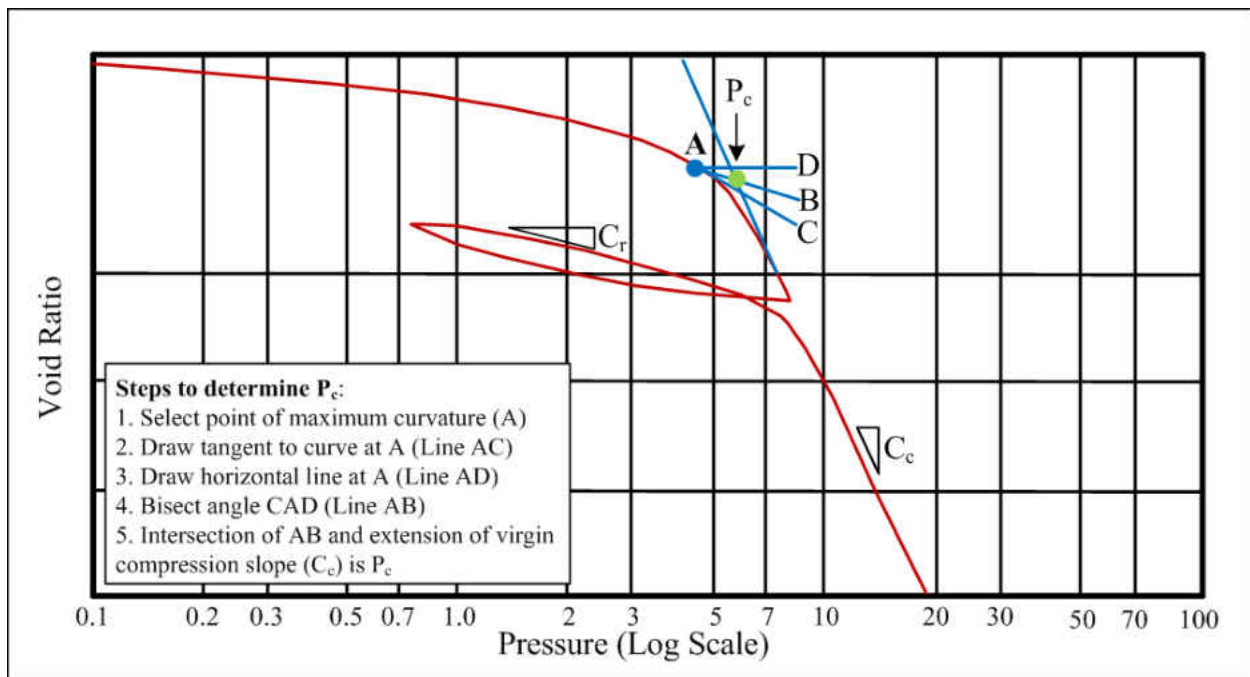


Figure 4: Determination of Maximum Past Stress

Source: NAVFAC, 1982

The compression indexes (C_c and C_r) can be determined from the slopes of various portions of the e - $\log \sigma$ curve. The Compression Index, C_c , is approximated as the slope of the e - $\log \sigma$ curve in the normally consolidated range. This is the behavior the soil exhibits when it's loaded to a stress beyond what it has been subjected to in its history. The Recompression Index, C_r , is computed as the slope of the curve in which the soil is being unloaded and reloaded. This portion of the curve captures the behavior when a loading has been removed from the soil and

then subsequently reloaded. This mimics field conditions when new construction with various loading conditions are applied to a previously loaded soil.

As can be seen in the settlement equations, the magnitude of the overall settlement depends on several variables such as the Compression Index, C_c , and Recompression Index, C_r . Due to the large amount of uncertainty for these parameters, engineers normally measure it directly via a consolidation test. This test is time consuming and can be relatively expensive due to the equipment and technical expertise needed. For this reason, correlations have been developed to approximate these compressibility indexes.

2.3 Predicting Settlement with Estimated Compressibility Indexes

For reasons previously stated, various attempts have been made to estimate the Compression Index, C_c , and Recompression Index, C_r , based on several soil descriptors. These descriptors can be obtained from a series of different lab tests that are quicker and significantly easier to administer than the consolidation test.

Existing correlations between index properties and consolidation parameters (C_c and C_r) are presented in the following table. The correlations range from single parameter models (e.g., void ratio (e), natural moisture content (w), etc.) to multi-parameter models. The multi-parameter models incorporate a combination of different data from common lab tests for soil descriptors. The majority that were obtained were for clays and were correlated to C_c . However, there were a few correlations for peats and all soils, and some date back to the 1950s. The strength of these correlations will be tested further in the study.

Table 3: Summary of Existing Correlations

Ind. Variable	Dep. Variable	Equation	Reference	Notes
C _c	w	$C_c = 0.01w - 0.05$	Azzouz (1976)	All soils
		$C_c = 0.01w$	Koppula (1981)	Clays
		$C_c = 0.01w - 0.075$	Herrero (1983)	Clays
		$C_c = 0.013w - 0.115$	Park, Lee (2011)	Clays
		$C_c = 0.0075w$	Miyakawa (1960)	Peat
		$C_c = 0.011w$	Cook (1956)	Peat
	e	$C_c = 0.54e - 0.19$	Nishida (1956)	Clays
		$C_c = 0.43e - 0.11$	Cozzolino (1961)	Clays
		$C_c = 0.75e - 0.38$	Sowers (1970)	Clays
		$C_c = 0.49e - 0.11$	Park, Lee (2011)	Clays
		$C_c = 0.4(e-0.25)$	Azzouz (1976)	All soils
		$C_c = 0.15e + 0.01077$	Bowles (1989)	Clays
		$C_c = 0.287e - 0.015$	Ahadiyan (2008)	Clays
		$C_c = 0.6e$	Sowers (1970)	Peat
		$C_c = 0.3(e-0.27)$	Hough (1957)	Clays
	LL	$C_c = 0.006(LL-9)$	Azzouz (1976)	Clays
		$C_c = (LL-13)/109$	Mayne (1980)	Clays
		$C_c = 0.009(LL-10)$	Terzaghi, Peck (1967)	Clays
		$C_c = 0.014LL-0.168$	Park, Lee (2011)	Clays
		$C_c = 0.0046(LL-9)$	Bowles (1989)	Clays
		$C_c = 0.011(LL-16)$	McClelland (1967)	Clays
	w, LL	$C_c = 0.009w + 0.005LL$	Koppula (1981)	Clays
		$C_c = 0.009w + 0.002LL - 0.01$	Azzouz (1976)	Clays
	G _s , e	$C_c = 0.141G_s^{1.2} * ((1+e)/G_s)^{2.38}$	Herrero (1983)	Fine Grained

Ind. Variable	Dep. Variable	Equation	Reference	Notes
	LL, G _s	$C_c = 0.0023 * LL * G_s$	Nagaraj, Murthy (1986)	Clays
	G _s , w	$C_c = 0.2343 * w * G_s$	Nagaraj, Murthy (1985)	Clays
	e, w	$C_c = 0.4(e + 0.001w - 0.25)$	Azzouz (1976)	All soils
	e, LL	$C_c = -0.156 + 0.411e - 0.00058LL$	Al-Khafaji, Andersland (1992)	Clays
	G _s , γ _{dry} , γ _{wet}	$C_c = 0.141 * G_s * (\gamma_{wet} / \gamma_{dry})^{12/5}$	Al-Khafaji, Andersland (1992)	Clays
	e, LL	$C_c = -0.023 + 0.271e + 0.001LL$	Ahadiyan (2008)	Clays
	e, w, LL	$C_c = 0.37(e + 0.003LL + 0.0004w - 0.34)$	Azzouz (1976)	Clays
	e, w, LL	$C_c = -0.404 + 0.341e + 0.006w + 0.004LL$	Yoon, Kim (2008)	Clays
	w, LL, e, γ _{dry}	$C_c = 0.1597(w^{-0.0187})(1 + e)^{1.592}(LL^{-0.0638})(\gamma_{dry}^{-0.8276})$	Ozer (2008)	Clays
	w, LL, e, γ _{dry}	$C_c = 0.151 + 0.001225w + 0.193e - 0.000258LL - 0.0699\gamma_{dry}$	Ozer (2008)	Clays
C _r	e	$C_r = 0.208e + 0.0083$	Peck, Reed (1954)	Clays
	w	$C_r = 0.14(e+0.007)$	Azzouz (1976)	All soils
		$C_r = 0.003(w + 7)$	Azzouz (1976)	All soils
	LL	$C_r = 0.002(LL + 9)$	Azzouz (1976)	All soils
	e, w	$C_r = 0.142(e - 0.009w + 0.006)$	Azzouz (1976)	All soils
	w, LL	$C_r = 0.003w + 0.0006LL + 0.004$	Azzouz (1976)	All soils
	e, LL	$C_r = 0.126(e + 0.003LL - 0.06)$	Azzouz (1976)	All soils
			$C_r = 0.156e + 0.0107$	Elnaggar, Krizek (1971)

Ind. Variable	Dep. Variable	Equation	Reference	Notes
	e, w, LL	$C_r = 0.135(e + 0.1LL - 0.002w - 0.06)$	Azzouz (1976)	All soils
	LL, G_s	$C_r = 0.000463 * LL * G_s$	Nagaraj, Murthy (1985)	Clays

2.4 Measuring Settlement with Settlement Plates

Measured settlement data is obtained via settlement indicators or plates. This apparatus is installed on site before a soil stress inducing agent is introduced, most commonly in the form of a surcharge (FDOT, 2013). A surcharge is a large layer of soil fill, most likely clean sands, that varies in height. This construction operation is introduced to extract primary consolidation settlement from deep pockets of thick problematic soil layers, such as high plasticity clays, mucks, and organic silts (NAVFAC, 1982). These soil layers will compress over time due to the stress change from the surcharge. If done correctly, the primary consolidation settlement will be extracted before the beginning of other construction operations (NAVFAC, 1982). The duration of the surcharge will largely be dependent on depth of problematic soil layers and thickness (NAVFAC, 1982). As the goal for every construction project is budget and time, outside factors will occasionally dictate the duration of the surcharge. The primary objective of this activity would be to ensure the structural integrity of facilities at ground surface on a long-term basis.

When settlement plates are implemented, they are placed in various locations where maximum settlement is predicted (FDOT, 2013). Their purpose is to record the amount and rate of changes in elevation due to underlying settlement, from stress change via surcharge. A settlement plate apparatus is composed of a square wooden platform or steel plate placed on

existing ground surface, prior to the surcharge being added (FDOT, 2013). A reference rod and protective pipe sleeve are attached to the platform. The reference rod is extended as needed, to account for additional lifts to the surcharge (FDOT, 2013). A schematic of a typical settlement plate apparatus is in the figure below.

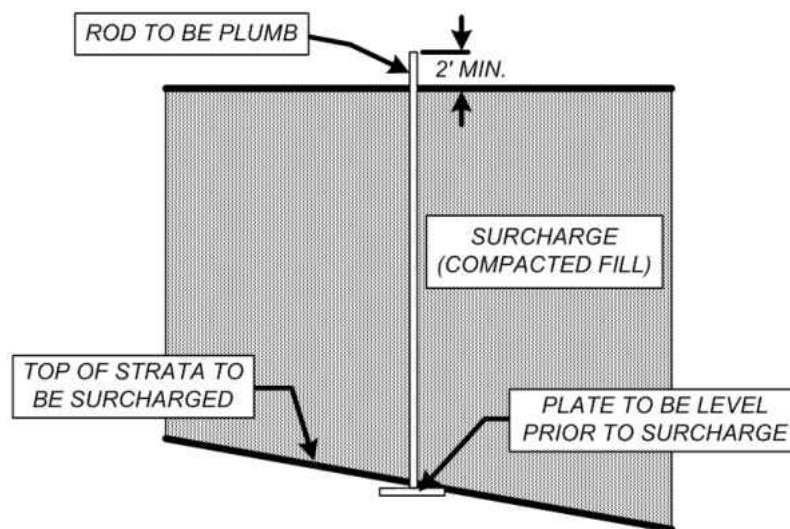


Figure 5: Settlement Plate Schematic

Readings are performed periodically by surveying the top of the rod, using benchmarks and reference datum. The platform elevation is first recorded, prior to the addition of the surcharge. All future readings are compared to the initial. The settlement readings from field observation are then recorded and plotted as a function of time, with respect to changes in fill height above ground surface, as seen in the figure below (FDOT, 2013).

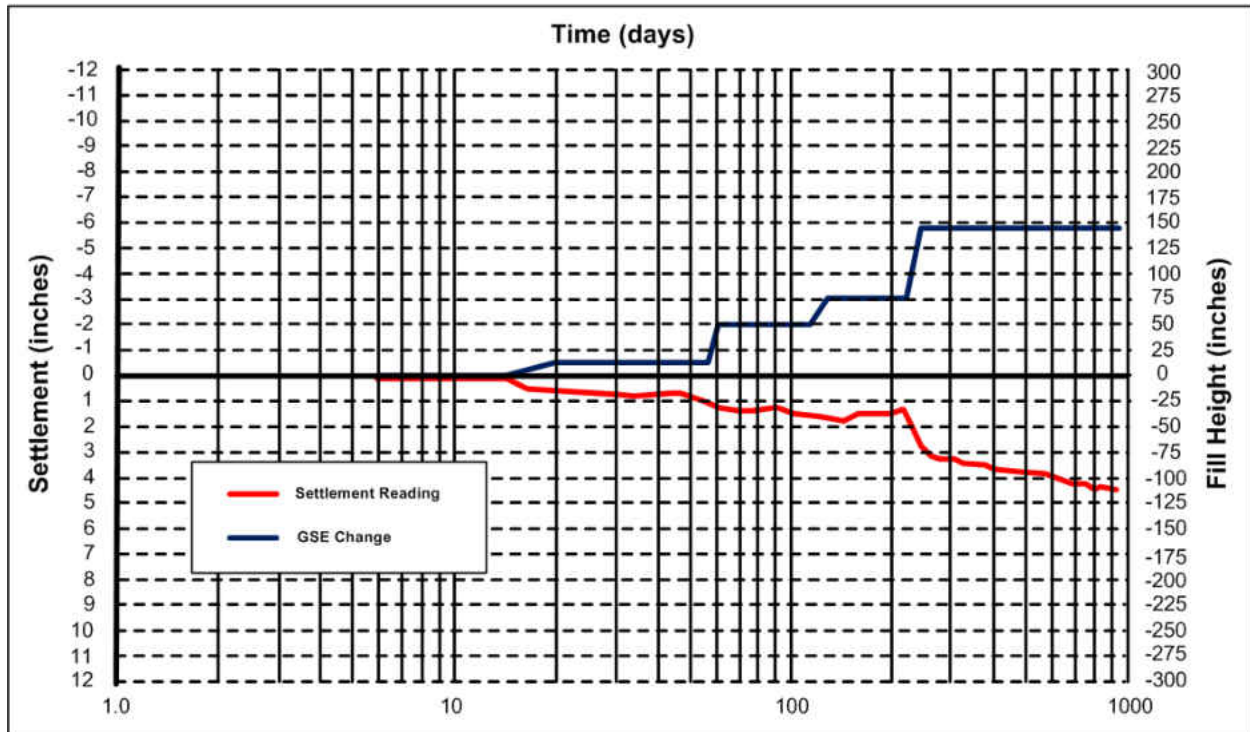


Figure 6: Typical Settlement Plate Measurement Plot

As can be seen in the figure, as the surcharge height increases, there is an associated increase in measured settlement. Fill height is measured in relation to the ground surface elevation (GSE). In this example, the measured settlement reached a total of 4.5 inches, due to 150 inches (12.5 feet) of surcharge. Actual settlement plate data for multiple locations will be presented further in the study, in a similar fashion.

2.5 Florida's Geological Formation

Florida's geology is unique from the Panhandle in the north, to the Central Highlands and Coastal Lowlands in the south (McVay, 2004). The Panhandle houses much of Florida's clayey sands and gravels, while the Central Highlands and Coastal Lowlands are comprised mainly of medium to fine sands and silts, shelly sands and clays, and large deposits of limestone, as noted in the figure below. A large portion of Florida's soils are clayey sands, defined as SC in the USCS (Unified Soil Classification System). Due to the compressive nature of clay particles in this particular soil and the sand particle's propensity for rearrangement during loading, there is a high settlement potential for this soil type that is unaccounted for in existing correlations, from previous literature.

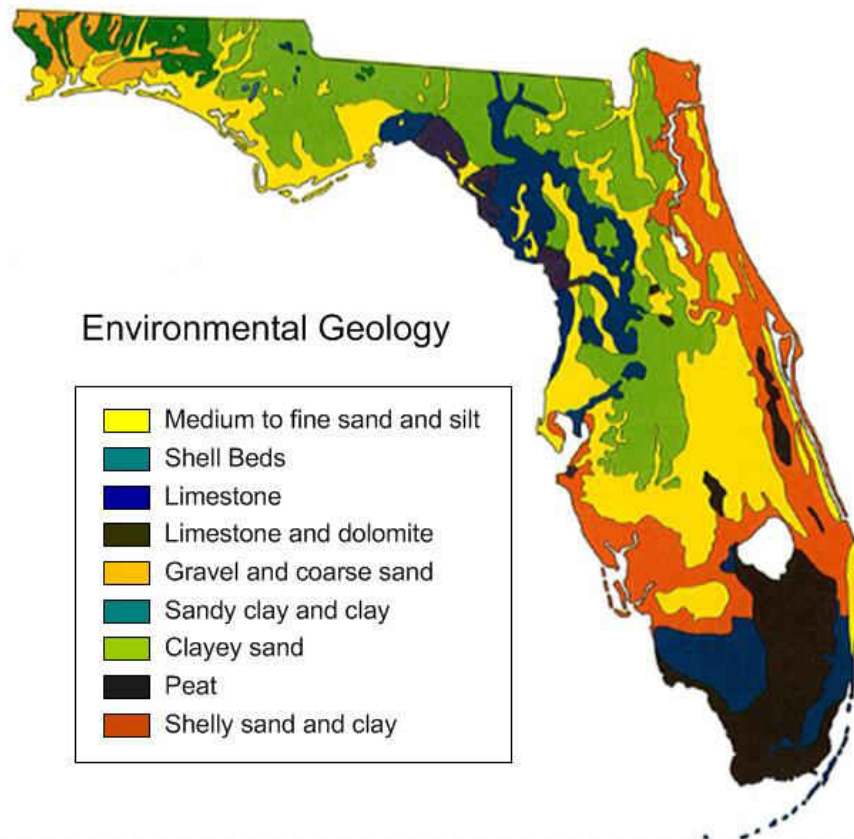


Figure 7: Geology of Florida

Source: Anderson, Krafft, Remington, 1981

Over-consolidation of soil can be observed due to one of many reasons. It could be that a greater depth of past overburden has eroded away over the course of time. Land shifts over many years and glacial movement are common causes of this. Cycles of wetting and drying could be subjected to the soil, such as shrinkage/swelling (Bowles, 1989). As Florida has very wet and dry seasons, moisture intrusion/drying is very likely. The soil could also be exposed to cycles of wetting and drying in the presence of certain sodium, calcium, and magnesium salts and there could be effective pressure changes from water table fluctuations (Bowles, 1989).

A brief look into Florida's geologic history will illustrate how unique the state really is. Florida's history begins out of the break-up of a supercontinent called Rodinia around 700 Ma (million years ago) into a new land mass called Gondwana. This process is composed of two parts: rifting and seafloor spreading. Rifting is the initial splitting apart of the continental mass and seafloor spreading is the formation of a new ocean basin (Hine, 2013). What is now North America was a separate land mass that collided with Gondwana approximately 350 Ma. When this occurred, it formed what we know as Florida today. The shifting and movement that occurred throughout this process displaced what is now Florida from the South Pole to its present location (Hine, 2013).

If one examines the topography of the state, the presence of numerous former beaches, scarps (steep slopes), and shorelines can be observed. This suggests that sediment movement is very likely (Hine, 2013). This occurs from the north to south orientation from peninsular Florida and must have occurred by breaking waves transporting soils from one location to another, much like how sand is moved in modern beaches today. This transport occurs when sea levels were at a higher elevation. When sea levels were lower, local streams and small rivers probably eroded into the former shorelines and moved various amounts of sediments from the east to west (Hine, 2013).

During the peak of the Middle Miocene era (18 Ma), approximately 300 feet of water covered south-central Florida, linking the Gulf of Mexico with the northern Straits of Florida (Hine, 2013). During this time, sea levels fluctuated with great regularity leaving portions of Florida to become shallower and, at times, were emergent, which allowed rivers to flow overland to estuaries and coastlines (Hine, 2013). There were, however, many time periods during this

time in which Florida was high and dry. This provided an environment where land animals and terrestrial creatures thrived due to the rich soils left behind from receding oceans. This sea level history of repeated flooding and exposing of land created one of the great fossil hunting locations in the world, mixing the remains of an abundance of land and marine organisms (Hine, 2013).

Given the geologic history of Florida, it is reasonable to assume that much of Florida's soils are over-consolidated to some degree, as large portions of Florida have been subjected to rising/lowering water tables and sediment transport, and there have been thousands of cycles of wetting/drying throughout the state's history. For this reason, when the soil is subjected to a change in stress and settlement ensues, it is reasonable to assume that a portion of the soil's behavior can be described by the unload-reload cycle of the consolidation curve. When this occurs, the Recompression Index, C_r , will be a factor in the primary consolidation settlement as described in Equations 2 and 3. Existing correlations for the Recompression Index, C_r , are not as abundant as for the Compression Index, C_c , particularly for fine grained and coarse grained soils.

The existing correlations utilize soil descriptors such as liquid limit (LL), void ratio (e), moisture content (w), and dry unit weight (γ_{dry}). While these soil descriptors are useful and relatively easy to obtain, there are several other parameters that also meet this criteria and could have as much, if not more, influence on the parameters that are directly proportional to primary consolidation settlement. These parameters include the wet unit weight (γ_{wet}), automatic hammer SPT blow count (N), overburden stress (σ), plasticity index (PI), and fine content (-200). Having a full spectrum of soil parameters to draw correlations from could yield stronger predictions of settlement.

2.6 Model Development Approach

The application of a machine learning approach will be implemented to develop soil compressibility prediction models, and subsequent field verification through settlement analysis. The concept of machine learning, in the form of classification, is the process of estimating the category of a previously unknown object/observation, out of a finite set of predefined categories based on a set of objects/observations whose category is known (Bishop, 2006). A pool of objects/observations that are pre-labeled, are used as the training set for machine learning algorithms. The training set is used to infer a mapping function. The mapping function is then used to predict the category of new objects/observations (Pappu et al., 2015; Panagopoulos et al., 2016).

Applications of machine learning in civil engineering include but are not limited to: The prediction of tunnel support stability using artificial neural networks (Leu et al., 2001), predicting the remaining service life of bridge decks (Melhem et al., 2003), predicting the ground surface settlement induced by deep excavation using artificial neural networks (Sou-Sen et al., 2004), optimizing the energy efficiency of buildings and their cooperation (Panagopoulos et al., 2015a; Alam et al., 2014; Panagopoulos et al., 2017), and predicting and optimizing building-integrated renewable energy resources (Panagopoulos et al., 2015b; Panagopoulos et al., 2012).

The data will be assumed to fall into different classifications and will be tested to determine if different models for each soil type are necessary. In addition to the correlated parameters summarized in Table 1, this study accounts for other soil descriptors including automatic hammer Standard Penetration Test (SPT) blow count (N), plasticity index (PI),

overburden stress (σ), and fines content (-200) of the soil, which is defined as the portion of the soil sample that has a particle diameter smaller than .074 mm (Bowles, 1989). These parameters may be able to increase the predictive capability of models generated. As part of the study, existing correlations will be tested to determine their predictive capability and they will be compared to the new models that are generated from data collected.

The correlations developed will then be tested through field study. Two different sites that have experienced a known surcharge via a roadway widening project, and have a measured settlement, will be compared to a series of settlement predictions using the models. The first settlement analysis will include direct measurements of C_c and C_r . The second analysis will incorporate predictions of C_c and C_r , using the respective models for each soil type. Comparisons will be drawn to determine the predictive capabilities of the models.

2.7 Summary

Predicting soil settlement is an essential component of any geotechnical design for roadways and structures. These predictions are based on many different factors, but perhaps the most difficult to obtain are the compressibility indexes. This data can either be measured or predicted. Measured compressibility indexes come in the form of consolidation testing which can be costly and time consuming. Estimations for compressibility indexes have been done in the past for a variety of different soils around the world. These correlations may or may not be applicable for Florida soils. The approximations include a variety of correlations for C_c , but not nearly as much for C_r . Given Florida's geologic history and propensity to have over

consolidated soils, where C_c is not applicable, the application of any existing C_r correlation comes into question. This will be vetted further in the study.

CHAPTER 3: DEVELOPMENT OF SOIL COMPRESSIBILITY PREDICTION MODELS - METHODOLOGY

3.1 Introduction

There have been many attempts to create predictions for compressibility indexes in the past. This will be discussed later in the study. When these predictions were made, data was gathered that included soil index parameters (LL, PI, w , e , etc.) and consolidation data. The measured C_c and C_r , from the consolidation test, were then determined if they could be predicted, based on what the index parameters were. In other words, if LL or PI or another parameter went up or down, C_c/C_r would act accordingly. This involved segregating data into certain categories and developing regression models. The specifics of how this was done was not always clear. This study will aim to develop classes for each soil type and create a regression model for each one. This all starts with data collection, which will now be discussed.

3.2 Data Collection

A total of 619 consolidation test data conducted on soils throughout the state of Florida were used in this analysis. Each consolidation test has an accompanying SPT boring to provide a description of the soil's stiffness. The vast majority of the data collected is from the Florida Department of Transportation (FDOT) District Five which includes the counties of Volusia, Seminole, Orange, Osceola, Brevard, Lake, Marion, Sumter, and Flagler.

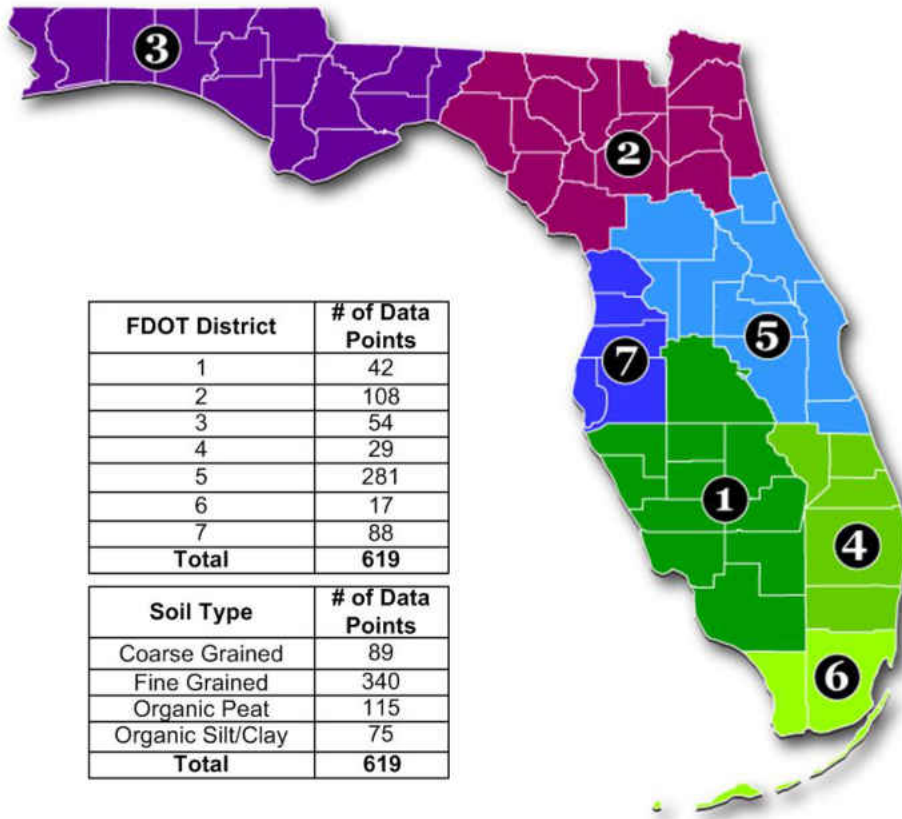


Figure 8: FDOT District Map

A breakdown of the data collected by location can be seen in the upper table in the figure above.

The soil types were assumed to fall into one of four categories. The first category is “Coarse Grained” materials, which is mainly comprised of sands with varying amounts of clays and silts intermingled. These materials are defined as SC (clayey sands) in the USCS (Unified Soil Classification System). Coarse grained materials are classified by having over half of the sample’s particle diameter larger than .074 mm, or the #200 sieve (Bowles, 1989). It’s important to note that all coarse grained samples had an element on fines intermixed with the sample taken from the field. The range of fine contents for each sample spanned from 12 to 49 percent of the sample. For this reason, there is a compressive element associated with this soil type.

The second category is “Fine Grained” materials, which is primarily composed of clays and silts. Fine grained materials are classified by having over half of the sample’s particle diameter smaller than .074 mm, or the #200 sieve (Bowles, 1989). These samples are identified as being CH (high plasticity clay), CL (low plasticity clay), MH (high plasticity silt), or ML (low plasticity silt), by the USCS classification system. The plasticity level of each sample is determined by where the plasticity falls on the A-line chart (Das, 2002). Clays and silts are differentiated by the segregation of their soil particles. Clays will have a larger amount of smaller particles, as compared to silts.

The third category was assumed to be soils with large deposits of organics, and is called “Organic Peat”. These fibrous soils are composed of decaying plant life and other degradable materials that are classified visually by inspection (Bowles, 1989). They are distinguished by the PT classification, when classified using USCS. They are often referred to as “muck” and are normally over-saturated with water. There is normally an associated smell when encountering this soil type in the field. It is highly compressible.

The last category that the soils were assumed to be grouped in is “Organic Silts/Clays”. These are fine grained soils with traces of organic materials. In order to have this classification, a series of Atterberg Limits needs to be performed for the soil, both before being oven dried and after. If the fraction of the Liquid Limit after being oven dried over the Liquid Limit before being oven dried is less than 0.75, the material is classified as an Organic Silt or Organic Clay, depending on the Plasticity Index. The assumed soil categories were tested to verify that separate correlations should be used based on soil type. The soil types in this category are OH

and OL, as defined by the USCS soil classification system, where the H and L are identified by their respective level of plasticity from the A-line chart (Das, 2002).

A Microsoft Access database has been created to store and sort the existing data for quick analysis. This database houses the general information of where the sample was taken (project numbers/description, FDOT District and County, etc.), specific information of where the sample was taken (latitude/longitude, boring number, sample depth), sample description (soil type, USCS Classification, fines content (-200), moisture content (w), initial void ratio (e_o), Atterberg limits (LL and PI), SPT automatic hammer blow count (N), specific gravity (G_s), etc.), and stress state of the soil (compression index (C_c), recompression index (C_r), effective overburden pressure (σ'_o), and preconsolidation pressure (P_c)).

Overburden pressure was computed using a correlation for SPT blow count to saturated unit weight of soil (Teng, 1962). This was determined for each soil strata above the depth from which the sample was taken and each unit weight was then multiplied by the height of each respective soil strata, taken from the SPT boring. The seasonal high water table was used to account for the effective overburden pressure computation.

The SPT borings were also used to help identify some of the missing data from the consolidation test report. If the moisture content (w) or fines content (-200) were not included on the consolidation test report, they may have been accounted for via lab tests in close proximity to where the undisturbed sample was taken, if these extra lab tests and undisturbed sample were taken from the same soil strata.

3.3 Methodology

3.3.1 Framework and Theoretical Background

A standard methodology is followed for data analysis. The collected data are first checked for completeness. Samples for which some of the descriptors (features) are missing are discarded. Data are then brought on the same scale through normalization. This ensures that all the descriptors will have an equal contribution to the machine learning model.

The next step aims to determine the number of distinct groups of soil that exist. Through this process, the goal is to decide if each soil type requires a different statistical model. The machine learning algorithm that is used at this step is Support Vector Machines (SVMs) (Vapnik, 2000). A portion of the data is used to train the SVMs. During the training, it is assumed that there are four distinct groups/classes (Coarse Grained, Fine Grained, Organic Peat, and Organic Silt/Clay). The four classes are highly variant in terms of size. The discrepancy in size between the classes has the potential to affect the efficient training of our model and thusly needs to be taken into consideration. To that end, when building the model, a class weighting scheme is utilized in the optimization process (Veropoulos et al., 1999; Xanthopoulos et al., 2014). This is done in order to address the issue of having a different number of samples from each soil type. The class weighting scheme we follow is a One-Versus-All approach of Support Vector Machines. The multiclass problem is decomposed into four binary classification problems. In particular, four binary classifiers are built where the n^{th} classifier separates the n^{th} class from the rest. The class of a new point is then determined according to a majority voting principle. The trained model is evaluated on the remaining data which encompasses the test set.

The classification results of the test set aid in the confirmation or rejection of the hypothesis that each soil type requires a different statistical model. Each group of samples will need a distinct statistical model, if, during the testing phase, the proportion of the correctly classified samples exceeds the 77% threshold. To that end, the hypothesis test is set to $H_0: p=.77$ and the $H_a: p>.77$.

The following notation is then introduced:

Let \mathbf{x}_i denote a multidimensional data point with dimensionality equal to the number of columns of the data matrix; that is every point has a dimension of seven, which is the number of variables that are used, namely the moisture content (w), initial void ratio (e_0), dry unit weight (γ_{dry}), wet unit weight (γ_{wet}), automatic hammer SPT blow count (N), overburden stress (σ), and fines content (-200).

y_i is denoted with the sign of the class/group membership. It can obtain two distinct values +1 or -1 which are used to represent the class of a sample. For example, when data are preprocessed in order to be inputted to the binary classifier, a sample that belongs to the Fine Grained class will obtain a corresponding y_i equal to +1 while the rest of the samples that belong to the other classes will obtain a value of y_i equal to -1.

The details of SVMs are presented below.

Let $S = \{(\mathbf{x}_i, y_i)\}$, $\mathbf{x}_i \in \mathbb{R}^d$, $y_i \in \{-1, +1\}$ $\forall i = 1, \dots, n$ be the training set.

Define the hinge loss function as,

$$l(y_i, f(\mathbf{x}_i)) = |1 - y_i f(\mathbf{x}_i)|_+ \quad (9)$$

During the training phase SVMs solve

$$\min_{\mathbf{w}} \frac{1}{2} \|\mathbf{w}\|^2 + C \sum_{i=1}^n l(y_i, f(\mathbf{x}_i)) \quad (10)$$

where C is a positive regularization parameter and $f(\mathbf{x}_i) = \langle \mathbf{w}, \mathbf{x}_i \rangle + \mathbf{b}$ is the desired linear classifier, with \mathbf{w} being the weight vector and \mathbf{b} the bias term.

For the case of imbalanced classification, different costs C^+ and C^- may be used for each class.

The optimization problem can be rewritten as,

$$\min_{\mathbf{w}} \quad \frac{1}{2} \|\mathbf{w}\|^2 + C^+ \sum_{\{i|y_i=+1\}} \xi_i + C^- \sum_{\{i|y_i=-1\}} \xi_i \quad (11)$$

$$\text{subject to} \quad y_i (\langle \mathbf{w}, \mathbf{x}_i \rangle + \mathbf{b}) \geq 1 - \xi_i, \quad \forall i=1, \dots, n$$

$$\xi_i \geq 0, \quad \forall i=1, \dots, n$$

SVMs can become non-linear through a transformation $\Phi: \mathbb{R}^d \rightarrow H$, such that $\Phi(\mathbf{x}_i) \in H$, where

H is a reproducing kernel Hilbert space with $\dim(H) > \dim(\mathbb{R}^d)$.

The Lagrangian function can be written as,

$$L(\mathbf{w}, \xi, \mathbf{b}, \alpha, \beta) =$$

$$\begin{aligned} & \frac{1}{2} \langle \mathbf{w}, \mathbf{w} \rangle + C^+ \sum_{\{i|y_i=+1\}} \xi_i + C^- \sum_{\{i|y_i=-1\}} \xi_i - \sum_{i=1}^n \alpha_i (y_i (\langle \mathbf{w}, \Phi(\mathbf{x}_i) \rangle + \mathbf{b}) - 1 + \xi_i) \\ & - \sum_{i=1}^n \beta_i \xi_i \end{aligned} \quad (12)$$

where α, β , are the Lagrange multipliers.

Since this is a convex problem, its Wolfe dual can be obtained from the following stationary first order conditions of the primal variables \mathbf{w} , \mathbf{b} and ξ .

$$\frac{\partial L}{\partial \mathbf{w}} = \mathbf{w} - \sum_{i=1}^n \alpha_i y_i \Phi(\mathbf{x}_i) = 0 \quad (13)$$

$$\frac{\partial L}{\partial \mathbf{b}} = \sum_{i=1}^n \alpha_i y_i = 0 \quad (14)$$

$$\frac{\partial L}{\partial \xi_k} = \begin{cases} C^+ - a_k - \beta_k = 0 & \text{if } y_k = +1 \text{ and } k = 1, \dots, n \\ C^- - a_k - \beta_k = 0 & \text{if } y_k = -1 \text{ and } k = 1, \dots, n \end{cases} \quad (15)$$

Substituting the equivalent expressions for \mathbf{w} , \mathbf{b} and ξ back in, the Wolfe dual can then be written as,

$$\max_{\alpha} \quad -\frac{1}{2} \sum_{i=1}^n \sum_{j=1}^n \alpha_i \alpha_j y_i y_j K(\mathbf{x}_i, \mathbf{x}_j) + \sum_{i=1}^n \alpha_i \quad (16)$$

subject to $\sum_{i=1}^n \alpha_i y_i = 0$

$$0 \leq \alpha_i \leq C^+ \quad \text{if } y_i = +1 \text{ and } i = 1, \dots, n$$

$$0 \leq \alpha_i \leq C^- \quad \text{if } y_i = -1 \text{ and } i = 1, \dots, n$$

The solution is used to evaluate,

$$\mathbf{w}^* = \sum_{i=1}^n \alpha_i y_i \Phi(\mathbf{x}_i) \quad (17)$$

Let $V^+ = \{ \alpha_i \mid 0 < \alpha_i < C^+ \text{ and } y_i = +1 \}$, $I^+ = \{ i \mid \alpha_i \in V^+ \}$

Let $V^- = \{ \alpha_i \mid 0 < \alpha_i < C^- \text{ and } y_i = -1 \}$, $I^- = \{ i \mid \alpha_i \in V^- \}$

The bias can be computed as,

$$\mathbf{b}^* = \frac{1}{|V^+|} \sum_{i \in I^+} (y_i - \sum_{j=1}^n \alpha_j y_j K(\mathbf{x}_i, \mathbf{x}_j)) + \frac{1}{|V^-|} \sum_{i \in I^-} (y_i - \sum_{j=1}^n \alpha_j y_j K(\mathbf{x}_i, \mathbf{x}_j)) \quad (18)$$

Then during the testing phase, the class of a new data point \mathbf{x} is determined as,

$$\text{class}(\mathbf{x}) = \text{sign}(\langle \mathbf{w}^*, \Phi(\mathbf{x}) \rangle + \mathbf{b}^*) = \text{sign}(\sum_{i=1}^n \alpha_i y_i K(\mathbf{x}_i, \mathbf{x}) + \mathbf{b}^*) \quad (19)$$

One of the most common kernels used in the training of SVMs is the Radial Basis Function

kernel defined by,

$$K(\mathbf{x}_i, \mathbf{x}_j) = \exp(-\gamma \|\mathbf{x}_i - \mathbf{x}_j\|^2), \quad \gamma \geq 0 \quad (20)$$

Parameter γ as well as parameter C is tuned by the user during the training phase.

If data can be separated with a hyperplane/decision surface in the trained SVMs, it will be an early indication that a regression model is needed for each distinct group/class; although the formal decision is made during the testing phase. The figures below demonstrate instances of trained SVMs. The straight line represents the two dimensional hyperplane/decision surface. In particular, Figure 9 depicts an instance in which data are separable and thus a regression model could be developed for each distinct group/class. This figure depicts the separation of a regression model for the Coarse Grained and Organic Peat class.

Figure 10 demonstrates an inseparable dataset. This example suggests that the Organic Silt/Clay class and Fine Grained class need to be grouped together when it comes to the development of the regression models. That is, a single regression model should be developed to represent the group of samples that encompasses both Organic Silt/Clay and Fine Grained.

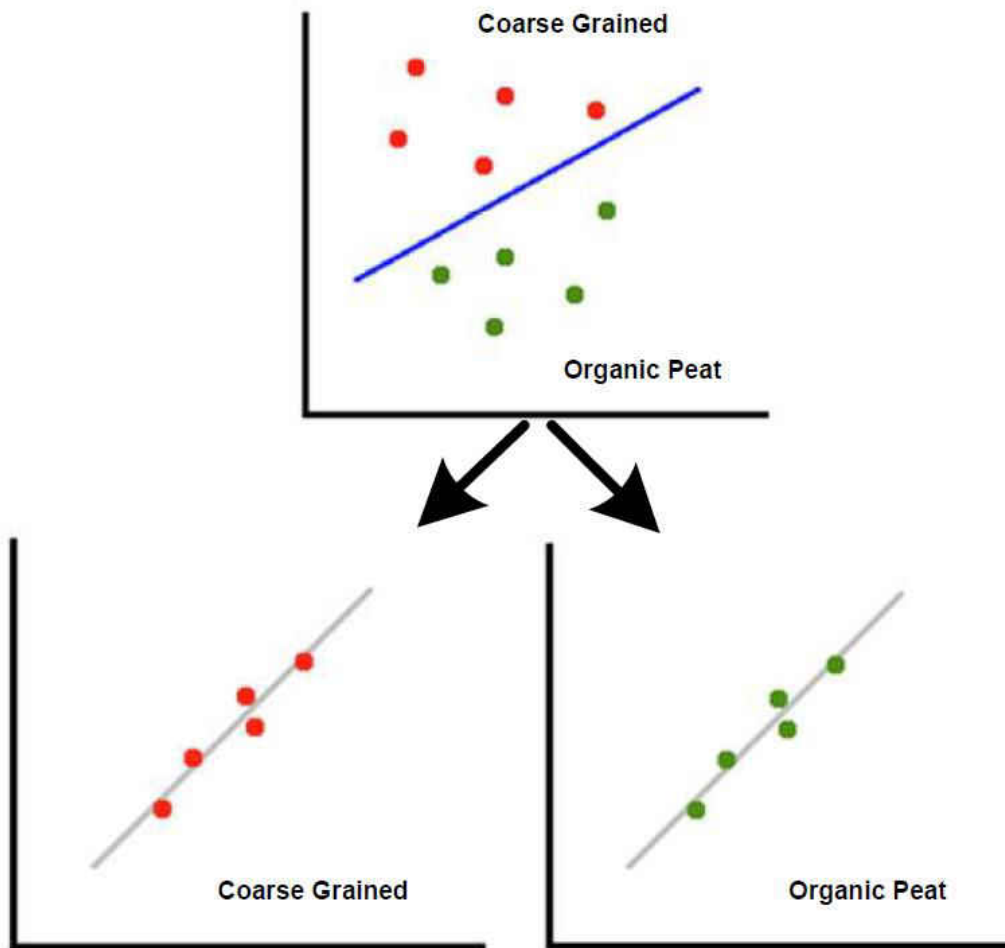


Figure 9: Hyperplane Generation for Coarse Grained and Organic Peat Classes

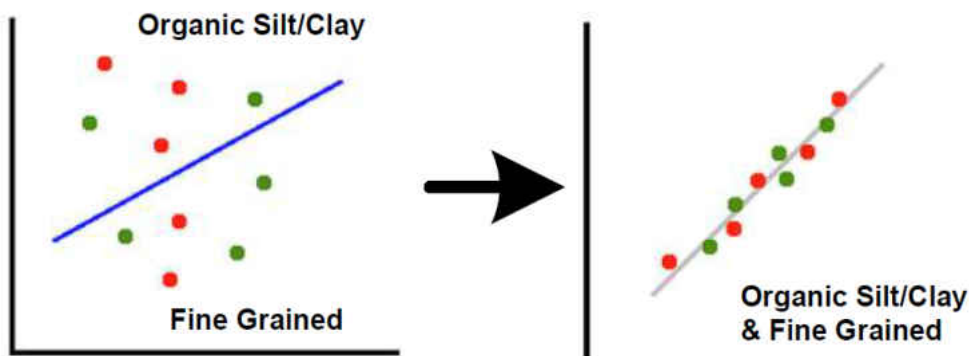


Figure 10: Hyperplane Generation for Organic Silt/Clay and Fine Grained Classes

Once the necessary number of distinct groups of soil has been determined, the corresponding C_c and C_r models are developed for each group.

A regression model is developed for each confirmed distinct group/class. The optimal models are developed through a forward selection stepwise regression procedure. The process begins with no predictors in the corresponding models and progresses by adding predictors, one by one, based on whether or not their addition increases the predictive power of the models. Interactions of predictors are considered as well as higher orders of the predictors in the models that can account for non-linearity. At each step of the procedure the regression model is evaluated based on a term-trusted “goodness of fit” measure.

The developed models are then compared to the ones presented in Table 3. All of the models are evaluated in terms of root mean square error (RMSE) (Levinson, 1946) values, coefficient of determination (R^2) (Nagelkerke, 1991) as well as adjusted coefficient of determination (R^2_{adj}) values (Theil, 1959). The overall predictive modeling framework for C_c and C_r appears in the figure below.

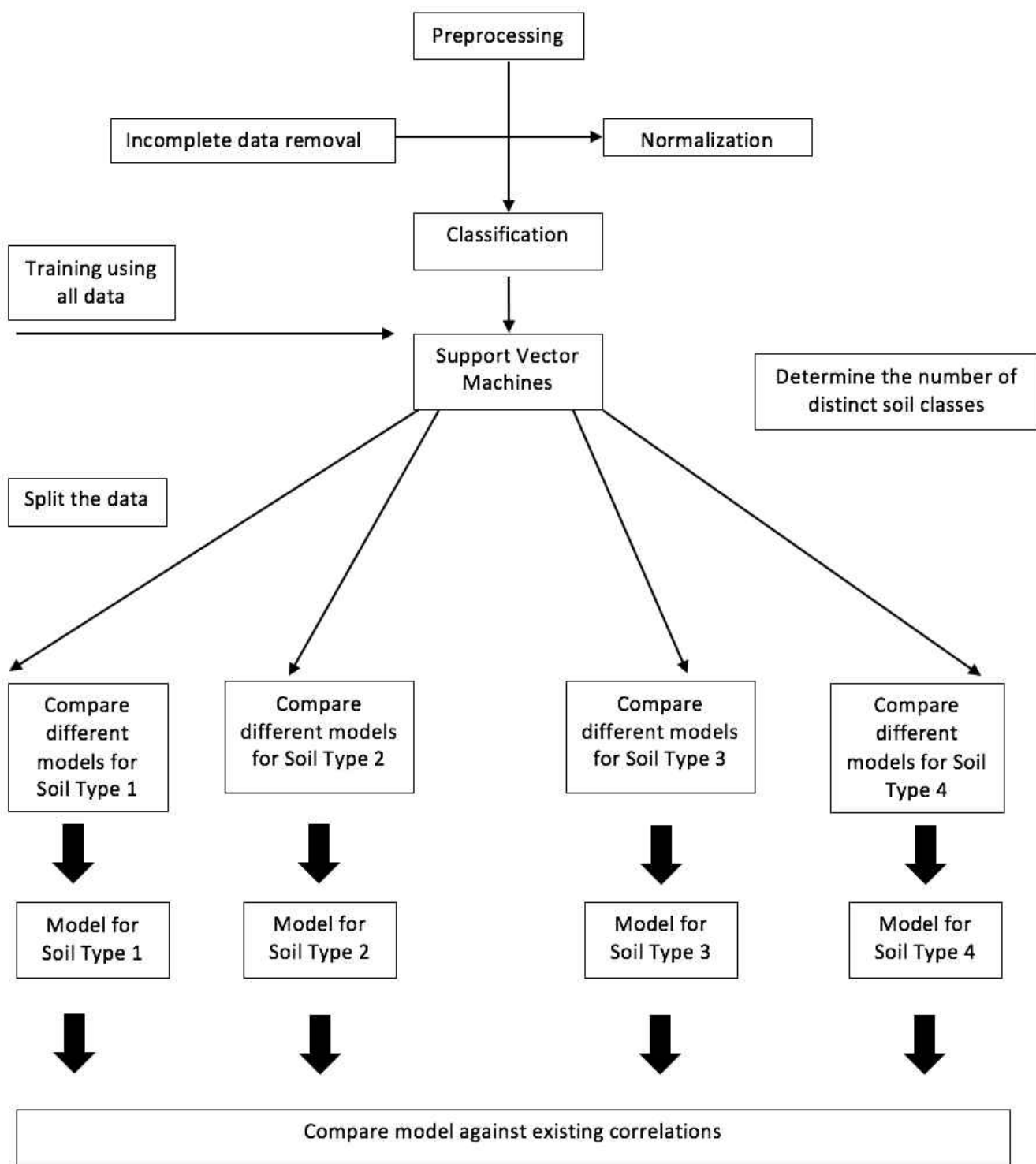


Figure 11: Overall Predictive Modeling Framework for C_c and C_r

The aforementioned framework is implemented in the following sections.

3.3.2 Preprocessing

In this portion of the study, full data sets were segregated from non-full data sets. A full data set includes all pertinent soil descriptors. The descriptors include moisture content (w), initial void ratio (e_0), dry unit weight (γ_{dry}), wet unit weight (γ_{wet}), automatic hammer SPT blow count (N), overburden stress (σ), fines content (-200), liquid limit (LL), plasticity index (PI), and specific gravity (G_s). Many data sets had a variety of soil descriptors missing from their profile. For simplification purposes, and abundance of full data sets, the non-full data sets were not included as part of the study.

Data is first normalized through z-score normalization. This process incorporates the means and standard deviations along the columns of the data matrix. This method preserves the range and the geometry of the data while offering a way to compare observations that have different units and are measured in different scale. Each soil classification has a unique dimensionality due to a varying number of full data sets.

3.3.3 Classification

In this stage, a classification model is developed that assists in determining the number of distinct groups of soil that exist, for classification purposes. Through this process, the goal is to confirm or reject the hypothesis that each soil type requires a different statistical model. If the hypothesis is confirmed, a specific model is then developed for each soil type. The data is

divided into two sets: the training set and the testing set. The training set is comprised of data used to teach the supervised learning algorithm, while the testing set will remain a set of unclassified data that will be used to evaluate the accuracy and predictive ability of the trained algorithm. Moreover, it will help determine the count of distinct groups that the data forms in the next steps.

The classification model is a One-Versus-All approach of Support Vector Machines. The classification performance is evaluated using five-fold cross validation: all experiments are conducted with 80/20 split on data, where 80% of the data is randomly selected for training the classification model and the remaining 20% is used to test its performance (Kohavi 1995). SVMs are implemented using LIBSVM (Chang, 2011) in MATLAB (Guide, 1998). Experiments are performed with a Haswell 2.60 GHz Intel Core i5 CPU running OS X with 8.0 GB of RAM.

The table below depicts the resulting contingency table (confusion matrix) which illustrates the performance of actual versus predicted classes based on the classifications derived from the testing data set. This matrix is used as a tool to evaluate how well the classifier performed. The table contains the numerical counts for each grouping, from the testing data set. The assumed classifications are contained within the rows, while the predicted classifications are contained within the columns. Ideally, there would be a diagonal line from top left to bottom right, which would house the testing data.

Table 4: Confusion Matrix

		Predicted Class			
		Coarse Grained	Fine Grained	Organic Peat	Organic Silt/Clay
Actual Class	Coarse Grained	11	1	1	-
	Fine Grained	1	44	-	1
	Organic Peat	-	-	12	1
	Organic Silt/Clay	-	7	1	3

As can be observed from the table above, the assumed classifications were confirmed by the testing data, with the exception of Organic Silt/Clay. The testing data predicted that this classification behaved more like Fine Grained soil. A group of samples will need a distinct statistical model if the proportion of the correctly classified samples exceeds the 77% threshold. The null and alternative hypotheses have been set to $H_0: p=.77$ and $H_a: p>.77$. The level of significance is chosen to be $\alpha = 0.05$. The corresponding p-values for the four assumed classifications are: $p_{\text{Coarse Grained}} = 0.04$, $p_{\text{Fine Grained}} \approx 0$, $p_{\text{Organic Peat}} \approx 0$ and, $p_{\text{Organic Silt/Clay}} \approx 1$. Therefore, at the selected alpha level we may reject the null hypothesis for the Coarse Grained, Fine Grained and Organic Peat groups of samples. A distinct statistical model should be developed for each of these groups of samples. However, for the Organic Silt/Clay the null hypothesis is rejected.

In order to properly classify an Organic Silt/Clay, according to the USCS system, the soil sample must undergo an organic test and a series of Atterberg Limit tests: the first before being oven dried and the second after being oven dried. If the equation below is verified as true, the sample can be classified as Organic Silt/Clay, depending on where the sample falls on the A-line (Das, 2002). If the equation below is not verified as true, the sample will be classified as a silt or clay (fine grained), depending on where the sample falls on the A-line.

$$\frac{LL_{\text{oven dried}}}{LL_{\text{not oven dried}}} < 0.75 \quad (21)$$

The process of identifying a sample as Organic Silt/Clay is time consuming. Often times, engineers will skip this step and instead rely on visual inspection and results from the organic test (Gray, 2016). If the sample has a high organic content, the engineer will label the sample as organic, although the USCS classification system demands the additional testing to use that classification. The results noted in Table 4 indicate that when the engineer used the Organic Silt/Clay classification without enough information, the majority of the time they were incorrect. For this reason, it was determined that only three predictive models would be used for C_c and C_r - those being Coarse Grained, Fine Grained, and Organic Peat, eliminating Organic Silt/Clay. Since the Organic Silt/Clay data set behaved more like Fine Grained, the two data sets were combined.

3.4 Summary

A total of 619 data sets were collected throughout the state of Florida, which included the following soil parameters (fines content (-200), moisture content (w), initial void ratio (e_o), Atterberg limits (LL and PI), SPT automatic hammer blow count (N), specific gravity (G_s), effective overburden pressure (σ'_o), organic content (o), and the wet and dry density). These parameters were used to describe the behavior of an assumed four soil classifications (Coarse Grained, Fine Grained, Organics, and Organic Silt/Clay). These classes were tested through Support Vector Machines, to confirm their existence. A training set of data was used to build the algorithms, while a testing set was used to confirm the presence of each soil type. When the algorithms were tested, it was determined that only three soil classes were evident. The Coarse Grained and Organics were classes were confirmed, while it was determined that the Organic Silt/Clay class behaved more like the Fine Grained class. For this reason, the Fine Grained class absorbed the data for Organic Silt/Clay. The goal going forward is to develop three regression models for C_c and C_r for each distinct soil class. Chapter 3 will highlight each regression model, graphical results, and a comparison of developed correlations to the correlation strength of existing models.

CHAPTER 4: DEVELOPMENT OF SOIL COMPRESSIBILITY PREDICTION MODELS - DATA ANALYSIS AND RESULTS

4.1 Introduction

With three distinct soil classes, in Chapter 4, regression models for each class will be developed. A graphical representation for each model will be presented to identify any anomalies in the data. Other observations and conclusions will be drawn from the results of the regression analysis. Correlational strength will then be identified for each existing correlation. Upon conclusion of this analysis, the correlational strength for the developed correlations will be compared to the correlation strength of correlations from existing literature.

4.2 Regression Models

A regression model was developed with interactions for each distinct group\class (Coarse Grained, Fine Grained, and Organic Peat). Higher order factors were taken into account. The optimal models are developed through a forward selection stepwise regression procedure in SAS JMP (SAS Institute, 2000) which minimizes the term-trusted “goodness of fit” measure Bayesian Information Criterion (BIC) (Claeskens & Hjort, 2008). The variable selection procedure that takes place during the forward selection stepwise regression takes into consideration the correlation coefficients of the participating variables to minimize multicollinearity (Freud & Littell, 2000). At the first step, of the process the initial regression model for every group of samples contains no variables. At each iteration, the present independent variables in the equation are held fixed and only the variable that is the most highly correlated with the response

variable (i.e. C_c/C_r) enters the regression model. This procedure leads to the most parsimonious model while trying to eliminate multicollinearity.

The table below presents the regression models (prediction expressions) that were developed. Strength of correlation parameters, such as root mean square error values, coefficient of determination as well as adjusted coefficient of determination values were noted. A perfect correlation yields an R^2 value of 1.0, and an RMSE value of 0.0. Note that the wet and dry densities (γ_{wet} and γ_{dry}) are in pcf and the fines and natural moisture (w) are in percent.

Table 5: Statistical Strength of Developed Correlations

Equation	Notes	R ²	R ² _{adj}	RMSE
$C_c = -0.146 + 0.001 * \gamma_{wet} - 0.003 * \gamma_{dry} + 0.007 * N + 0.005 * \text{Fines} + 0.373 * e_o - 0.0006 * [(\gamma_{wet} - 115.484) * (N - 6.493)] + 0.001 * [(\gamma_{wet} - 115.484) * (\text{Fines} - 31.584)] + 0.032 * [(\text{Fines} - 31.584) * (e_o - 1.028)] + 0.001 * [(\gamma_{wet} - 115.484) * (\gamma_{wet} - 115.484)] - 0.0003 * [(\gamma_{dry} - 86.024) * (\gamma_{dry} - 86.024)] - 0.0005 * [(N - 6.493) * (N - 6.493)]$	Coarse Grained	0.9079	0.8888	0.1108
<p style="text-align: center;"><u>Reduced Model</u></p> $C_c = 0.759 + 0.0048 * \gamma_{wet} - 0.012 * \gamma_{dry} - 0.002 * N - 0.0012 * e_o - 0.0006 * [(\gamma_{wet} - 115.484) * (\gamma_{wet} - 115.484)]$		0.8308	0.8133	0.1436
$C_c = -0.217 + 0.006 * w + 0.287 * e_o$	Fine Grained	0.6487	0.6462	0.3906
$C_c = 1.272 + 0.006 * w - 0.021 * \text{Fines} + 0.121 * e_o - 0.000009 * [(w - 359.133) * (\text{Fines} - 65.666)] - 0.000985 * [(w - 359.133) * (e_o - 5.543)] + 0.0521 * [(e_o - 5.543) * (e_o - 5.543)]$	Organic Peat	0.7724	0.7480	1.0904
$C_r = 0.0607 + 0.0004 * w - 0.0024 * \text{Fines} + 0.0303 * e_o - 0.00001 * [(w - 359.133) * (\text{Fines} - 65.666)] + 0.00549 * [(e_o - 5.543) * (e_o - 5.543)]$	Organic Peat	0.8101	0.7935	0.1387

Table 5 does not include models generated for C_r for the coarse or fine grained categories. The reason for this is because the models weren't strong enough to report. Upon this finding, it was postulated that the addition of other parameters to the analysis would yield better results. One will note the R² parameters for comparison between Table 5 and Table 6. In Table 5, the R² values for coarse grained (C_c), fine grained (C_c), and organic peat (C_c and C_r) are 0.9079, 0.6487, 0.7724, and 0.8101, respectively.

The models were then updated to include the soil parameters LL (liquid limit), PI (plasticity index), and G_s (specific gravity). As can be seen in Table 6, the addition of these parameters had a positive overall effect on the developed correlations. The R^2 value for the fine grained C_c increased from 0.6487 to 0.6740. Also, the C_r models for coarse and fine grained increased in reliability and are now worthy of reporting, with R^2 values of 0.695 and 0.532, respectively. One will note that LL was added to the strongest models for the coarse and fine grained C_r models. PI was added to the strongest model for the fine grained C_c model, and G_s was added to the strongest model for the fine grained C_r model.

Table 6: Statistical Strength of Developed Correlations

Equation	Notes	R ²	R ² _{adj}	RMSE
$C_c = -0.146 + 0.001 * \gamma_{wet} - 0.003 * \gamma_{dry} + 0.007 * N + 0.005 * \text{Fines} + 0.373 * e_o - 0.0006 * [(\gamma_{wet} - 115.484) * (N - 6.493)] + 0.001 * [(\gamma_{wet} - 115.484) * (\text{Fines} - 31.584)] + 0.032 * [(\text{Fines} - 31.584) * (e_o - 1.028)] + 0.001 * [(\gamma_{wet} - 115.484) * (\gamma_{wet} - 115.484)] - 0.0003 * [(\gamma_{dry} - 86.024) * (\gamma_{dry} - 86.024)] - 0.0005 * [(N - 6.493) * (N - 6.493)]$	Coarse Grained	0.9079	0.8888	0.1108
<p style="text-align: center;"><u>Reduced Model</u></p> $C_c = 0.759 + 0.0048 * \gamma_{wet} - 0.012 * \gamma_{dry} - 0.002 * N - 0.0012 * e_o - 0.0006 * [(\gamma_{wet} - 115.484) * (\gamma_{wet} - 115.484)]$		0.8308	0.8133	0.1436
$C_r = 0.071 + 0.006 * \sigma - 0.0005 * \gamma_{wet} + 0.0004 * N + 0.0002 * \text{Fines} - 0.0001 * LL - 0.0006 * [(\sigma - 1.966) * (\text{Fines} - 32.934)] - 0.00005 * [(\gamma_{wet} - 117.148) * (N - 6.439)] - 0.00003 * [(\gamma_{wet} - 117.148) * (LL - 50.943)] - 0.00001 * [(\gamma_{wet} - 117.148) * (\gamma_{wet} - 117.148)]$		0.695	0.666	0.013
$C_c = -0.296 + 0.001 * PI + 0.485 * e + 0.001 * [(PI - 65.685) * (e - 1.859)]$	Fine Grained	0.6740	0.6700	0.3600
$C_r = -0.276 + 0.003 * \gamma_{dry} + 0.002 * w - 0.0003 * \text{Fines} + 0.0002 * LL - 0.005 * G_s + 0.00005 * [(\gamma_{dry} - 61.171) * (w - 71.207)] + 0.000007 * [(w - 71.207) * (LL - 98.843)] - 0.002 * [(w - 71.207) * (G_s - 2.595)] + 0.004 * [(\text{Fines} - 80.226) * (G_s - 2.595)]$		0.532	0.516	0.058
$C_c = 1.272 + 0.006 * w - 0.021 * \text{Fines} + 0.121 * e_o - 0.000009 * [(w - 359.133) * (\text{Fines} - 65.666)] - 0.000985 * [(w - 359.133) * (e_o - 5.543)] + 0.0521 * [(e_o - 5.543) * (e_o - 5.543)]$	Organic Peat	0.7724	0.7480	1.0904
$C_r = 0.0607 + 0.0004 * w - 0.0024 * \text{Fines} + 0.0303 * e_o - 0.00001 * [(w - 359.133) * (\text{Fines} - 65.666)] + 0.00549 * [(e_o - 5.543) * (e_o - 5.543)]$		0.8101	0.7935	0.1387

The C_c model for the Coarse Grained class is able to explain 91% of the variability of the data. This is the strongest predictive model that was obtained. Its corresponding RMSE value of 0.1108 is the lowest among all the existing correlations in the literature. This confirms that not only is a separate, distinct model necessary for Coarse Grained soils, but also that the generated model is accurate to a high degree. The C_r model has noticeably more variability, but is stronger than the strongest C_r correlations from existing literature, as one will notice further in the study.

The C_c model for the Fine Grained materials, which includes data from the previous Organic Silt/Clay category, is able to explain 67% of the variability of the data while achieving a low RMSE score of 0.360. This is within the same range as other correlations generated in previous literature, per Table 4 (Nishida (1956), Sowers (1970)). Again, the C_r model is markedly weaker and less able to predict the actual C_r for this soil class, but is still on par with the strength of existing C_r models for this soil class.

Two strong models were developed for the Organic Peat class. The C_c model achieves an R^2_{adj} value of 0.772 and a RMSE value of 1.09. The explanatory power of this model is higher than the models found in the literature. The C_r model for the Organic Peat class explains 81% of the variability of the data while achieving a very low RMSE value of 0.1372. This model outperforms the existing correlations for C_r .

Predicted versus Measured Plots as well as the Residual versus Predicted Plots for each soil class can be seen in the following figures.

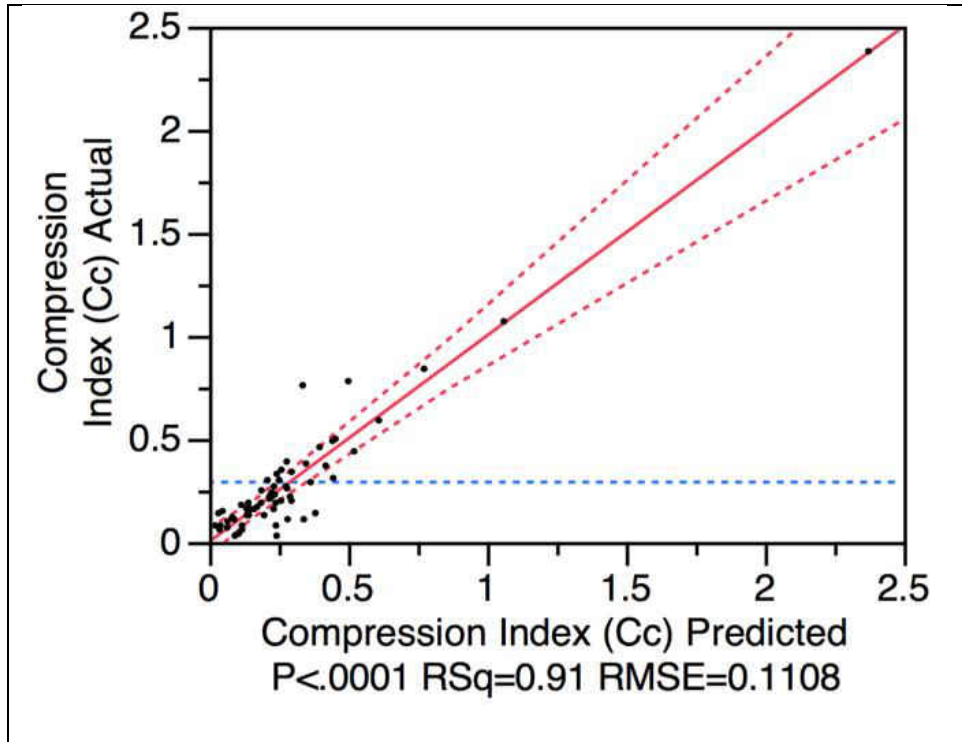


Figure 12: Predicted versus Measured Plot for C_c model of Coarse Grained

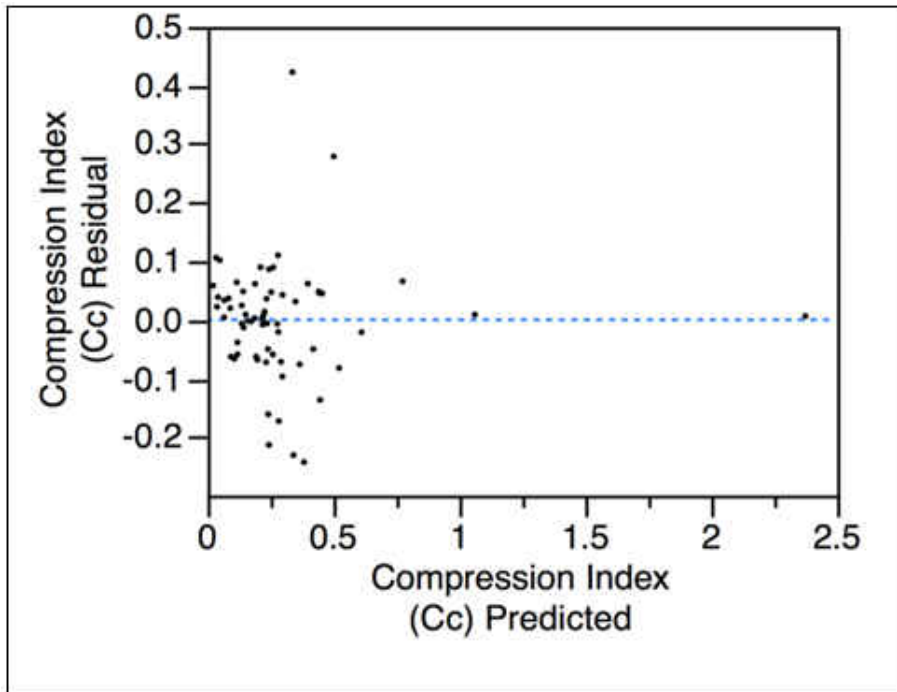


Figure 13: Residual by Predicted Plot for C_c Model of Coarse Grained

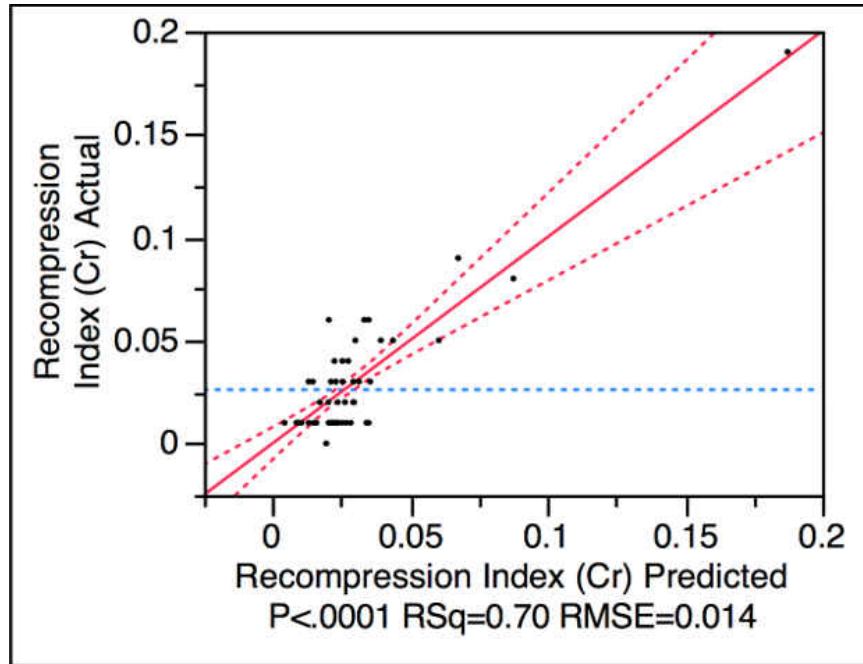


Figure 14: Predicted versus Measured Plot for C_r model of Coarse Grained

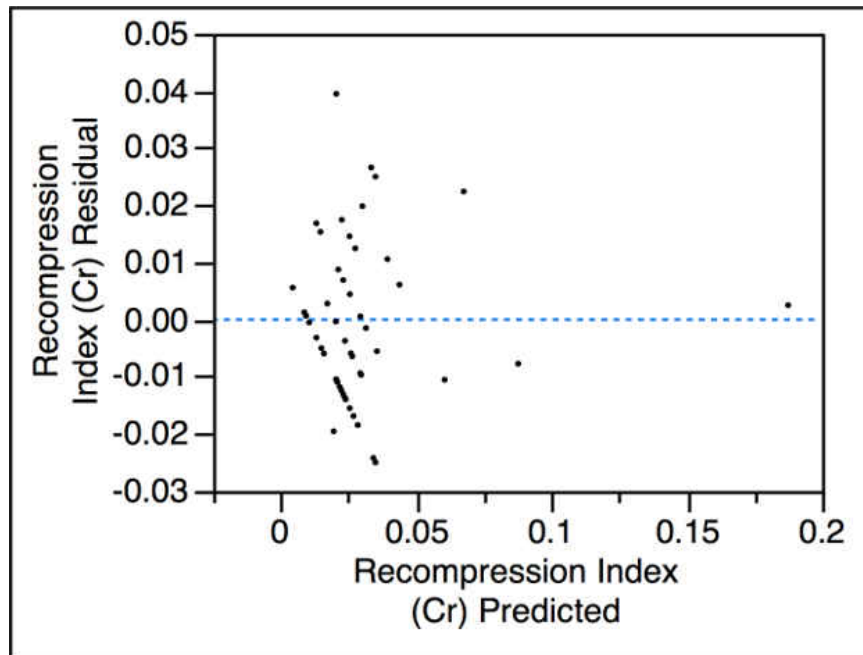


Figure 15: Residual by Predicted Plot for C_r Model of Coarse Grained

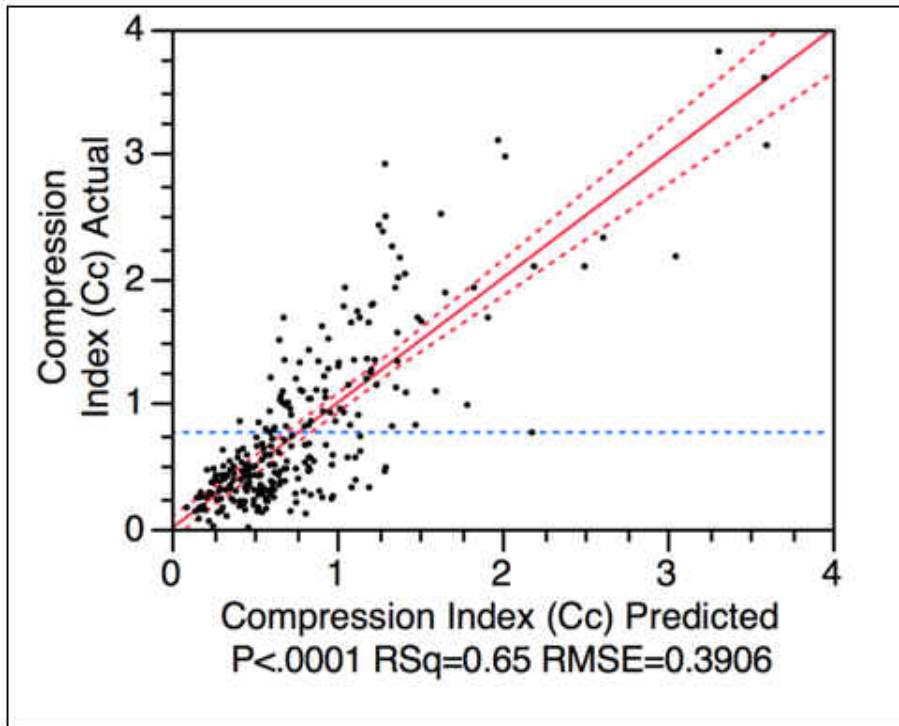


Figure 16: Predicted versus Measured Plot for C_c model of Fine Grained

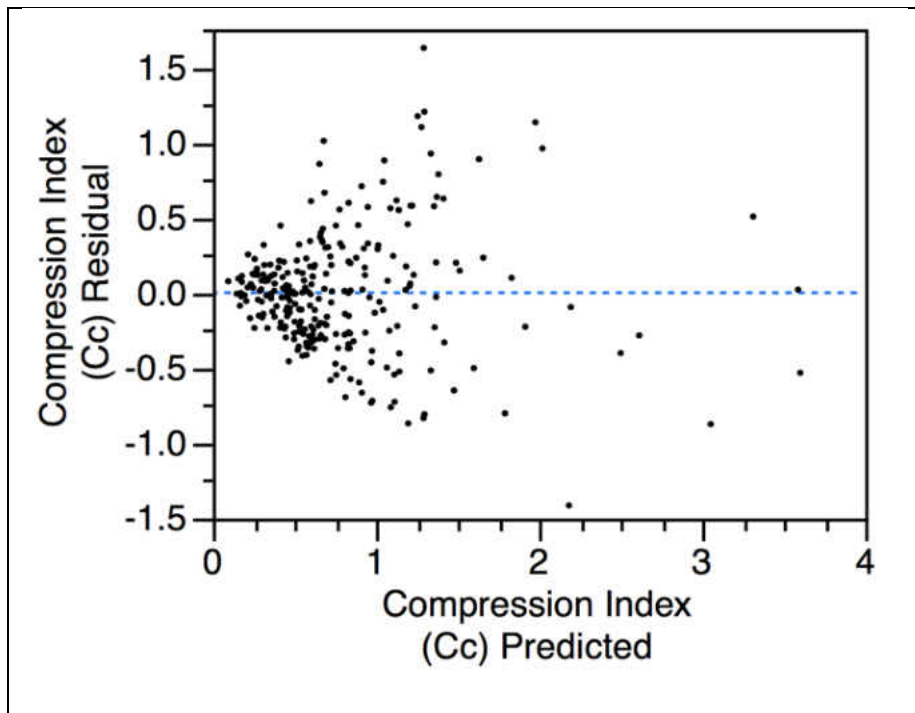


Figure 17: Residual by Predicted Plot for C_c Model of Fine Grained

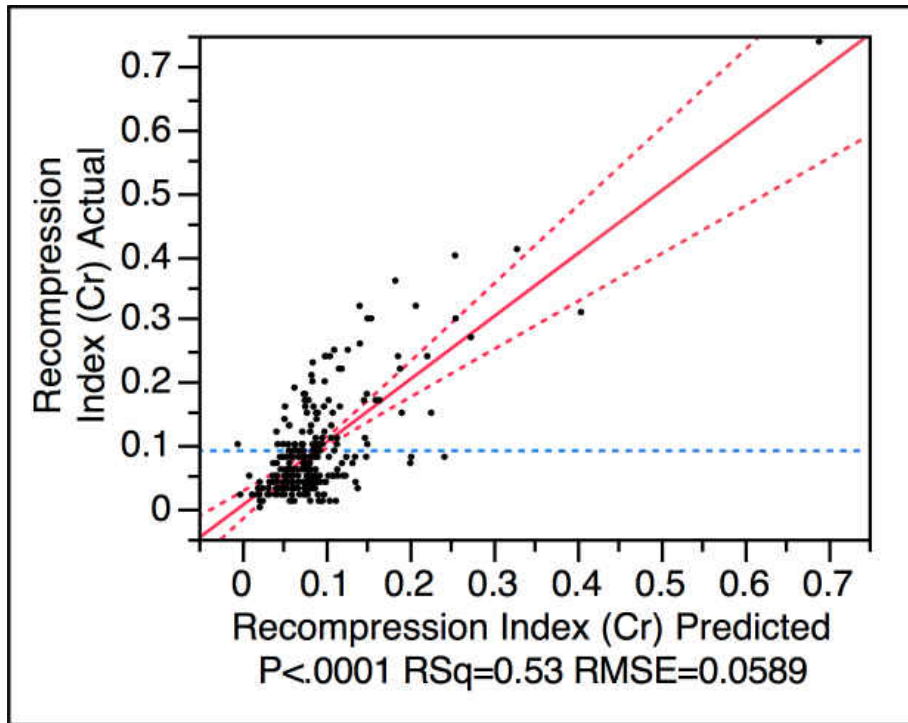


Figure 18: Predicted versus Measured Plot for C_r model of Fine Grained

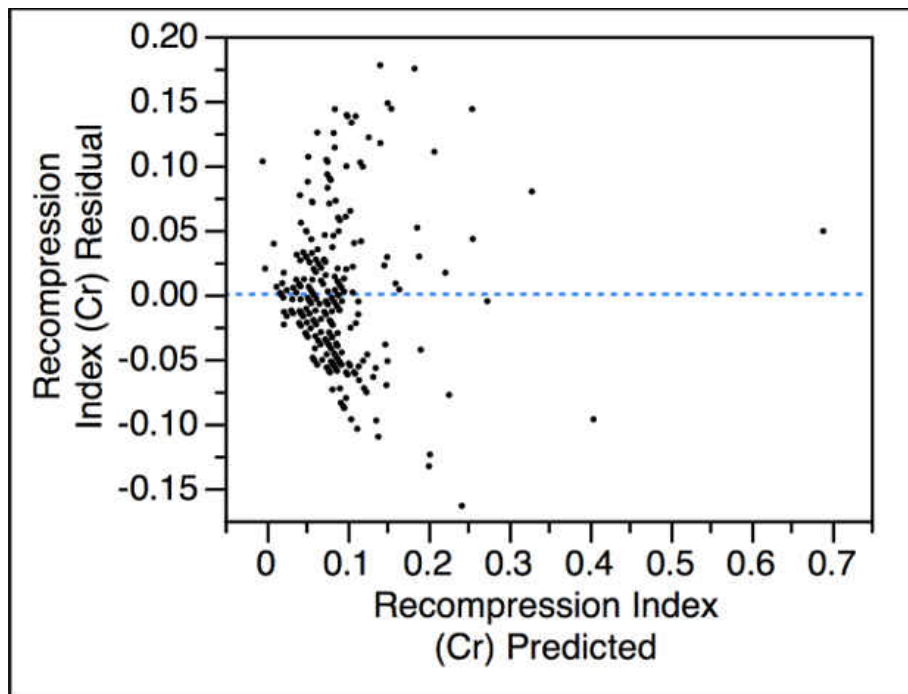


Figure 19: Residual by Predicted Plot for C_r Model of Fine Grained

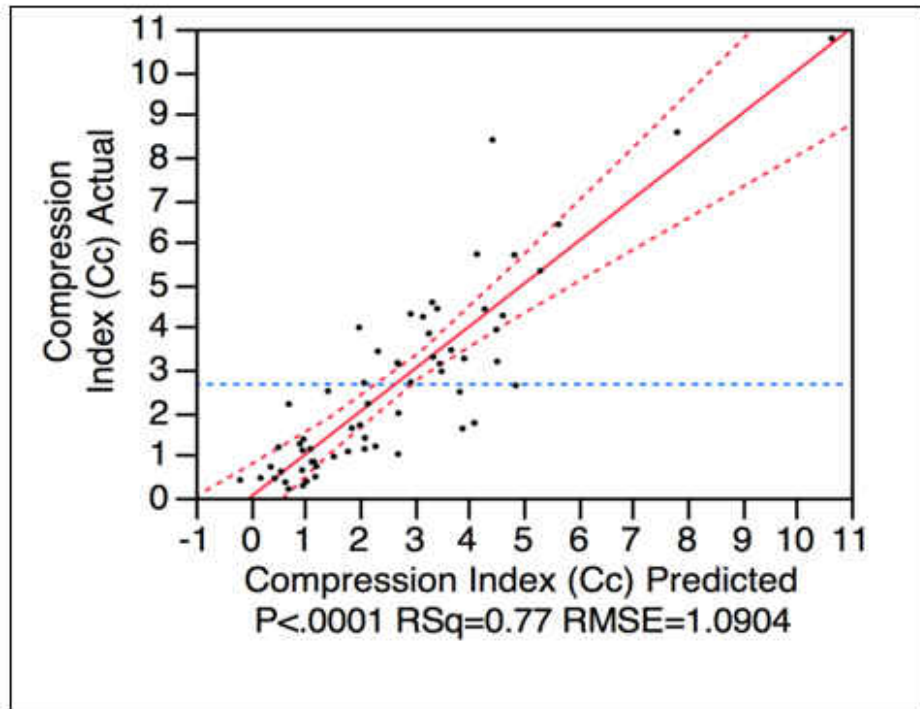


Figure 20: Predicted versus Measured Plot for C_c Model of Organic Peat

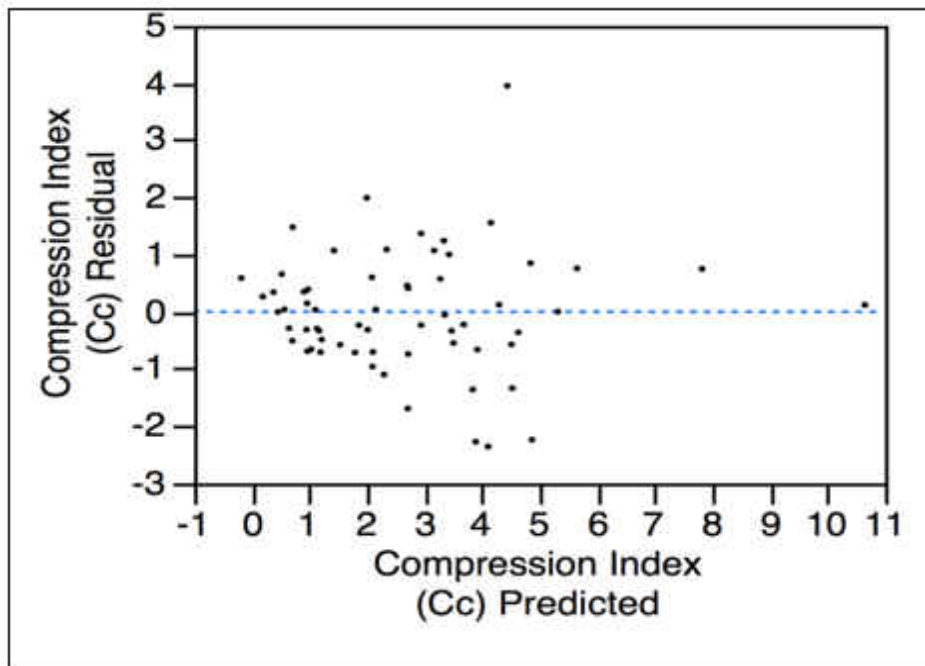


Figure 21: Residual by Predicted Plot for C_c Model of Organic Peat

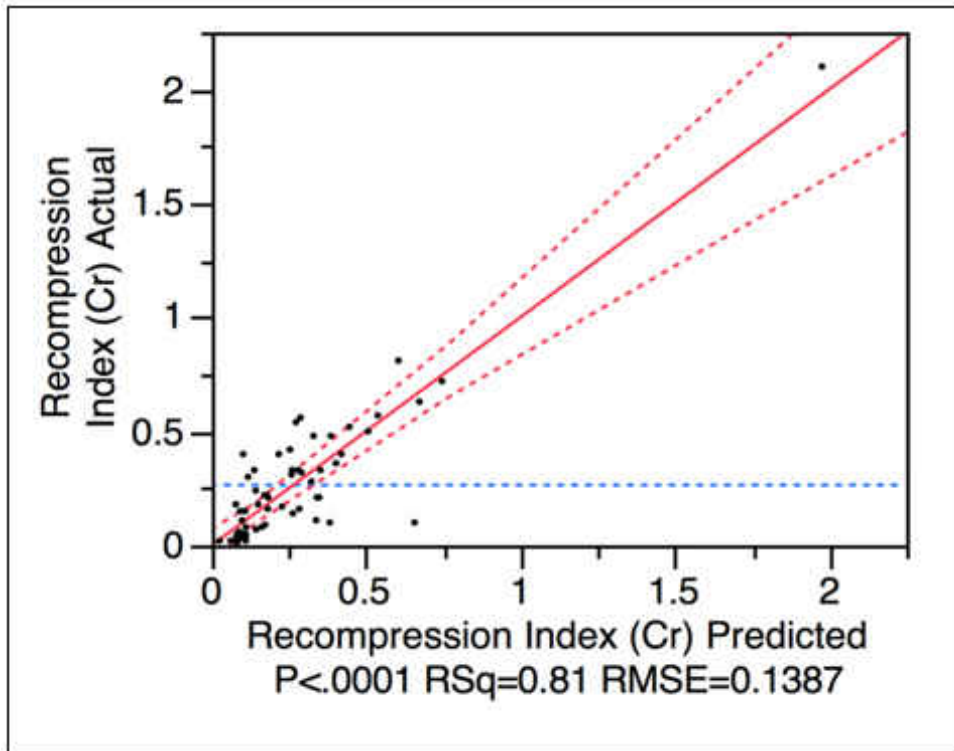


Figure 22: Predicted versus Measured Plot for C_r Model of Organic Peat

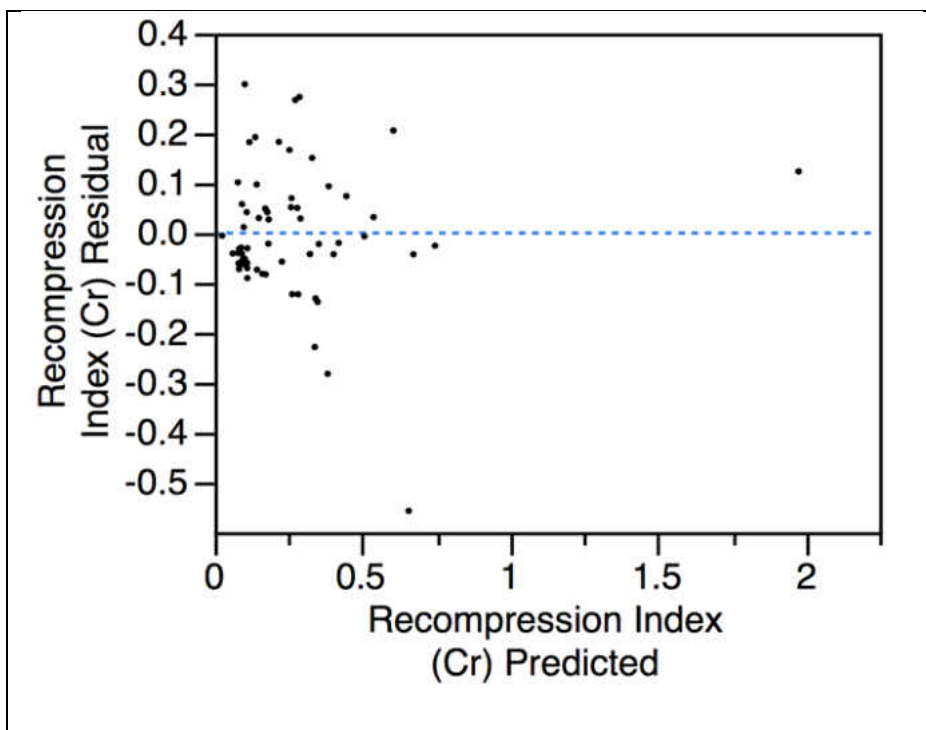


Figure 23: Residual by Predicted Plot for C_r Model of Organic Peat

In the Predicted versus Measured Plots the solid red line is the line of fit and the dashed red curves are the confidence bands for an alpha level set at 5%. The dashed horizontal blue line is set at the mean of the C_c and C_r leverage residuals.

In the Residual versus Predicted Plots, the dashed horizontal blue line is set at zero. The Predicted versus Measured Plot suggests very strong goodness of fit of the C_c model for the Coarse Grained class. The random pattern in the residuals for this class indicate that the predictor variables of the model indeed capture all explanatory information.

The funnel shape that can be observed in the Residual versus Predicted Plot for the C_c model of Fine Grained including Organic Silt/Clay is an indication of non-constant variance. This means that when the predicted C_c is low, relatively speaking, the actual C_c will be either slightly higher or lower. This indicates a small amount of uncertainty. As the predicted C_c gets higher, the actual C_c will vary by a higher degree. This indicates a growing amount of uncertainty, as the predicted C_c rises.

This can be attributed to disturbance of the soil sample during extraction or preparation for testing. As the level of disturbance increases, the remolded strength decreases, and the sensitivity subsequently increases. Sensitivity is a concern for cohesive soils such as silts and clays, where minimal amounts of disturbance can largely effect the strength. The growing uncertainty of this soil classification, for C_c , confirms the ideal that this correlation should be limited to fine grained soils with low sensitivity (Bowles, 1989). This demonstrates one of the limitations of using correlations to quantify the settlement potential of highly compressible soils.

All the points are close to the regressed diagonal line while being minimally dispersed. In addition, there is not a non-random pattern in the residuals. This suggests that the response variable C_c is accurately predicted by the developed model for the Organic Peat class. The predicted values are indeed close to the actual values. The random pattern of the residuals suggests that the developed C_r model for the Organic Peat class is sufficient and any error in the model is of stochastic nature.

Through the analysis, it's evident that separate models for each soil type are needed. The correlations generated having varying degrees of predictive capabilities. The C_c model for Fine Grained (clays and silts) is strong and compares well with existing correlations. It's unfortunate that a reasonable model for C_r could not be obtained. The C_c and C_r models for Coarse Grained (sands) are very strong and in fact are stronger than all the other existing correlations for any soil type, which is an important finding. The C_c and C_r models for the Organic Peat class are also very strong and are indeed considerably stronger than the existing correlations for this soil type, as seen in the table below. The correlations generated also incorporate parameters not seen in existing correlations such as the fines content (-200), automatic hammer blow count (N), and the interactions between the wet and dry density (γ_{wet} and γ_{dry}). This confirms that the addition of parameters to the generation of soil compressibility models has the potential to increase their predictive capability, not detract from it.

4.3 Comparison of Existing Correlations

The focus of this study is to find the best predictors for C_c and C_r . The strength of existing correlations was analyzed for comparison to the previous findings. The coefficient of determination (R^2) and the root mean squared error (RMSE) were used to evaluate the strength of the existing correlations, with respect to the data that was gathered for the various soil types. The predicted C_c and C_r was compared to the measured C_c and C_r . As previously stated, a perfect correlation yields an R^2 value of 1.0, and an RSME value of 0.0. The table below represents a summary of these statistical values for the strength of the various existing correlations, based on the data collected.

Table 7: Statistical Strength of Existing Correlations

Equation	Reference	Notes	R^2	RMSE
$C_c = 0.01w - 0.05$	Azzouz (1976)	All soils	0.7448	0.8359
$C_c = 0.01w$	Koppula (1981)	Clays	0.5202	0.4191
$C_c = 0.01w - 0.075$	Herrero (1983)	Clays	0.5189	0.4336
$C_c = 0.013w - 0.115$	Park, Lee (2011)	Clays	0.6729	0.3953
$C_c = 0.0075w$	Miyakawa (1960)	Peat	0.5784	1.5194
$C_c = 0.011w$	Cook (1956)	Peat	0.6611	1.9601
$C_c = 0.54e - 0.19$	Nishida (1956)	Clays	0.7236	0.3945
$C_c = 0.43e - 0.11$	Cozzolino (1961)	Clays	0.6120	0.4046
$C_c = 0.75e - 0.38$	Sowers (1970)	Clays	0.7362	0.5552
$C_c = 0.49e - 0.11$	Park, Lee (2011)	Clays	0.6847	0.3924
$C_c = 0.4(e - 0.25)$	Azzouz (1976)	All soils	0.5676	0.7501
$C_c = 0.15e + 0.01077$	Bowles (1989)	Clays	0.3157	0.7536

Equation	Reference	Notes	R ²	RMSE
$C_c = 0.287e - 0.015$	Ahadiyan (2008)	Clays	0.3847	0.7692
$C_c = 0.6e$	Sowers (1970)	Peat	0.6715	1.7876
$C_c = 0.3(e-0.27)$	Hough (1957)	Clays	0.4081	0.5425
$C_c = 0.006(LL - 9)$	Azzouz (1976)	Clays	0.2857	0.6213
$C_c = (LL-13)/109$	Mayne (1980)	Clays	0.4323	0.5638
$C_c = 0.009(LL - 10)$	Terzaghi, Peck (1967)	Clays	0.4236	0.5641
$C_c = 0.014LL - 0.168$	Park, Lee (2011)	Clays	0.5569	0.7921
$C_c = 0.0046(LL-9)$	Bowles (1989)	Clays	0.2780	0.6989
$C_c = 0.011(LL-16)$	McClelland (1967)	Clays	0.5094	0.5991
$C_c = 0.009w + 0.005LL$	Koppula (1981)	Clays	0.5701	0.5518
$C_c = 0.009w + 0.002LL - 0.01$	Azzouz (1976)	Clays	0.5866	0.4875
$C_c = 0.141G_s^{1.2} * ((1+e)/G_s)^{2.38}$	Herrero (1983)	Fine Grained	0.7217	0.4992
$C_c = 0.0023 * LL * G_s$	Nagaraj, Murthy (1986)	Clays	0.2111	0.5212
$C_c = 0.2343 * w * G_s$	Nagaraj, Murthy (1985)	Clays	0.3229	0.5373
$C_c = 0.4(e + 0.001w - 0.25)$	Azzouz (1976)	All soils	0.7057	0.7414
$C_c = -0.156 + 0.411e - 0.00058LL$	Al-Khafaji, Andersland (1992)	Clays	0.5276	0.3881
$C_c = 0.141 * G_s * (\gamma_{wet}/\gamma_{dry})^{12/5}$	Al-Khafaji, Andersland (1992)	Clays	0.6439	0.8965
$C_c = -0.023 + 0.271e + 0.001LL$	Ahadiyan (2008)	Clays	0.3400	0.4597
$C_c = 0.37(e + 0.003LL +).0004w - 0.34)$	Azzouz (1976)	Clays	0.5014	0.3888
$C_c = -0.404 + 0.341e + 0.006w + 0.004LL$	Yoon, Kim (2006)	Clays	0.6805	0.4991
$C_c = 0.1597(w^{-0.0187})_{0.8276}(1 + e)^{1.592}(LL^{-0.0638})(\gamma_{dry}^{-0.8276})$	Ozer (2008)	Clays	0.6824	0.5886
$C_c = 0.151 + 0.001225w + 0.193e - 0.000258LL - 0.0699\gamma_{dry}$	Ozer (2008)	Clays	0.3006	0.5204
$C_r = 0.156e + 0.0107$	Elnaggar, Krizek (1971)	Clays	0.5330	0.2536
$C_r = 0.208e + 0.0083$	Peck, Reed (1954)	Clays	0.5419	0.3643
$C_r = 0.14(e+0.007)$	Azzouz (1976)	All soils	0.6016	0.3369

Equation	Reference	Notes	R ²	RMSE
$C_r = 0.003(w + 7)$	Azzouz (1976)	All soils	0.5780	0.4415
$C_r = 0.002(LL + 9)$	Azzouz (1976)	All soils	0.5485	0.1682
$C_r = 0.142(e - 0.009w + 0.006)$	Azzouz (1976)	All soils	0.6089	0.1802
$C_r = 0.003w + 0.0006LL + 0.004$	Azzouz (1976)	All soils	0.5674	0.2344
$C_r = 0.126(e + 0.003LL - 0.06)$	Azzouz (1976)	All soils	0.5808	0.2109
$C_r = 0.135(e + 0.1LL - 0.002w - 0.06)$	Azzouz (1976)	All soils	0.5548	0.3131
$C_r = 0.000463*LL*G_s$	Nagaraj, Murthy (1985)	Clays	0.3418	0.0862

The following observations can be drawn from the generated correlations:

1. Existing correlations for C_c and C_r were gathered for a variety of different soil types and regions throughout the world. The predictive ability of these correlations were tested, based on soil samples collected throughout the State of Florida. Based on this analysis, it was determined that the Azzouz (1976) correlation for all soils (moisture content), the Nishida (1956) correlation for clay (void ratio), and the Herrero (1983) correlation for clay (void ratio and specific gravity) were the strongest, from previous literature.
2. When new correlations were created, it was determined that three distinct soil classes are evident, these being Coarse Grained, Fine Grained, and Organic Peat. Each soil class has a separate model for predictive ability for C_c and C_r .
3. The model for the Coarse Grained classification performs very well, with respect to C_c , which is an important observation considering the dearth of previous correlations generated for this classification and the abundance of this soil type in the State of Florida, per Figure 1.

4. The model for the Fine Grained classification absorbed the data from the Organic Silt/Clay classification. When including all representative data for this class, it was determined that the predictive capability for C_c is comparable to the strength of existing correlations.
5. The model for the Organic Peat classification performed considerably better than that of existing correlations, with respect to both C_c and C_r . This observation is especially critical for settlement predictions in the southern portion of the State of Florida, where wetlands are widespread.
6. The correlations generated incorporate several factors not utilized in correlations from previous literature. These factors include the fines content (-200), plasticity index (PI), and the interactions between the wet and dry density (γ_{wet} and γ_{dry}).

Correlations are a useful tool to make preliminary predictions of settlements, but should not be relied upon with any degree of accuracy for a final design. Only correlations that have been developed using site-specific laboratory consolidation test data should be relied upon (Sabatini et al., 2002). Evidence suggests that the soil structure, geological history, and other factors strongly influence the compression index, and for this reason any correlation used should be with caution (Bowles, 1989).

4.4 Identification of Influential Parameters

With the abundance of soil parameters included in the study, and the noticeable absence of some of them in the Fine Grained and Organic models (i.e. overburden stress, automatic hammer blow count, etc.), it is evident that some parameters have more influence on C_c and C_r

than others. This has been hypothesized in previous studies, but the concept has been mostly untested. Table 8 outlines influential factors from previous studies.

Table 8: Existing Delineational Models for Soil Compressibility

Correlation	Applicability	Influential Factor	Source
$C_c = 0.75e - 0.38$	Soils w/low plasticity	e	Sowers (1970)
$C_c = 0.006*(LL-9)$	Clays (LL<100)	LL	Azzouz (1976)

As can be determined from these correlations, they were developed in an attempt to delineate soil classes using a certain influential parameter. How this influential parameter was identified is uncertain. It's fair to assume that soils with high plasticity, as is the case for the Sowers correlation, would be treated with a different model for soil compressibility. The same can be said about the Azzouz correlation for clays above 100. During their study, there must have been a noticeable behavior change when this dividing line was crossed.

With the updated correlations generated for compressibility indexes, a separate analysis will now be performed to determine influential factors for each respective class. Data analysis begins with the evaluation of the relationships between key index parameters and soil compressibility (C_c and C_r). The key index parameters that were examined include effective overburden pressure (ksf), wet density (pcf), dry density (pcf), natural moisture (%), automatic hammer blow count, fines (-200) (%), liquid limit (LL), plasticity index (PI), initial void ratio (e), and specific gravity (G_s).

The data was split into five categories. The first three are identical to the soil classifications derived from the previous study – Coarse Grained, Fine Grained, and Organics. In the last two categories, the Fine Grained class was split into clays and silts. This was done for two reasons, the first being an abundance of data, particularly for clays, and the second being the majority of existing correlations for compressibility indexes are for fine grained materials. When fine grained materials were more closely analyzed, there was a tendency to focus on clays, due to its highly compressible nature. For this reason, it was decided to split clays out for more detailed analysis of influential parameters and determine if a delineational model exists. Since clays were being split out, it was decided to perform the same operation for silts, due to this category being largely unstudied.

A Pearson's Correlation Coefficient analysis was implemented to identify "better" performing parameters in the prediction of C_c and C_r of a specific soil (Lee Rodgers et al., 1988). A high (positive) correlation coefficient indicates that there is a strong, directly proportional, relationship between key index parameters and soil compressibility (C_c and C_r). Such a relationship implies that as an index parameter increases, the C_c and C_r will increase as well. On the contrary, a low (negative) correlation coefficient indicates that there is a strong, inversely proportional, relationship between key index parameters and soil compressibility (C_c and C_r). Such a relationship indicates that as an index parameter increases, the C_c and C_r will decrease and vice versa. Thusly, the closer the Pearson's Correlation Coefficient is to 1 or -1, the more influence it will have on the outcome of the compressibility index. The closer it is to zero, the less likely it is to have any influence at all.

Coefficient of Determination and Root Mean Square Error values were calculated to quantify the performance level of the key index parameters. The results appear in tables below. The rows highlighted in light red illustrate the top three negative Pearson's Correlation Coefficient, and the rows highlighted in light blue illustrate the top three positive Pearson's Correlation Coefficient.

Table 9: Silts: Pearson's Correlation Coefficient for C_c

Soil Type	Compressibility Index	Parameter	Pearson's Correlation Coefficient	R^2	RMSE
Silts	C_c	Effective Overburden Pressure (ksf)	0.0566	0.0032	0.8855
		Wet Density (pcf)	-0.5679	0.3225	0.7300
		Dry Density (pcf)	-0.6111	0.3734	0.7021
		Natural Moisture (%)	0.7388	0.5458	0.5977
		Automatic Hammer Blow Count	-0.0566	0.0032	0.8855
		Fines (-200) (%)	-0.6704	0.4495	0.6580
		Liquid Limit (LL)	0.7469	0.5578	0.5897
		Plasticity Index (PI)	0.7347	0.5398	0.6016
		Initial Void Ratio (e)	0.5699	0.3248	0.7287
		Specific Gravity (G_s)	-0.7154	0.5118	0.6196

Table 10: Silts: Pearson's Correlation Coefficient for C_r

Soil Type	Compressibility Index	Parameter	Pearson's Correlation Coefficient	R^2	RMSE
Silts	C_r	Effective Overburden Pressure (ksf)	0.0039	0.0001	0.1974
		Wet Density (pcf)	-0.5505	0.3031	0.1648
		Dry Density (pcf)	-0.5752	0.3308	0.1615
		Natural Moisture (%)	0.7176	0.5150	0.1375
		Automatic Hammer Blow Count	-0.2678	0.0717	0.1902
		Fines (-200) (%)	-0.6351	0.4034	0.1525
		Liquid Limit (LL)	0.6159	0.3793	0.1555
		Plasticity Index (PI)	0.6336	0.4014	0.1527
		Initial Void Ratio (e)	0.5380	0.2894	0.1664
		Specific Gravity (G_s)	-0.7426	0.5514	0.1322

As illustrated in the tables above, w , LL, and PI are the strongest positive factors with respect to both C_c and C_r , for the Silts classification. The strongest negative factors are also the same for the Silts classification, with respect to both C_c and C_r . The factors are γ_{dry} , fines content, and G_s .

Table 11: Fine Grained: Pearson's Correlation Coefficient for C_c

Soil Type	Compressibility Index	Parameter	Pearson's Correlation Coefficient	R^2	RMSE
Fine Grained	C_c	Effective Overburden Pressure (ksf)	0.0510	0.0026	0.6212
		Wet Density (pcf)	-0.6288	0.3954	0.4836
		Dry Density (pcf)	-0.6888	0.4744	0.4509
		Natural Moisture (%)	0.7645	0.5845	0.4009
		Automatic Hammer Blow Count	-0.2349	0.0552	0.6046
		Fines (-200) (%)	-0.0566	0.0032	0.6210
		Liquid Limit (LL)	0.5332	0.2843	0.5262
		Plasticity Index (PI)	0.4542	0.2063	0.5541
		Initial Void Ratio (e)	0.7641	0.5838	0.4012
		Specific Gravity (G_s)	-0.0748	0.0056	0.6203

Table 12: Fine Grained: Pearson's Correlation Coefficient for C_r

Soil Type	Compressibility Index	Parameter	Pearson's Correlation Coefficient	R^2	RMSE
Fine Grained	C_r	Effective Overburden Pressure (ksf)	-0.0656	0.0043	0.0847
		Wet Density (pcf)	-0.4260	0.1815	0.0768
		Dry Density (pcf)	-0.4764	0.2270	0.0746
		Natural Moisture (%)	0.5762	0.3320	0.0694
		Automatic Hammer Blow Count	-0.1311	0.0172	0.0841
		Fines (-200) (%)	-0.0616	0.0088	0.0847
		Liquid Limit (LL)	0.4906	0.2407	0.0740
		Plasticity Index (PI)	0.3947	0.1558	0.0780
		Initial Void Ratio (e)	0.5236	0.2742	0.0723
		Specific Gravity (G_s)	-0.1292	0.0167	0.0842

Illustrated in Table 8 and Table 9, w , LL, and e are the strongest positive factors with respect to both C_c and C_r , for the Fine Grained classification. The strongest negative factors are also the same for the Fine Grained classification, with respect to both C_c and C_r . The factors are γ_{wet} , γ_{dry} , and N .

Table 13: Clays: Pearson's Correlation Coefficient for C_c

Soil Type	Compressibility Index	Parameter	Pearson's Correlation Coefficient	R^2	RMSE
Clays	C_c	Effective Overburden Pressure (ksf)	0.0693	0.0048	0.5981
		Wet Density (pcf)	-0.6266	0.3926	0.4673
		Dry Density (pcf)	-0.6912	0.4778	0.4332
		Natural Moisture (%)	0.7725	0.5967	0.3807
		Automatic Hammer Blow Count	-0.2396	0.0574	0.5821
		Fines (-200) (%)	0.1679	0.0282	0.591
		Liquid Limit (LL)	0.5132	0.2634	0.5146
		Plasticity Index (PI)	0.4366	0.1906	0.5394
		Initial Void Ratio (e)	0.7913	0.6262	0.3666
		Specific Gravity (G_s)	-0.0063	0.00004	0.5996

Table 14: Clays: Pearson's Correlation Coefficient for C_r

Soil Type	Compressibility Index	Parameter	Pearson's Correlation Coefficient	R ²	RMSE
Clays	C_r	Effective Overburden Pressure (ksf)	-0.0500	0.0025	0.0711
		Wet Density (pcf)	-0.3965	0.1572	0.0653
		Dry Density (pcf)	-0.4589	0.2106	0.0632
		Natural Moisture (%)	0.4999	0.2499	0.0616
		Automatic Hammer Blow Count	-0.1086	0.0118	0.0708
		Fines (-200) (%)	0.1049	0.011	0.0708
		Liquid Limit (LL)	0.5007	0.2507	0.0616
		Plasticity Index (PI)	0.3953	0.1563	0.0654
		Initial Void Ratio (e)	0.4893	0.2394	0.0621
		Specific Gravity (G_s)	-0.0141	0.0002	0.0712

Illustrated in tables above, w , LL, and e are the strongest positive factors with respect to both C_c and C_r , for the Clay classification. The strongest negative factors are also the same for the Clay classification, with respect to both C_c and C_r . The factors are γ_{wet} , γ_{dry} , and N . These are the same influential factors for the Fine Grained classification, which would be expected due to this classification being predominantly clays.

Table 15: Organics: Pearson's Correlation Coefficient for C_c

Soil Type	Compressibility Index	Parameter	Pearson's Correlation Coefficient	R^2	RMSE
Organics	C_c	Effective Overburden Pressure (ksf)	-0.2610	0.0681	2.1162
		Wet Density (pcf)	-0.3743	0.1401	2.0328
		Dry Density (pcf)	-0.6022	0.3626	1.7501
		Natural Moisture (%)	0.7062	0.4987	1.5521
		Automatic Hammer Blow Count	-0.1625	0.0264	2.1631
		Fines (-200) (%)	-0.1865	0.0348	2.1537
		Organic Content (%)	0.4358	0.1899	1.9731
		Initial Void Ratio (e)	0.7162	0.5129	1.5299
		Specific Gravity (G_s)	-0.1967	0.0387	2.1493

Table 16: Organics: Pearson's Correlation Coefficient for C_r

Soil Type	Compressibility Index	Parameter	Pearson's Correlation Coefficient	R^2	RMSE
Organics	C_r	Effective Overburden Pressure (ksf)	-0.2218	0.0492	0.297
		Wet Density (pcf)	-0.2726	0.0743	0.293
		Dry Density (pcf)	-0.4668	0.2179	0.2694
		Natural Moisture (%)	0.5412	0.2929	0.2561
		Automatic Hammer Blow Count	-0.1819	0.0331	0.2995
		Fines (-200) (%)	-0.1811	0.0328	0.2995
		Organic Content (%)	0.2546	0.0648	0.2945
		Initial Void Ratio (e)	0.8230	0.6774	0.173
		Specific Gravity (G_s)	-0.0071	0.00005	0.3046

Illustrated in tables above, w, o, and e are the strongest positive factors with respect to both C_c and C_r , for the Organic classification. The strongest negative factors are also the same for the Organic classification, with respect to both C_c and C_r . The factors are γ_{wet} , γ_{dry} , and effective overburden pressure.

Table 17: Coarse Grained: Pearson's Correlation Coefficient for C_c

Soil Type	Compressibility Index	Parameter	Pearson's Correlation Coefficient	R^2	RMSE
Coarse Grained	C_c	Effective Overburden Pressure (ksf)	0.0872	0.0076	0.2980
		Wet Density (pcf)	-0.7348	0.5400	0.2029
		Dry Density (pcf)	-0.7664	0.5874	0.1921
		Natural Moisture (%)	0.8854	0.7839	0.1390
		Automatic Hammer Blow Count	-0.0911	0.0083	0.2979
		Fines (-200) (%)	0.0678	0.0046	0.2984
		Liquid Limit	0.7276	0.5294	0.2052
		Plasticity Index	0.5549	0.3079	0.2488
		Initial Void Ratio (e)	0.8592	0.7383	0.1530
		Specific Gravity (G_s)	-0.2706	0.0732	0.2879

Table 18: Coarse Grained: Pearson's Correlation Coefficient for C_r

Soil Type	Compressibility Index	Parameter	Pearson's Correlation Coefficient	R^2	RMSE
Coarse Grained	C_r	Effective Overburden Pressure (ksf)	0.1300	0.01690	0.0241
		Wet Density (pcf)	-0.5958	0.3550	0.0195
		Dry Density (pcf)	-0.5695	0.3243	0.0200
		Natural Moisture (%)	0.6914	0.4781	0.0176
		Automatic Hammer Blow Count	0.1095	0.0120	0.0242
		Fines (-200) (%)	0.0063	0.0001	0.0243
		Liquid Limit	0.5332	0.2843	0.5262
		Plasticity Index	0.3838	0.1473	0.0225
		Initial Void Ratio (e)	0.6711	0.4504	0.0180
		Specific Gravity (G_s)	-0.2581	0.0666	0.0235

Illustrated in tables above, w , LL , and e are the strongest positive factors with respect to both C_c and C_r , for the Coarse Grained classification. The strongest negative factors are also the same for the Coarse Grained classification, with respect to both C_c and C_r . The factors are γ_{wet} , γ_{dry} , and G_s .

4.5 Discussions

The following table outlines the results of the influential parameter analysis for compressibility indexes. The influential parameters are listed from highest to lowest influence

on compressibility indexes and include the statistical value of influence in parentheses. Only the top three most positive and negative factors are noted.

Table 19: Influential Parameter Breakdown by Soil Classification

Soil Classification	Positive Factor		Negative Factor	
	C _c	C _r	C _c	C _r
Silts	LL (0.75)	w (0.72)	G _s (-0.72)	G _s (-0.74)
	w (0.74)	PI (0.63)	-200 (-0.67)	-200 (-0.63)
	PI (0.74)	LL (0.62)	γ _{dry} (-0.61)	γ _{dry} (-0.58)
Fine Grained	w (0.77)	w (0.58)	γ _{dry} (-0.69)	γ _{dry} (-0.48)
	e (0.76)	e (0.52)	γ _{wet} (-0.63)	γ _{wet} (-0.43)
	LL (0.53)	LL (0.49)	N (-0.23)	N (-0.13)
Clay	e (0.79)	LL (0.50)	γ _{dry} (-0.69)	γ _{dry} (-0.46)
	w (0.77)	w (0.50)	γ _{wet} (-0.63)	γ _{wet} (-0.40)
	LL (0.51)	e (0.49)	N (-0.24)	N (-0.11)
Organic	e (0.72)	e (0.82)	γ _{dry} (-0.60)	γ _{dry} (-0.47)
	w (0.71)	w (0.54)	γ _{wet} (-0.37)	γ _{wet} (-0.27)
	o (0.44)	o (0.25)	σ (-0.26)	σ (-0.22)
Coarse Grained	w (0.89)	w (0.69)	γ _{dry} (-0.77)	γ _{wet} (-0.60)
	e (0.86)	e (0.67)	γ _{wet} (-0.74)	γ _{dry} (-0.57)
	LL (0.73)	LL (0.53)	G _s (-0.27)	G _s (-0.26)

There are several things that can be noted from this analysis. The first is that LL, w, and e, were the most positive influential factors for every category, with the exception of PI for Silts and o for Organics. The most negative influential factors were noticeably less consistent, in regards to inclusion for all soil classifications. The only consistently included negative influential factor is γ_{dry}. In fact, it was the most negative influential factor for four out of the five classifications, with the exception of Silts. γ_{wet} also follows γ_{dry} for each of the same classifications, with respect to most negative influential factor, with the same exception of the

Silts classification. This makes sense as these two parameters are interconnected through a relationship with moisture content (Das, 2002).

Results for the most influential factors typically illustrate Pearson's Correlation Coefficients in the range of 0.60 to 0.70 for the most positive, and -0.60 to -0.70 for most negative for predictions for compressibility index. For C_r , the most influential parameters (both positive and negative) appeared to be of smaller magnitude. This stands to reason, since C_r correlations, developed during this study, are noticeably weaker than C_c correlations. The Pearson's coefficients for the Clays and Silts appear to be on par with the others. This leads one to believe that relatively strong predictions for C_c and C_r , based on developed correlations in the future, could be made.

The strongest Pearson's Correlation Coefficients were for the Coarse Grained classification (0.89 for moisture content and 0.86 for void ratio, both being for C_c) and for the Organic classification (0.82 for void ratio, for C_c). Note that the strongest coefficients were both positive influential factors and were contained in predictions for C_c . In a future study, where delineational models for C_c and C_r are to be examined, these would be good places to start looking for data trends. If such a trend exists, delineational models may be present that would create two separate, distinct models, once a certain threshold is crossed. For example, if $w < 85$, a separate correlation for C_c may be needed than if w is greater than or equal to 85.

Geotechnically speaking, many of these influential factors make sense. For example, as the void ratio goes up, one would expect C_c and C_r to increase proportionally. As the voids in the soil skeleton become greater, so would the soil's propensity to collapse once loaded (Bowles, 1989). The same can be said about the moisture content. The more the soil has a tendency to

hold water, the greater the propensity to expel it once loaded (Hough, 1957). Also, as the wet and dry densities increase, one would expect the soil to be stiffer and more resilient to deformations once loaded (Lambe et al., 1969). All of these phenomena have been statistically endorsed through data analysis. However, one would also expect that the fines content would play a larger part in these compressibility index predictions. As the percentage of smaller particles in the soil skeleton increases, so does the tendency to behave like a cohesive soil (i.e. clay/silt). These soils have a tendency to be sensitive to changes in stress due to its honeycomb composition (Bowles, 1989). Its stability and subsequent ability to compress increases when loaded.

The next noteworthy item worthy of discussion is the inclusion/exclusion of some of the most influential parameters in the developed correlations. This is best illustrated with a summary as noted in the following table. It includes all factors included in the correlation for each classification and also Pearson's Correlation Coefficient in parentheses for that respective parameter.

Table 20: Pearson's Correlation Coefficient of Parameters Included in Compressibility Correlations

Compressibility Index	Soil Classification	Included Parameter in Correlation
C _c	Coarse Grained	σ (0.09)
		γ _{wet} (-0.74)
		γ _{dry} (-0.77)
		w (0.89)
		N (-0.09)
		-200 (0.07)
		LL (0.73)
		PI (0.55)
		e (0.86)
		G _s (-0.27)
	Fine Grained	w (0.77)
		-200 (-0.06)
		PI (0.45)
		e (0.76)
		Organic
w (0.71)		
-200 (-0.19)		
o (0.44)		
e (0.72)		
C _r	Coarse Grained	σ (0.13)
		γ _{wet} (-0.60)
		N (0.11)
		-200 (0.01)
		LL (0.53)
	Fine Grained	γ _{dry} (-0.48)
		w (0.58)
		-200 (-0.06)
		LL (0.49)
		G _s (-0.13)
	Organic	w (0.54)
		-200 (-0.18)
		e (0.82)

The table above includes the same shading pattern for the most positive and negative influential factors, as seen in the previous tables, where red is strongest negative factors, while blue is the strongest positive factors. One will note that all of the most positive and negative influential factors were included in the developed correlation for Coarse Grained soils. However, the developed correlation also incorporates parameters that are seemingly not as important, such as the overburden pressure, automatic hammer SPT blow count, plasticity index, and fines content. According to the Pearson's Correlation Coefficient for PI, N, and -200, these parameters should have little to no influence at all, since they are so close to zero. For this reason, one could conclude that their removal would have little to no impact in the strength of the correlation.

The Fine Grained classification has a correlation that includes moisture content, fines content, plasticity index, and void ratio. Of these parameters, only the moisture content and void ratio were identified to have significant influence on the compression index. These were the top two most positive influential factors. However, the wet and dry densities, as identified in Table 19, were the top negative influential factors and neither of them were incorporated into the developed correlations. This classification also included the fines content, which has a Pearson's Correlation Coefficient very close to zero. This signifies that if a reduced model were to be used for better more efficient field use, the parameter could be excluded with little to no effect on compressibility predictions.

The developed correlation for compression index for the Organic classification included the top three most influential factors, those being void ratio, moisture content, and organic content. However, only one of the top negative influential factors was included, this being the

wet density. This seems a bit out of place, since the dry density had a much stronger Pearson's Correlation Coefficient (-0.60 and compared to -0.37 for wet density), but was not included in the prediction for compression index. This correlation also included the fines content and specific gravity, with both of their coefficients being closer to zero. This, again, leads one to believe that a reduced model could be created for easier field application.

The Organic classification also included a prediction for the recompression index. However, only two of the top positive influential factors, these being moisture content and void ratio were included, and none of the top negative influential factors were included. The exclusion of the top influential factors makes a bit of sense, as none of the top negative parameters has a Pearson's Correlation Coefficient below -0.50. Also, the third best positive influential parameter, the organic content, only had a Pearson's Correlation Coefficient of 0.25. Again, the fines content appeared in the prediction of the compressibility index, although the coefficient was relatively low. This is a consistent observation with each of the soil classifications.

4.6 Summary

Regression models were developed for each distinct soil classification. The model for the Coarse Grained classification performs very well, with respect to C_c , which is an important observation considering the dearth of previous correlations generated for this classification. The model for the Fine Grained classification absorbed the data from the Organic Silt/Clay classification. The predictive capability for C_c is comparable to the strength of existing

correlations. The model for the Organic Peat classification performed considerably better than that of existing correlations, with respect to both C_c and C_r . The correlations generated incorporate several factors not utilized in correlations from previous literature, such as the fines content (w_{200}), plasticity index (PI), and the interactions between the wet and dry density (γ_{wet} and γ_{dry}).

When the influential parameter analysis was performed, it was noted that LL, w, and e, were the most positive influential factors for every category, with the exception of PI for Silts and o for Organics. The most negative influential factors were noticeably less consistent, in regards to inclusion for all soil classifications. Some of the Pearson's Correlational Coefficients were strongly negative or positive. This leads one to conclude that viable delineational models, segregating the data based on a dividing line (i.e. $LL > 50$) and subsequently creating different regression models for each data set, may be possible. When the influential parameters were examined, in relation to their inclusion in the regression models, it was noted that some were included and some weren't. This leads one to believe that the regression models that have been generated can likely exclude certain parameters, for simplicity of use purposes, without losing much correlational strength.

CHAPTER 5: VERIFICATION OF SOIL COMPRESSIBILITY PREDICTION MODELS

5.1 Introduction

The developed correlations show promise for their predictive capabilities. In the next portion of the study, the strength of the correlations will be tested through additional field exploration and comparison to existing data. This will be accomplished through comparison of measured field settlement data to settlement predictions derived from measured compression indexes and predicted compression indexes from developed correlations.

In order for this to be achieved with any level of confidence, sites must be chosen with a known soil stratigraphy, measured settlement from a known source, and preferably, existing consolidation data. A known soil stratigraphy provides a general concept of the types of soil on site, thickness of soil layers, and depths. An accurate settlement prediction cannot be achieved without this information. It would also be preferable to have existing consolidation data on site for some of the soil layers. Although it would be ideal if there was a consolidation test for each soil layer on site and each depth interval, due to budgetary and time constraints, most consultants will test only the most problematic clay or organic layers, if any at all. This leads their settlement predictions to be less accurate. Having at least some consolidation tests would provide a better sense of soils on site, and eliminate the need for extracting additional samples.

Two locations were chosen for further study that meet the criteria specified above. They both are at SR 415 in Volusia County, Florida. This portion of SR 415 has been previously surcharged and has existing settlement data, as well as a wealth of SPT borings and consolidation

testing data. This translates to a known soil stratigraphy which is instrumentally helpful in the event that further field /lab testing needs to be performed. Each site will now be explained in detail.

5.2 Site Description

The SR 415 corridor was once a two-lane roadway through the border of Volusia and Seminole county, crossing the St. John's River Bridge. In order to meet the increasing traffic demand in the area, a large roadway section from Reed Ellis Rd. in Volusia County to the Seminole County line was widened, including the construction of an additional bridge to house the traffic moving southbound. The entire area throughout this corridor is littered with pockets of thick, problematic soils, such as organic sandy clay and peat. There were several SPT borings, lab tests for index properties and consolidation tests performed for this project.



Figure 24: Site Plan

Sample SPT borings from the original widening project are below:

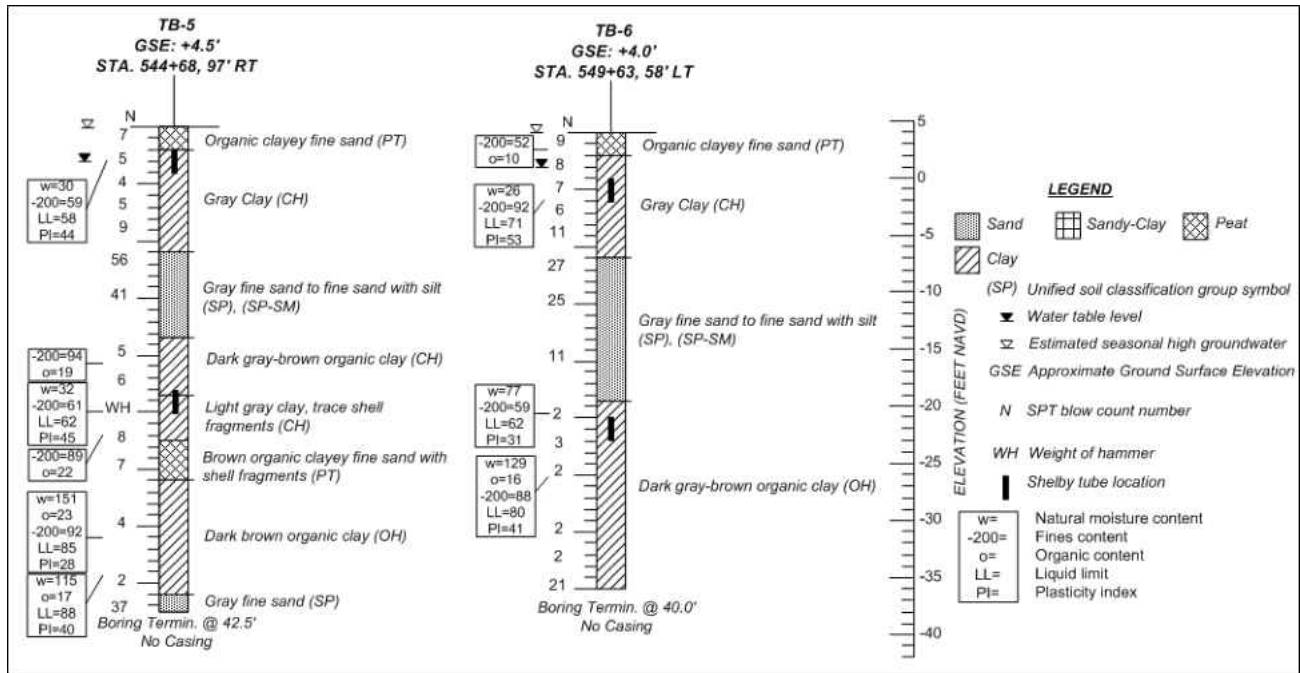


Figure 25: Sample SPT Borings

Source: Sewell & Abboud, 2012

As can be seen in the sample SPT borings above, sand pockets are intermingled with larger clay strata. The clays are loose and highly compressible, as demonstrated by relative low SPT blow counts (less than 10), Atterberg limits above 50, and several high moisture content readings (above 70%). Seasonal high-water table is at or near ground surface. This leads one to believe that this area is continually saturated year-round. When these soils were encountered, engineers deemed consolidation testing necessary, due to a high probability of significant soil settlement when loaded.

5.3 Field Testing Program

5.3.1 Settlement Measurement and Monitoring

As part of this project, an embankment would need to be constructed for the roadway and bridge approaches. This embankment would be contained with the construction of new MSE walls. Due to large stress changes from these overlying loads and construction activities, along with the soil profile having thick clay layers, engineers deemed it necessary to surcharge the area to extrude the hazardous settlement (Sewell & Abboud, 2012). This surcharge was installed in 2007 and concluded in December of 2009, for a total of just over 2 years. The fill was composed of clean sands and was over 20 feet high in certain locations (Sewell & Abboud, 2012). The figure below depicts the surcharge details and is not to scale.

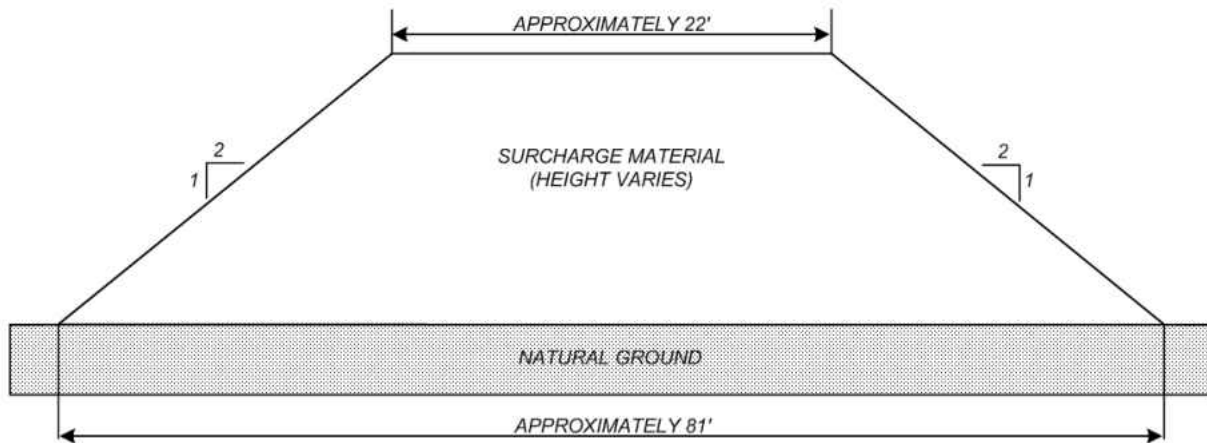


Figure 26: Surcharge Details

Settlement plates were incorporated into surcharge operations to monitor the settlement of the area. Settlement readings were performed weekly for the first three months after

installation, then bi-weekly for six months, and then on a monthly basis afterwards (Sewell & Abboud, 2012). The following table represents a summary of the readings taken for the site:

Table 21: Settlement Plate Data

Settlement Plate Info			Primary Settlement Reading (in.)
Settlement Plate #	Station	Offset	
S-4	523+00	40' LT	8.6
S-5	523+50	40' LT	7.3
S-6	524+00	40' LT	7.2
S-7	525+00	40' LT	10.0
S-8	530+00	40' LT	2.3
S-9	535+00	40' LT	3.7
S-10	540+00	40' LT	4.5
S-11	545+00	40' LT	5.5
S-12	550+00	40' LT	3.0
S-13	555+00	40' LT	4.0
S-14	560+00	40' LT	3.2
S-15	565+00	40' LT	3.5
S-16	570+00	40' LT	5.2
S-17	575+00	40' LT	2.6
S-18	580+00	40' LT	3.2
S-19	585+00	40' LT	5.0
S-20	590+00	40' LT	5.1
S-21	595+00	40' LT	4.2
S-22	600+00	40' LT	3.0

Source: Sewell & Abboud, 2012

As can be seen in the table above, all of the locations within the surcharge area experienced settlements less than one foot, and were frequently in the range of three to five inches. The observed variation in settlement throughout this area can be attributed to varying surcharge height and change in soil stratigraphy.

The following figures detail the measured settlement and surcharge history of settlement plate S-12 and S-18. These two locations will be discussed in greater detail, further in the study.

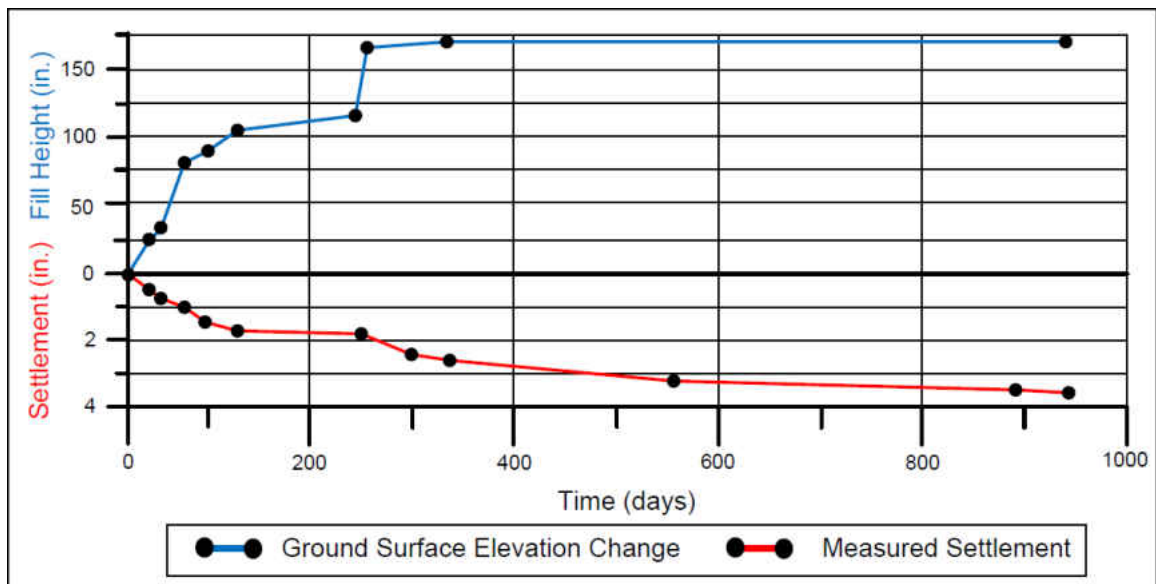


Figure 27: Measured Settlement and Surcharge History for S-12

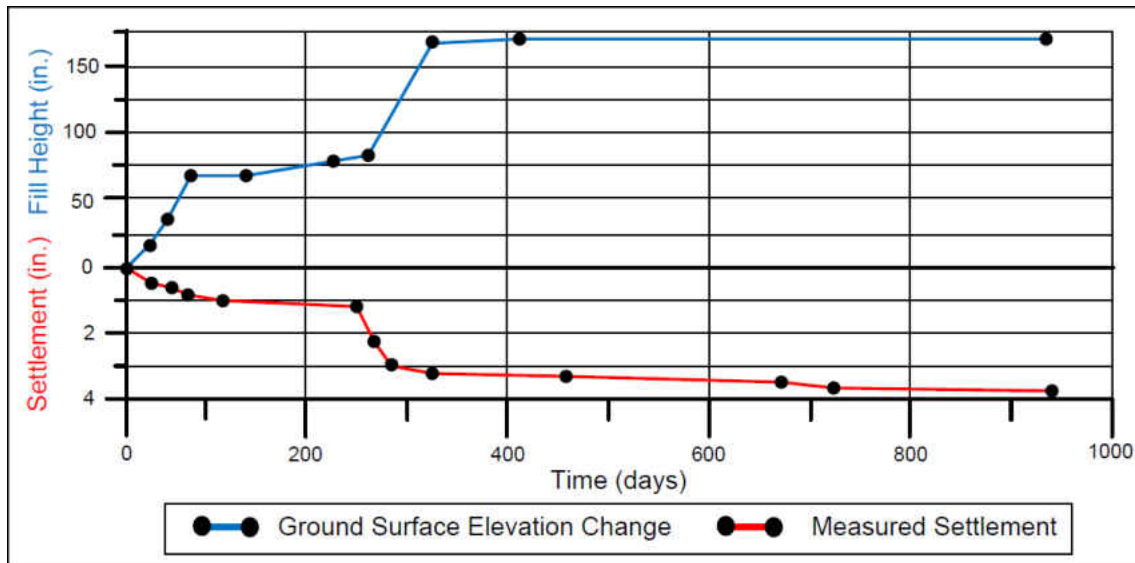


Figure 28: Measured Settlement and Surcharge History for S-18

5.3.2 Site Characterization

There were two locations chosen for additional testing at the SR 415 site. These were chosen due to a SPT boring being performed in close proximity to where a settlement plate was later placed, similar to the criteria in Location 1. The SPT boring provides information for the soil profile underneath the surcharge, and the settlement plate provides the information for how it behaves during loading. With a known surcharge loading, a settlement analysis can be performed to compare the predicted settlement to the measured.

The two locations that were chosen for further study were at SPT boring location TB-6 and TB-12. A summary of these locations is below.

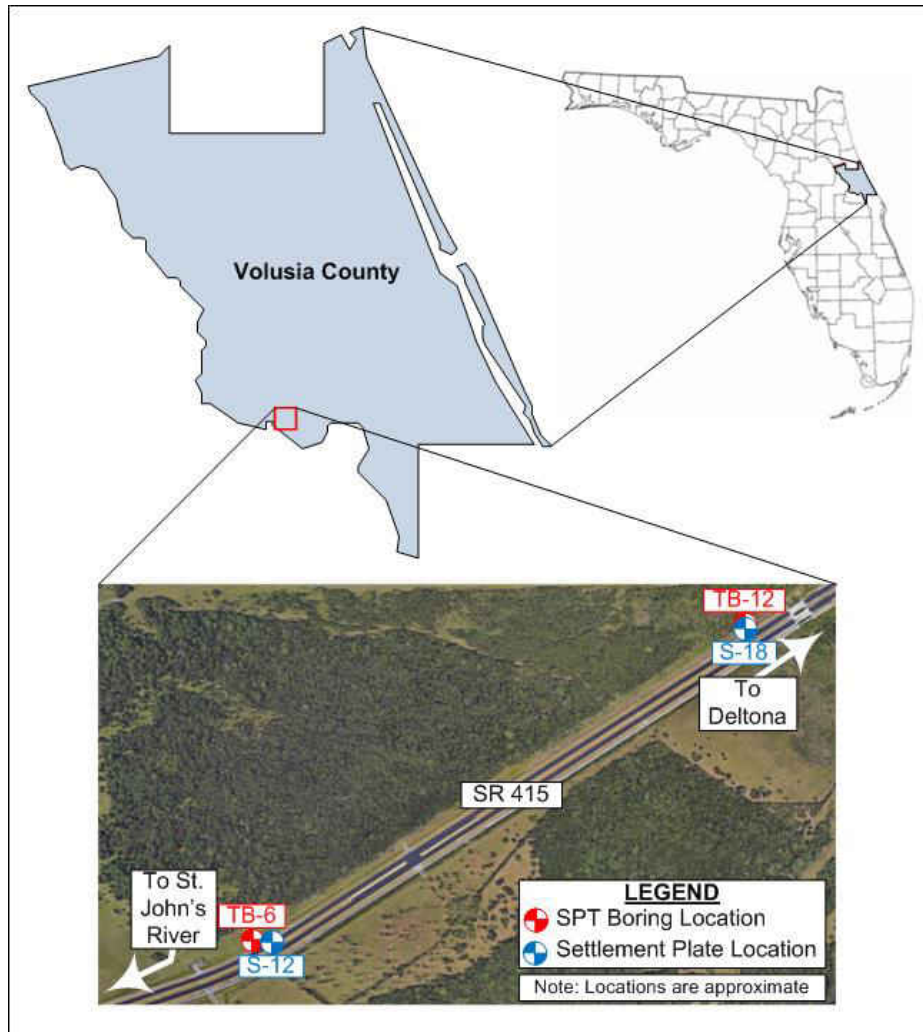


Figure 29: Additional Field Testing Locations

The figure above depicts the locations in which an SPT boring was performed and its proximity in relation to where settlement plate data exists. In this case, the SPT boring TB-6 closely relates to the location of settlement plate S-12 and SPT boring TB-12 closely relates to the location of settlement plate S-18. For further description of these locations, please see the table below.

Table 22: Field Testing Locations

Location	Boring #	Station	Offset	Settle. Plate #	Station	Offset
Location 1	TB-6	549+63	58' LT	S-12	550+00	40' LT
Location 2	TB-12	580+00	83' LT	S-18	580+00	40' LT

As can be seen, at SPT location TB-6, a settlement plate was later placed 37 feet further east and 18 feet closer to the centerline of the roadway. At SPT location TB-12, a settlement plate was later placed at the exact same station, but 43 feet closer to centerline. These were the locations that had closest proximities between existing SPT borings and settlement plates. Soil spatially varies in thickness and depth, which will ultimately have an influence on total settlement. While the SPT borings are fairly consistent in this project, with respect to depth and thickness of soil layers, it may not be a safe assumption that the settlement plate reading would be the same at the SPT location, had one been placed there. This will be vetted during settlement predictions and compared to measured settlement.

In order to confirm site soils, CPT soundings were performed at the existing SPT locations, prior to additional SPT borings and laboratory testing. The CPT profile for the location of SPT TB-6 matches up fairly well with the SPT boring profile. According to the CPT sounding profile, there should be approximately four feet of fill for this area. While the settlement plate data specifies 12.5 feet (discussed later in the study), the surcharge was stated to be partially removed for roadway embankment construction, upon completion of the surcharge program (Sewell & Abboud, 2012). The CPT sounding profile suggests that approximately 8.5 feet of fill was removed at this location, leaving approximately four feet to remain. The clay and

sand layers match up reasonably well, with the exception of the second clay layer, which appears to behave more like a sand, according to the CPT sounding profile.

The zone of influence is defined as the depth in which there is significant stress change so as to influence soil settlement. This depth is on the magnitude of $2 \cdot H$ below ground surface of the surcharge, where H is the surcharge height. At this depth, stress change generally falls to 10% of the stress change at ground surface, due to loading (Bowles, 1989). This largely depends on the unit weight of the soil layers above the influence zone depth. Typical subsoil investigation underneath an embankment calls for borings to be taken at a depth of twice the proposed embankment height or 10% of the original overburden pressure (FDOT, 2013).

For the SPT boring TB-6 location, two consolidation tests were carried out on the two clay layers within the influence zone of 25 ft. beneath the fill ($2H$ for this area would be 2×12.5 ft. of fill). The sand layer was viewed as incompressible. The SPT boring profile in Figure 30 continues to 40 ft. If the fill is eliminated, this accounts for a profile 36 ft. deep, which is 11 ft. beyond the conventional influence zone of settlement. The entire boring profile will be included in the settlement analyses.

The CPT profile for the location of SPT TB-12 illustrates approximately 4 ft. of fill. This varies from the 13.5 ft. of fill specified within the settlement plate results, but, as specified previously, a portion of the surcharge fill was later removed to account roadway embankment construction. The clay layer looks to be dispersed with silty sands, according to the CPT sounding profile. Note that the sand layer was viewed as incompressible. The SPT boring profile for TB-12 continues to 40 ft. With the same influence zone of settlement, as in boring TB-6 (25 ft.), if the fill is eliminated, the boring profile contains 11 additional feet below the

conventional influence zone of settlement. Both SPT locations will include a deeper than conventional influence zone of settlement in the settlement predictions. The results of the applicability of the conventional influence zone of settlement will be vetted in the results.

A depiction of the CPT sounding profile is highlighted in the figure below.

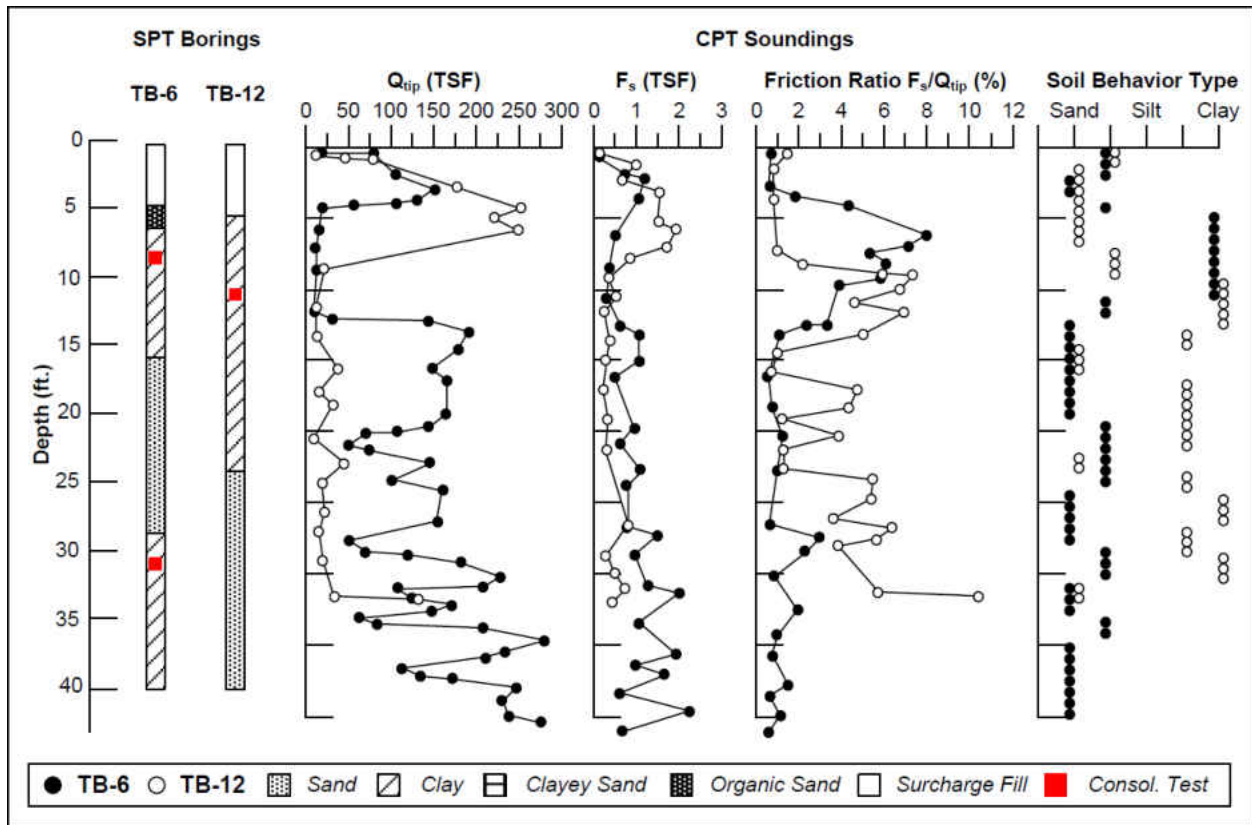


Figure 30: Geotechnical Profile at both SPT Locations

Details of the proposed additional testing are below. With this information, settlement analyses can be performed and compared to measured settlement.

Table 23: Additional Index Parameters Needed to Complete Soil Profile

Location	Depth (ft.)	Specific Gravity (G_s)	Fines (-200)	Atterberg Limits (LL, PI)	Moisture Content (w)	Wet Unit Weight (γ_{wet})	Organic Content (o)
TB-6	20	X	X		X	X	
TB-12	30	X	X		X	X	

SPT borings were then performed in close proximity to where the existing borings were taken in the past and had very little variation in soil stratigraphy. Note that they could not be performed in the exact location, due to utilities and other conflicts in the area. The SPT borings were performed in an effort to gather the required index properties for the use of correlations in the settlement analyses. Although the SPT borings were performed in slightly different locations, the naming convention will be kept the same. The SPT borings, and accompanying lab testing, can be seen in Figure 31. Table 24 houses a tabular version of the laboratory testing.

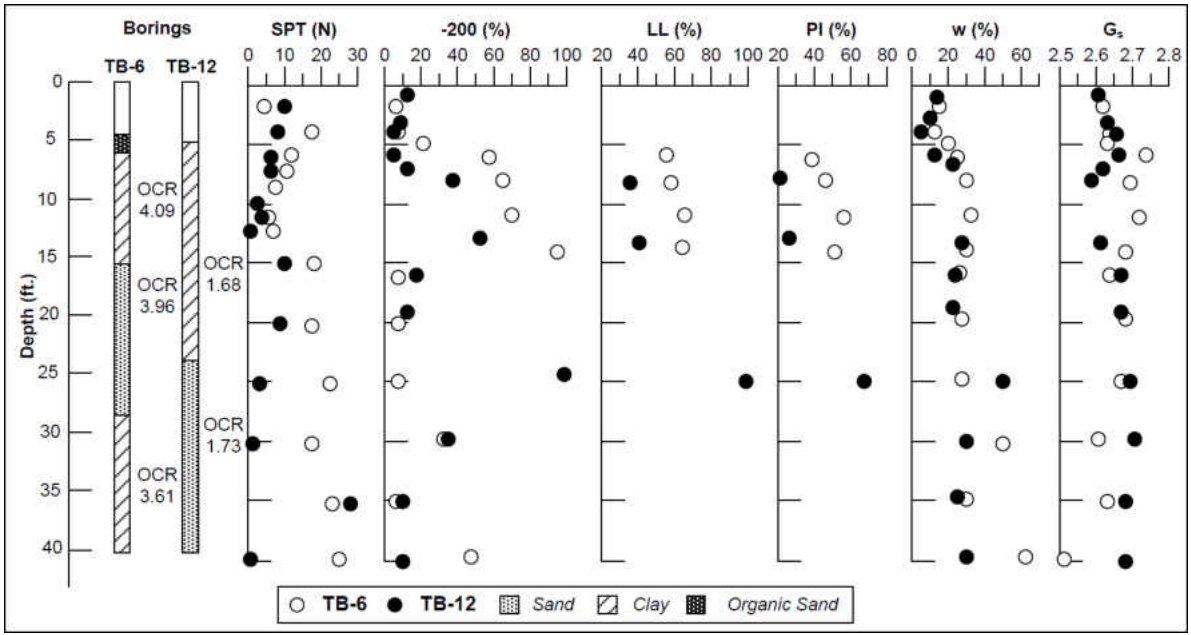


Figure 31: SPT Results and Lab Testing for Complete Soil Profiles

Table 24: Additional Laboratory Testing

SPT Boring	Depth	USCS	-200 (%)	LL (%)	PI (%)	w (%)	G _s
TB-6	2	SP-SM	7	-	-	14	2.61
	4	SP-SM	8	-	-	12	2.67
	5	SM	23	-	-	20	2.63
	6	CH	58	56	40	23	2.75
	8	CH	64	60	47	29	2.68
	11	CH	68	69	54	33	2.72
	14	CH	92	64	50	29	2.69
	16	SP-SM	6	-	-	24	2.64
	20	SP-SM	6	-	-	27	2.67
	25	SP-SM	7	-	-	27	2.66
	30	SM	32	-	-	47	2.59
	35	SP-SM	6	-	-	28	2.64
40	SM	49	-	-	64	2.52	
TB-12	1	SP-SM	11	-	-	11	2.60
	3	SP-SM	8	-	-	10	2.63
	4	SP	3	-	-	5	2.65
	6	SP	4	-	-	11	2.65
	7	SM	15	-	-	25	2.61
	8	SC	37	32	18	25	2.58
	13	SC	50	42	28	28	2.61
	16	SM	19	-	-	25	2.66
	19	SM	16	-	-	23	2.66
	25	CH	97	99	67	52	2.68
	30	SM	34	-	-	34	2.72
	35	SP-SM	11	-	-	22	2.66
40	SP-SM	11	-	-	26	2.65	

Two clay samples were taken for consolidation testing for TB-6 and one clay sample was tested for TB-12. The consolidation test results can be seen in Figure 32. For TB-6, the upper clay layer shows C_c of 0.49 and C_r of 0.10 while the lower clay layer shows C_c of 2.50 and C_r of 0.09. For TB-12, the clay layer shows C_c of 0.43 and C_r of 0.08.

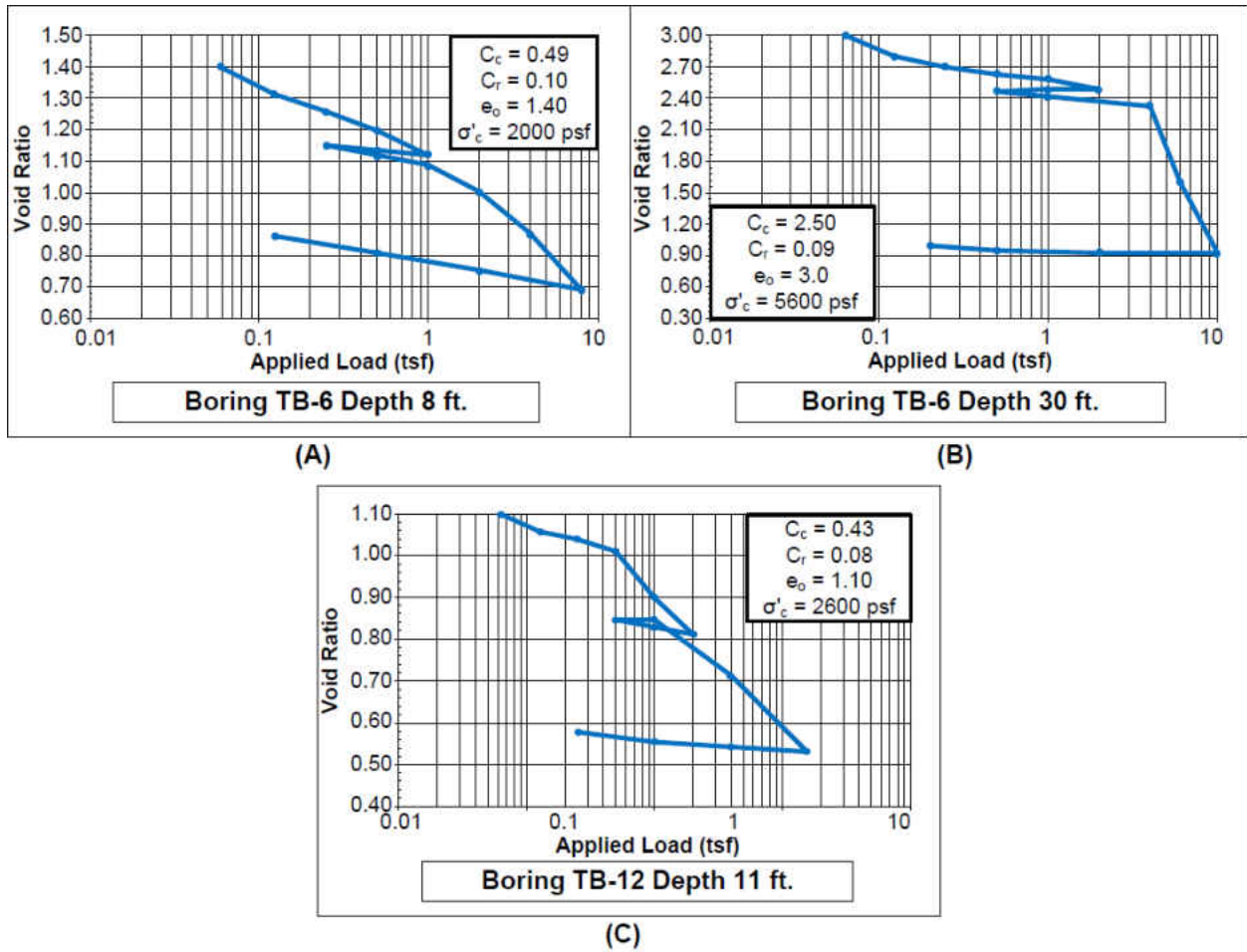


Figure 32: Consolidation Test Results

5.4 Case Studies Comparing Predicted Settlement to Measured Settlement

5.4.1 Case Study 1: SPT Boring TB-6 Analysis

Settlement can be computed using Equations 1 through 3 for all soil types, as discussed during the introduction. The stress state of the soil will dictate which equation is used. If the sample is normally consolidated, Equation 1 will be used. If the sample is overly consolidated, Equation 2 or 3 will be used, depending on the maximum past pressure, as previously discussed.

The settlements for each soil type will be determined, and then summed for a total primary consolidation settlement.

The settlement analyses are organized via a case study for each location. Two different analyses were performed for each location, including: (1) settlement computed using the measured compressibility indexes by consolidation test and (2) settlement computed using the predicted compressibility indexes via the developed correlations. The computed settlements are then compared with the measured settlements. In the settlement analyses, three different C_r indexes were used, including (1) measured C_r from consolidation test, (2) predicted C_r from the correlation, and (3) predicted C_r from a rule of thumb correlating C_c to C_r . In addition to this, the predicted C_r from the strongest C_r prediction model from existing literature will be used (Azzouz).

The site geometry below, will be used in the analysis. Note that depths are taken prior to surcharge fill operations.

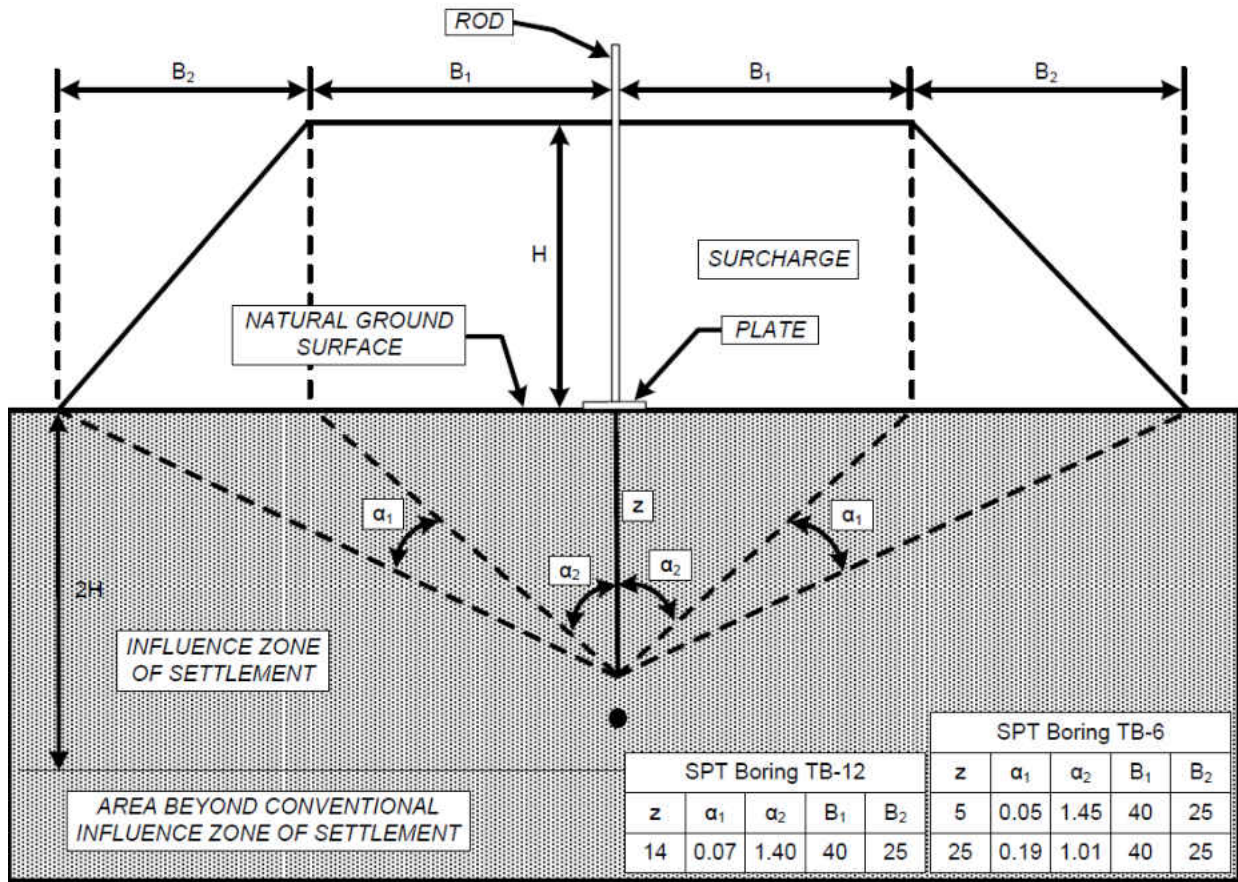


Figure 33: SPT Results and Lab Testing for Complete Soil Profiles

The applicable data will be input in a series of tables for clarity.

The depths of interest are 5 and 25 feet. The depths are taken prior to surcharge operations, in the middle of the soil layer. This is done in order to determine the initial stresses, before any stress changes occur.

Table 25 includes information for the settlement equations, and total settlement (Δ) computed for this location, using measured C_r . The predicted settlement, Δ , is determined from total surcharge height at the end of fill operations. The maximum past stress, σ'_c , is taken directly

from the consolidation tests. The change in pressure for each depth is determined by spatial geometry, with respect to depth of interest and location of settlement plate.

Table 25: Predicted Settlement from Measured C_r , SPT Boring TB-6

Soil #	H (ft.)	σ'_o (psf.)	$\Delta\sigma$ (psf.)	σ_r (psf.)	σ'_c (psf.)	1C_r	e_o	Δ (in.)	Total Δ (in.)	2 Measured Δ (in.)
1	11.5	488	785	1273	2000	0.10	1.31	2.17	2.92	3.60
3	11.5	1550	755	2305	5600	0.09	3.05	0.75		

¹ C_r is measured by consolidation test

² Settlement was measured by the field test

The maximum past stress, σ'_c , is taken directly from the consolidation tests. The change in pressure for each depth is determined by spatial geometry, with respect to depth of interest and location of settlement plate.

The critical piece of information that will change with Analysis #2, is the compressibility index(s). This will now be predicted using the correlations generated. All other information involved in the settlement analysis will remain the same.

The predicted settlement is highlighted in the table below. Note that index properties were either taken from existing information, where there was no additional testing, or was taken as an average of index properties from that soil layer. Also note that the sand layer is treated as a compressible layer and is incorporated into the analysis.

Table 26: Predicted Settlement from Predicted C_r , SPT Boring TB-6

Layer #	H (ft.)	σ_f (psf.)	σ'_o (psf.)	1C_r	e_o	Δ (in.)	Total Δ (in.)	2 Measured Δ (in.)
1	11.5	1273	488	0.03	1.31	0.98	2.43	3.60
2	13	1848	1071	0.01	0.66	0.39		
3	11.5	2305	1550	0.07	3.05	1.06		

¹ C_r is the predicted value using Table 6 and applicable index parameters

² Settlement was measured by the field test

As the overall site has exhibited being heavily over-consolidated (see Figure 5), with the maximum past stress significantly higher than the final stress (from embankment surcharge construction), it was assumed that the same settlement equation would apply for this analysis.

One will notice that in Table 6, the correlations generated for C_c are significantly stronger than C_r , particularly for coarse grained soils. Although C_c is not applicable for this site, due to stress history, there is a rule of thumb that can be used, such that the recompression index is 1/5 of the compression index (Das, 2002). It is governed by the equation below:

$$C_r = 0.20(C_c) \quad (22)$$

This correlation of C_r to C_c may be able to compensate for the lack of correlational strength of coarse and fine grained soils, with respect to the comparison of C_r to C_c , using Table 6. Note that as previously stated in Figure 8, a total of 619 consolidation tests were collected for the State of Florida. These consolidation tests identify the compressibility indexes, both C_c and C_r . For this reason, the rule of thumb previously stated in Equation 22 can be tested for each soil type. Results of this analysis can be seen in the table below.

Table 27: C_c to C_r Ratio for Each Soil Type

Soil Type	C_c/C_r Ratio
Coarse Grained	0.13
Fine Grained	0.24
Organic	0.11
Average	0.16

As can be seen, there was some variability with the ratios for each soil type, with coarse grained being 0.13, fine grained being 0.24, and organic being 0.11. The average of these soil types came to 0.16, which is within close proximity to 0.20, so Equation 22 will apply.

Table 28: Total Settlement from Predicted Compressibility Index(s) using the C_c correlation to C_r

Layer #	H (ft.)	σ_r (psf.)	σ'_o (psf.)	σ'_c (psf.)	1C_c	2C_r	e	Δ (in.)	Total Δ (in.)	3 Measured Δ (in.)
1	11.5	1273	488	2000	0.40	0.08	1.31	1.73	3.03	3.60
2	13	1848	1071	3400	0.09	0.02	0.66	0.39		
3	11.5	2305	1550	5600	0.53	0.11	3.05	0.91		

1C_c is the predicted value using Table 2 and applicable index parameters

2C_r is computed by Eq. 22

3 Settlement was measured by the field test

The settlement plate data for location S-12 (SPT Boring TB-6) can be seen in Figure 8, with various line colors representing the measured and predicted settlements. The settlement using the correlation of C_c to C_r exhibits the closest values to the measured settlement and the error is within 15%. On the other hand, the settlement by the predicted C_r shows lowest

predicted values over time and the error range is up to 31%. Since the recompression of soils is typically small and much lower than C_c , its sensitivity to other index properties can be much less sensitive compared to C_c . In addition, the accuracy of C_r correlation exhibits much lower than C_c as shown in Table 6.

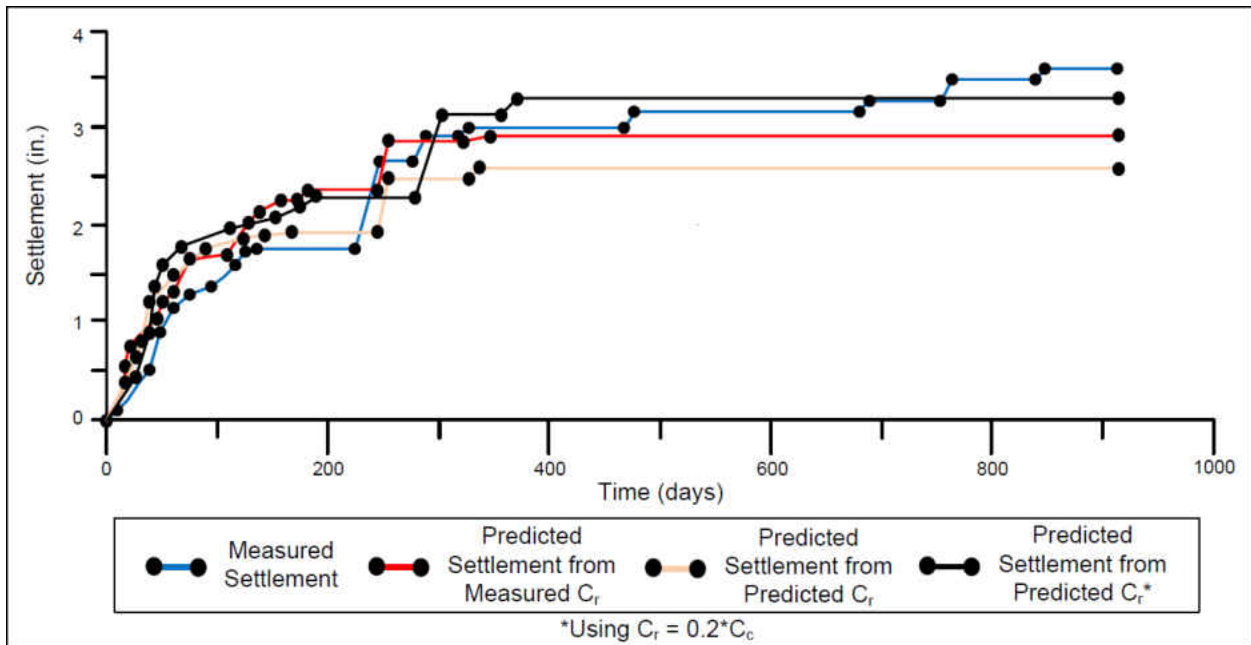


Figure 34: Settlement Plate Results for Location S-12 (TB-6 Location)

Along with using the developed correlations, the settlement will now be predicted from the strongest of the existing correlations for C_r , this being the Azzouz correlation using moisture content and void ratio. The following table includes the pertinent information and computed settlement using Azzouz's correlation for C_r for all soil types:

Table 29: Total Settlement from Predicted C_r using Azzouz's correlation ($C_r = 0.142(e - 0.009w + 0.006)$) for all soils

Layer #	σ_f (psf.)	σ'_o (psf.)	H (ft.)	w (%)	e_o	C_r	Δ (in.)	Total Δ (in.)
1	1273	488	11.5	26	1.31	0.15	3.31	7.40
2	1848	1071	13	29	0.66	0.06	1.28	
3	2305	1550	11.5	77	3.05	0.34	2.82	

With the exception of the settlement prediction from using the Azzouz correlation, the remainder of the settlement predictions are all below the measured settlement. This leads one to believe that there is a missing component of immediate settlement that can be compensated by examining the elastic contribution. This is determined by accounting for the change in Modulus of Elasticity within the influence zone of settlement (Bowles, 1989). This parameter can be correlated using information from the SPT Boring N value (blow count) for coarse grained materials with varying amounts of fine particles, or using information from the CPT tip resistance for fine grained materials (NAVFAC, 1982), using the table below:

Table 30: Correlations for Modulus of Elasticity for Various Soil Types

Soil Type	Correlation	Field Test Used
Silts, sandy silts, slightly cohesive silt-sand mixtures	E = 4N	SPT
Clean, fine to medium, sands and slightly silty sands	E = 7N	SPT
Coarse sands and sands with little gravel	E = 10N	SPT
Sandy gravels and gravel	E = 12N	SPT
Fine grained materials	E = 2*q _{tip}	CPT

This procedure involves splitting up to subsurface profile in layers, similar to what has already been performed. The Modulus of Elasticity will then be computed using Table 30. The influence factor will then be determined for each soil layer using spatial geometry and depth of interest (NAVFAC, 1982). Lastly, a creep correction factor is applied to compensate for any long-term contribution for settlement over time. This process is outlined in the following table.

Table 31: Elastic Settlement Parameters SPT Boring TB-6

Layer	H (ft.)	Type	N	q _{tip}	E multiplier	E (tsf)	¹ I	I/E*H (in/tsf)
1	11.5	Clay	-	25	2.5	62.5	0.49	1.08
2	13	Sand	21	N/A	7	147	0.47	0.50
3	11.5	Clay	-	150	2.5	375	0.47	0.17
Sum								1.75

¹Influence Factor underneath embankment loading (NAVFAC, 1982)

Total elastic settlement can then be computed using Equation 23

$$\Delta H = C * q * \Sigma \left(\frac{I}{E} \right) (H) \quad (23)$$

Where C is a creep correction factor, determined from Equation 24, q is the final surcharge pressure (tsf), and ΔH is the elastic settlement (in.).

$$C = 1 + 0.2\log(10t) \quad (24)$$

Note that t is in years. For immediate settlement, t is zero, so C = 1.

The elastic settlement can then be computed using the table below.

Table 32: Elastic Settlement SPT Boring TB-6

q (tsf)	C	I/E*H (in/tsf)	ΔH (in.)
0.81	1	1.75	1.42

The total immediate settlement can then be computed for SPT Boring TB-6.

Table 33: Total Settlement SPT Boring TB-6

¹ Consolidation Settlement (in.)	Elastic Settlement (in.)	Total Settlement Prediction (in.)	² Measured Settlement (in.)
3.03	1.42	4.45	3.60

¹Settlement Prediction using the Predicted C_r (Using C_r = 0.2*C_c)

²Settlement was measured by the field test

Note that when the elastic settlement component was examined, the total settlement prediction increased to 4.45 inches, which is less than an inch above the measured settlement. As the zone of settlement was taken 11 feet beyond the conventional influence zone, one would expect that if the influence zone of settlement was taken as 2H below ground surface, settlement

predictions would move closer to the measured. Table 28 will now be revised to account for the reduced influence zone of settlement.

Table 34: Total Settlement from Predicted Compressibility Index(s) using the C_c correlation to C_r using Conventional Influence Zone of Settlement

Layer #	H (ft.)	σ_r (psf.)	σ'_o (psf.)	σ'_c (psf.)	1C_c	2C_r	e	Δ (in.)	Total Δ (in.)	3 Measured Δ (in.)
1	11.5	1273	488	2000	0.40	0.08	1.31	1.73	2.52	3.60
2	13	1848	1071	3400	0.09	0.02	0.66	0.39		
3	1	1958	1200	5600	0.53	0.11	3.05	0.40		

1C_c is the predicted value using Table 2 and applicable index parameters

2C_r is computed by Eq. 22

3 Settlement was measured by the field test

Tables 31 and 32 will now be modified for the reduction in the influence zone of settlement.

Table 35: Elastic Settlement Parameters SPT Boring TB-6 using Conventional Influence Zone of Settlement

Layer	H (ft.)	Type	N	q_{tip}	E multiplier	E (tsf)	1I	$I/E*H$ (in/tsf)
1	11.5	Clay	-	25	2.5	62.5	0.49	1.08
2	13	Sand	21	N/A	7	147	0.47	0.50
3	1	Clay	-	150	2.5	375	0.47	0.01
Sum								1.59

1 Influence Factor underneath embankment loading (NAVFAC, 1982)

Table 36: Elastic Settlement SPT Boring TB-6 using Conventional Influence Zone of Settlement

q (tsf)	C	I/E*H (in/tsf)	ΔH (in.)
0.81	1	1.59	1.29

Table 33 will now be modified for the reduction in influence zone of settlement.

Table 37: Total Settlement SPT Boring TB-6 using Conventional Influence Zone of Settlement

¹Consolidation Settlement (in.)	Elastic Settlement (in.)	Total Settlement Prediction (in.)	²Measured Settlement (in.)
2.52	1.29	3.81	3.60

¹Settlement Prediction using the Predicted C_r (Using $C_r = 0.2 * C_c$)

²Settlement was measured by the field test

As can be seen, using a conventional influence zone of settlement ($2 * H$ below ground surface), and accounting for elastic settlement improved the results for the settlement prediction, as it moved closer to the measured settlement at this location. The same procedure will be replicated at the TB-12 location, first assuming a deeper than conventional influence zone of settlement and then using conventional, if needed.

5.4.2 Case Study 2: SPT Boring TB-12 Analysis

According to the SPT boring (TB-12) in Figure 31, the clay layer has a depth of interest at 13.5 ft. The depth is taken prior to surcharge operations, in the middle of the soil layer. Table 38 includes the predicted settlement from measured C_r .

The following table includes information for the settlement equations, and total settlement computed for this location, using the pertinent measured compressibility index(s):

Table 38: Predicted Settlement from Measured C_r

Layer #	H (ft.)	σ'_o (psf.)	$\Delta\sigma$ (psf.)	σ_f (psf.)	σ'_c (psf.)	1C_r	e_o	Δ (in.)	2 Measured Δ (in.)
1	15	548	809	1357	2600	0.08	1.10	2.72	3.80

1C_r is measured by consolidation test

2 Settlement was measured by the field test

The predicted settlement, as described in the SPT Boring TB-12 from Figure 31, is highlighted in Table 39. Note that in this analysis, the sand layer is treated as compressible and the applicable model from Table 6 is applied.

Table 39: Predicted Settlement from Predicted C_r , SPT Boring TB-12

Layer #	H (ft.)	σ_f (psf.)	σ'_o (psf.)	1C_r	e	Δ (in.)	Total Δ (in.)	2 Measured Δ (in.)
1	15	1357	548	0.05	1.10	1.70	2.25	3.80
2	19	3045	2305	0.03	0.98	0.55		

1C_r is the predicted value using Table 6 and applicable index parameters

2 Settlement was measured by the field test

The predicted settlement using a correlation of predicted C_c to C_r is highlighted in Table 40.

Table 40: Total Settlement from Predicted Compressibility Index(s) using the C_c correlation to C_r

Layer #	H (ft.)	σ_f (psf.)	σ'_o (psf.)	1C_c	2C_r	e	Δ (in.)	Total Δ (in.)	3 Measured Δ (in.)
1	15	1357	548	0.30	0.06	1.10	2.01	2.76	3.80
2	19	3045	2305	0.20	0.04	0.98	0.75		

1C_c is the predicted value using Table 2 and applicable index parameters

2C_r is computed by Eq. 22

3 Settlement was measured by the field test

The settlement plate data for location S-18 (SPT Boring TB-12) can be seen in Figure 35, with various line colors representing the measured and predicted settlements. The same trend is observed as shown in Figure 34. The settlement using the correlation of C_c to C_r exhibits closest values to the measured settlement, and the settlement by the measured C_r and the settlement by the predicted C_r are followed in order.

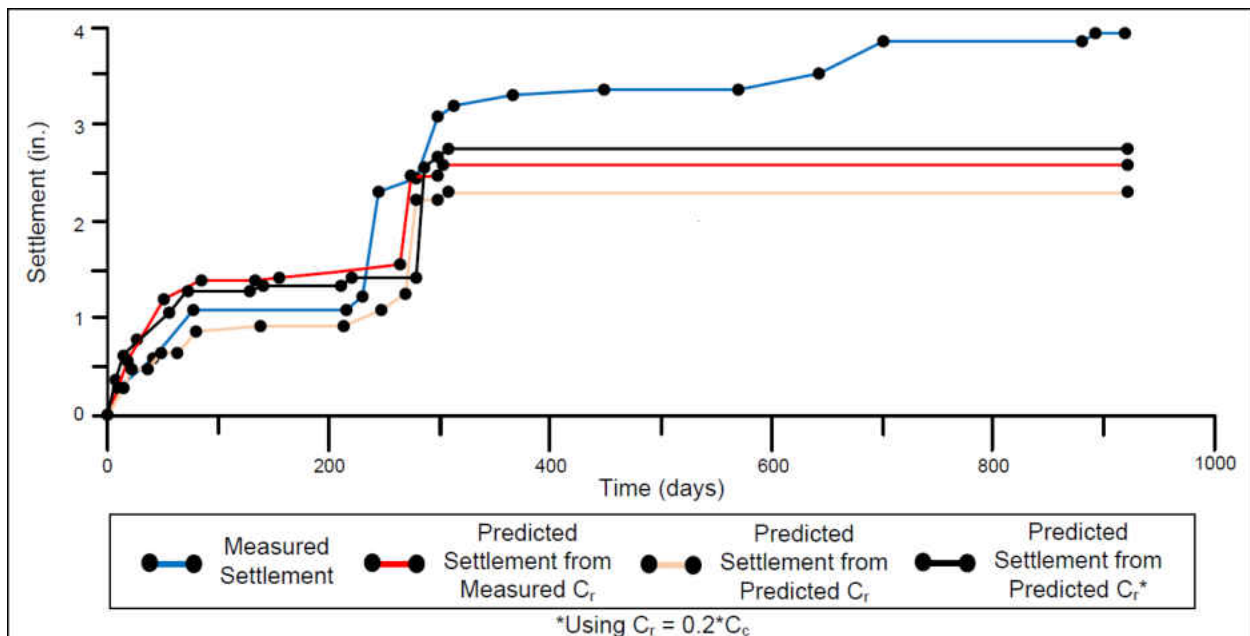


Figure 35: Settlement Plate Results for Location S-18 (TB-12 Location)

Along with using the developed correlations, the settlement will now be predicted from the strongest of the existing correlations for C_r , this being the Azzouz correlation using moisture content and void ratio. The following table includes the pertinent information and computed settlement using Azzouz's correlation for C_r for all soil types:

Table 41: Total Settlement from Predicted C_r using Azzouz's correlation ($C_r = 0.142(e - 0.009w + 0.006)$) for all soils

Layer #	σ_r (psf.)	σ'_o (psf.)	H (ft.)	w (%)	e_o	C_r	Δ (in.)	Total Δ (in.)
1	1357	548	15	26	1.10	0.13	4.22	6.08
2	3045	2305	19	29	0.98	0.11	1.86	

With the exception of the settlement prediction from using the Azzouz correlation, the remainder of the settlement predictions are all below the measured settlement, similar to what was observed at the previous location. As the TB-6 location yielded better results when elastic settlement was considered, the same procedure will be implemented for the TB-12 location.

Table 42 outlines the elastic settlement parameters for this location.

Table 42: Elastic Settlement Parameters SPT Boring TB-12

Layer	H (ft.)	Type	N	q_{tip}	E multiplier	E (tsf)	¹ I	I/E*H (in/tsf)
1	15	Clay	-	25	2.5	62.5	0.49	1.41
2	19	Sand	15	N/A	7	105	0.47	1.02
Sum								2.43

¹Influence Factor underneath embankment loading (NAVFAC, 1982)

The elastic settlement can then be computed using the table below.

Table 43: Elastic Settlement SPT Boring TB-12

q (tsf)	C	I/E*H (in/tsf)	ΔH (in.)
0.81	1	2.43	1.97

The total immediate settlement can then be computed for SPT Boring TB-6.

Table 44: Total Settlement SPT Boring TB-12

¹Consolidation Settlement (in.)	Elastic Settlement (in.)	Total Settlement Prediction (in.)	²Measured Settlement (in.)
2.76	1.97	4.73	3.80

¹Settlement Prediction using the Predicted C_r (Using $C_r = 0.2 * C_c$)

²Settlement was measured by the field test

Note that when the elastic settlement component was examined, the total settlement prediction increased to 4.73 inches. Similar to the TB-6 location, the total settlement is less than an inch above the measured settlement. As the zone of settlement was taken 11 feet beyond the conventional influence zone. Similar to the TB-6 location, one would expect that if the influence zone of settlement was taken as 2H below ground surface, settlement predictions would move closer to the measured. Table 40 will now be revised to account for the reduced influence zone of settlement.

Table 45: Total Settlement from Predicted Compressibility Index(s) using the C_c correlation to C_r using Conventional Influence Zone of Settlement

Layer #	H (ft.)	σ_f (psf.)	σ'_o (psf.)	1C_c	2C_r	e	Δ (in.)	Total Δ (in.)	3 Measured Δ (in.)
1	15	1357	548	0.30	0.06	1.10	2.01	2.32	3.80
2	8	2592	1800	0.20	0.04	0.98	0.31		

1C_c is the predicted value using Table 2 and applicable index parameters

2C_r is computed by Eq. 22

3 Settlement was measured by the field test

Tables 42 and 43 will now be modified for the reduction in the influence zone of settlement.

Table 46: Elastic Settlement Parameters SPT Boring TB-12 using Conventional Influence Zone of Settlement

Layer	H (ft.)	Type	N	q_{tip}	E multiplier	E (tsf)	1I	I/E*H (in/tsf)
1	15	Clay	-	25	2.5	62.5	0.49	1.41
2	8	Sand	15	N/A	7	105	0.47	0.43
Sum								1.84

1 Influence Factor underneath embankment loading (NAVFAC, 1982)

Table 47: Elastic Settlement SPT Boring TB-12 using Conventional Influence Zone of Settlement

q (tsf)	C	I/E*H (in/tsf)	ΔH (in.)
0.81	1	1.84	1.49

Table 44 will now be modified for the reduction in influence zone of settlement.

Table 48: Total Settlement SPT Boring TB-12 using Conventional Influence Zone of Settlement

¹ Consolidation Settlement (in.)	Elastic Settlement (in.)	Total Settlement Prediction (in.)	² Measured Settlement (in.)
2.32	1.49	3.81	3.80

¹Settlement Prediction using the Predicted C_r (Using $C_r = 0.2 * C_c$)

²Settlement was measured by the field test

As can be seen, using a conventional influence zone of settlement ($2 * H$ below ground surface), and accounting for elastic settlement greatly improved the results for the settlement prediction. In fact, the results very closely match the measured settlement. This is a positive indicator that using a conventional influence zone of settlement and including the elastic settlement component, in conjunction with using the 0.2 factor relating C_c to C_r , can yield accurate settlement predictions.

5.5 Discussions

The root mean squared error (RMSE) method was implemented to summarize the variance between the predicted and measured values for each settlement prediction and evaluate their performance, statistically. A perfect predictive model yields an RMSE value of 0.0. The lower the RMSE value of a predictive model the better the model performs. In a perfect model, the predicted settlements as seen in figures above would coincide with the measured settlement. The closer the predicted settlement follows the measured settlement, the better the model performs.

$$\text{RMSE} = \sqrt{(f - o)^2/n} \quad (25)$$

Where f = predicted settlement (per day), o = measured settlement (per day), and n = number of observations.

For each increment of time in which a settlement reading was taken, the difference between predicted settlement and measured settlement is evaluated and this statistical operation is a summary of those differences.

The following table presents a summary of this measure for each location. Keep in mind that these statistical parameters are for the predictions made using a deeper than conventional influence zone of settlement and a non-elastic settlement contribution.

Table 49: Statistical Strength of Prediction Models

RMSE		Settlement Prediction Method
Location TB-6 (S-12)	Location TB-12 (S-18)	
0.131	0.200	Settlement Prediction from the Measured C_r
0.208	0.305	Settlement Prediction from the Predicted C_r
0.128	0.186	Settlement Prediction using the Predicted C_r (Using $C_r = 0.2 * C_c$)

As can be determined from the table above, the predicted C_r (using a correlation from predicted C_c) was the strongest settlement prediction at both locations. The differences between predicted and measured settlements can be attributed to a number of factors. As stated

previously, the settlement plates were not placed at the exact location of the SPT borings. As soil varies spatially and with depth, there is the potential that the soil stratigraphy could be different between where the settlement plate was placed and where the SPT boring was performed. The soil sampling may also not have occurred as frequently as it needed to be. There is a chance that slight variances and small pockets of varying soils could have been missed between sampling intervals.

Table 50 illustrates the comparison between the settlement using the measured and predicted compressibility index(s) and the measured settlement. The measurements and predictions are reported for the last observed reading of the settlement plate, as noted in Figures 34 and 35. The predicted settlement from the predicted C_r from both locations was noticeably less accurate when comparing to the measured settlement. With the weakness of correlational strength between measured and predicted C_r for coarse and fine grained soils (as compared to the correlational strength of C_c), it was then hypothesized to use a standard rule of thumb to equate C_c to C_r . When this analysis was performed, it yielded better results, when compared to the measured settlement. Although this ratio has been widely accepted and adopted in field practice, it is still a generalization that may not be applicable for all soils, including those encountered at this site. This generalization may have had an effect on the settlement predictions.

Table 50: Measured vs. Predicted Settlement Summary

Settlement Plate Location	Measured Settlement (in.)	Predicted Settlement w/Measured ¹ C _r (in.)	Predicted Settlement w/Predicted ² C _r (in.)	Predicted Settlement w/Predicted ³ C _r (in.)	Predicted Settlement w/Predicted ⁴ C _r (in.)
S-12 (TB-6)	3.60	2.92	2.43	3.03	7.40
S-18 (TB-12)	3.80	2.72	2.25	2.76	6.08

¹C_r is measured from consolidation test

²C_r is the predicted value from the correlation shown in Table 2.

³Using a correlation from C_c to C_r

⁴Using the strongest correlation from existing literature (Azzouz)

The influence zone of settlement was taken as two times the surcharge height below ground surface. The other rule of thumb for this depth is wherever the stress change from the overlying load moves to 10%. The slight variance between predicted and measured settlements can be attributed to ambiguity of the identification of the influence zone of settlement. As can be determined from the previous table, the predicted settlements were less than the measured. This leads one to believe that the influence zone of settlement is deeper than 2H below ground surface.

The elastic settlement contribution was considered and added to the analyses for the last measured settlement reading at both locations. When this contribution was added to the study, settlement predictions increased beyond the measured settlement at both locations. For this reason, the influence zone of settlement was brought back to 2H below ground surface. Results of this analysis can be seen in Table 51.

Table 51: Measured vs. Predicted Settlement Summary, Considering Conventional Influence Zone of Settlement and Elastic Settlement Contribution

Settlement Plate Location	Measured Settlement (in.)	Predicted Settlement w/Predicted ¹C_r (in.)
S-12 (TB-6)	3.60	3.81
S-18 (TB-12)	3.80	3.81

¹Using a correlation from C_c to C_r

5.6 Summary and Conclusions

The following conclusions can be made:

- In general, C_r correlations show lower accuracy than C_c correlations. C_r values are smaller than C_c and its sensitivity to other soil index properties may be lower. Using the rule of thumb, C_r=0.2*C_c, is an alternative when the C_r correlation has low performance.
- The predicted settlement from predicted C_r (using a correlation from predicted C_c) was the most accurate settlement prediction for both locations.
- The predicted settlement using the predicted C_r values exhibits the weakest settlement prediction but still in reasonable prediction range. The difference in settlement prediction between the measured and predicted C_r approaches is over an inch for both locations and the error range is from 16% to 17%.
- When elastic settlements were considered and predicted settlements subsequently increased in excess of the measured settlement, the influence zone of settlement was reduced to 2H below ground surface. This yielded much stronger settlement predictions.

As depicted in Table 49, at both settlement plate locations, the predicted settlement from measured compressibility indexes was more accurate than the predicted settlement using predicted compressibility indexes. With the weakness of correlational strength between measured and predicted C_r for coarse and fine grained soils (as compared to the correlational strength of C_c), it was then hypothesized to use a standard rule of thumb to equate C_c to C_r . When this analysis was performed, it yielded much better results, compared to the measured settlement. The difference between predicted and measured settlement was about an inch for the S-18 location and about half an inch for the S-12 location. This is an important finding, as the predicted settlement using this method is much more favorable to measured settlement than that of predictions using the strongest correlation from existing literature. Although this ratio has been widely accepted and adopted in field practice, it is still a generalization that may not be applicable for all soils, including those encountered at this site. This generalization may have had an effect on the settlement predictions.

When the strongest correlation from existing literature was used (Azzouz, 1976) for both SPT boring locations, the predicted settlements (7.40 inches and 6.08 inches, for SPT boring location TB-6 and TB-12, respectively) were both significantly higher than the measured settlement for these locations (3.6 inches and 3.8 inches, respectively). The strongest settlement prediction for both SPT boring locations, continues to be using the derived C_c correlations from this study (stronger than derived C_r correlations) and a subsequent rule of thumb applied, such that $C_r = 0.2 * C_c$. This signifies that using C_c correlations derived from this study can have a positive effect on having an accurate computation of predicted settlement, when a correlation for

C_r is used in conjunction with it. This is a critical finding to engineers and designers trying to determine how long and how high to design a surcharge for.

The differences between predicted and measured settlements can be attributed to a number of factors. As stated previously, the settlement plates were not placed at the exact location of the SPT borings. As soil varies spatially and with depth, there is the potential that the soil stratigraphy could be different between where the settlement plate was placed and where the SPT boring was performed. The soil sampling may also not have occurred as frequently as it needed to be. There is a chance that slight variances and small pockets of varying soils could have been missed between sampling intervals.

The following table summarizes the optimal correlations to use in the field:

Table 52: Optimal Correlations for Field Use

Equation	Notes
$C_c = 0.759 + 0.0048 * \gamma_{wet} - 0.012 * \gamma_{dry} - 0.002 * N - 0.0012 * e_o - 0.0006 * [(\gamma_{wet} - 115.484) * (\gamma_{wet} - 115.484)]$	Coarse Grained
$C_c = - 0.296 + 0.001 * PI + 0.485 * e + 0.001 * [(PI - 65.685) * (e - 1.859)]$	Fine Grained

Note that the recommendation is to use the reduced model for coarse grained soils (C_c). For C_r , coarse and fine grained soils, research suggests using the 0.2 factor for C_c to C_r will likely provide better results in settlement analyses than using the developed models in Table 6. For the organic classification, the developed models in Table 6 appear applicable, although they were not field verified as part of this study.

The influence zone of settlement was taken as two times the surcharge height below ground surface. The other rule of thumb for this depth is wherever the stress change from the overlying load moves to 10%. The slight variance between predicted and measured settlements can be attributed to ambiguity of the identification of the influence zone of settlement. In this study, soil profiles were examined that extended beyond the conventional influence zone of settlement. As can be determined from Table 50, the predicted settlements were less than the measured. When the elastic settlement contribution was added and in the influence zone of settlement reduced to 2B below ground surface, settlement predictions were much stronger. This signifies that elastic settlement needs to be included in all settlement predictions.

CHAPTER 6: CONCLUSIONS AND RECOMMENDATIONS

6.1 Conclusions

The following conclusions can be drawn from this study:

1. The predicted settlement from measured compressibility index(s) was largely more accurate, when comparing to measured settlement, than the predictions using predicted index(s).
2. The predicted settlement using the predicted C_c values, and a subsequent rule of thumb for correlating to C_r , were the strongest predictions of settlement made during this study, for both locations.
3. When elastic settlement was considered and the influence zone of settlement moved to $2H$ below ground surface, predictions improved dramatically and were far more favorable to measured settlement.
4. A complete soil profile, with index parameters, is imperative for accurate settlement predictions.
5. Settlement predictions using the strongest existing correlation from Azzouz were significantly higher than the measured settlement for both locations, and compared less favorably than that of predictions using predicted C_r from other methods.
6. There are strong Pearson's Correlation Coefficients present for each soil classification. This signifies that data trends may be present and reliable delineational models for certain soil classifications may be able to be generated.

7. Evidence suggests that reduced models can be created for the Fine Grained and Organic models for C_c .
8. Based on influential parameter analysis, it appears evident that reliable models for C_c can be created for Clays and Silts and it should also be determined if models for C_r can be developed for these classifications.
9. The fines content is included in all of the generated prediction models but none of them have a strong Pearson's Correlation Coefficient.
10. Moisture content, void ratio, and liquid limit have demonstrated to be directly proportional to the influence of compressibility indexes, while the wet and dry densities have proven to be equally as inversely proportional.

The following comprises opportunities for future studies:

1. The SR 415 site had organic soil layers throughout its limits. Unfortunately, the locations identified that had a measured settlement in close proximity to an existing boring, and somewhat complete soil profile, did not contain any organic soil layers. There were several areas in which a settlement plate was placed near an existing SPT boring containing organic layers, but the soil profile with existing consolidation tests was largely absent. In a future study, this soil type will need to be verified in a similar manner as what was performed in this field verification process. This can be accomplished through further study at this site, or a new one altogether.
2. The areas of SR 415 that were examined had a mostly sandy profile. For this reason, when existing correlations were to be used for settlement predictions, it appeared only prudent to examine those correlations that were applicable for all soils, since there were

no existing correlations for coarse grained materials only. As it happened, the strongest existing correlation worked out to be applicable for all soils. In the future, sites with a clayey profile should be examined to determine the applicability of existing correlations for fine grained materials to settlement predictions.

3. The SR 415 site was observed to be heavily over consolidated, such that C_c was not applicable in settlement predictions. For this reason, the C_r prediction models were exclusively used for settlement predictions. As can be observed in Table 6, there is a noticeable drop off in statistical strength of generated models from C_c to C_r for both of these soil types. When settlement predictions were made using predicted C_r , there was a wider margin of error, as compared to measured settlement, than that of predictions using other methods. A site with normally consolidated soils, where C_c would be more applicable for settlement predictions, should be evaluated in the future, so that the stronger compressibility prediction models can be tested.
4. As developed correlations get fine-tuned by adding index parameters, this study should be revisited and settlement predictions updated. The addition of these index parameters to the generated models could have the potential to develop reliable models for C_r for Coarse Grained and Fine Grained models as well as improve upon the existing models for C_c . These improvements could thusly increase the accuracy of settlement predictions.
5. Upon the completion of data analysis and the evidence of strong influential parameters, it has been postulated that delineational models exist. It should be researched to determine if they can be developed with any reliability. If they can, they can be

compared to those presented from previous literature, as outlined in Table 7. It would be an important finding, as there is a dearth of these models from previous studies.

6. The Clay and Silt data sets should also be analyzed to determine if reliable prediction models for C_c and C_r can be created. According to data analysis, these classes have strong influential factors, similar to the data sets in which prediction models have been derived. Previous models for clays have been generated, but nothing substantial for silts.

6.2 Limitations and Recommendations

As previously discussed, this study pertains to primary settlement. This is said to occur immediately. However, primary settlement is difficult to quantify, as the definition of “immediate settlement” is arbitrary. If one observes the measured settlement in Figures 27 and 28, one will notice that the settlement reading “jumps” when additional fill was added did not occur on the same day. Often, there was a short duration in which the settlement change took place. In this time duration, there could have likely been other factors affecting the overall settlement, aside what would be expected from the sudden increase in load. These factors could have likely come from creep settlement, which is the slow expulsion of water from overly saturated cohesive soils over time.

When deciding on how high or how long to stage a surcharge, accurate settlement predictions are of critical importance. This will likely call for several consolidation tests for measured compressibility indexes. Where there is not enough time or money in the budget, settlement predictions will need to be made without consolidation tests. When this happens, it is imperative that a full soil profile be examined. This includes taking index parameters (LL , PI , w ,

-200, etc.) for each soil layer. Without having a complete idea of the characteristics of each soil layer, the accuracy of settlement predictions will come into question, particularly if the correlations derived from this study are to be used.

When an SPT boring is performed and an “undisturbed” sample gathered, there will always be a fair amount of disturbance. This is especially true with silts and desiccated clays, whose soil structure is susceptible to instability when encountered, particularly under a loading. As previously stated, as the level of soil disturbance increases, the remolded strength of a soil sample decreases, and the sensitivity subsequently increases. Sensitivity is a concern for cohesive soils such as silts and clays, where minimal amounts of disturbance can largely effect the strength. The growing uncertainty of this soil classification, for C_c , confirms the ideal that this correlation should be limited to fine grained soils with low sensitivity (Bowles, 1989). This demonstrates one of the limitations of using correlations to quantify the settlement potential of highly compressible soils. The sensitivity could also affect correlations developed for other fine grained classes in the future, such a separating the category into clays and silts.

It is also apparent from this study that performing settlement predictions with measured compressibility indexes is still a reliable method and should be a continued practice (as seen in the statistical strength Table 49). The only exception to this, in this study, is when predictions were made using a correlation for C_c to C_r . These were the strongest predictions made during the study (accounting for elastic settlement and influence zone of settlement $2H$ below ground surface). This signifies that there is a fair amount of variability with these correlations and a standard rule of thumb should be avoided for blanket use. As previously stated, correlations are a useful tool to make preliminary predictions of settlements, but should not be relied upon with

any degree of accuracy for a final design. Only correlations that have been developed using site-specific laboratory consolidation test data should be relied upon (Sabatini, Bachus, Mayne, Schneider, Zettler, 2002). Evidence suggests that the soil structure, geological history, and other factors strongly influence the compression index, and for this reason any correlation used should be with caution (Bowles, 1989).

It is recommended that normally consolidated soils be tested in the future. This would provide an opportunity to examine the prediction potential of the C_c correlations which are considerably stronger than the C_r correlations, statistically speaking. For this reason, it is a reasonable assumption that settlement predictions on normally consolidated soils from predicted C_c would likely more closely match the measured settlements. Observations from this exercise will likely shed more light on the applicability of using compressibility correlations for settlement predictions.

**APPENDIX:
FIELD TESTING PICTURES**



Figure A1: Cone Penetration Test Rig on SR 415



Figure A2: Cone Penetration Test Push Rods



Figure A3: Cone Penetration Test Hydraulic Press for Ground Penetration

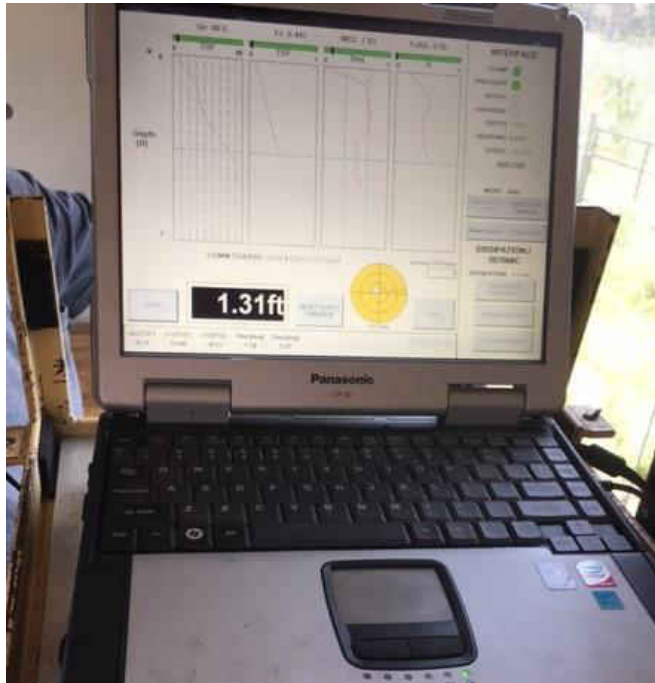


Figure A4: Cone Penetration Test Real Time Ground Resistance



Figure A5: SPT Drill Rig on SR 415



Figure A6: Sample Collection from SPT Test



Figure A7: SPT Test Preparation – Adding Drill Rods

REFERENCES

- Abu-Farsakh, M, and Yu X (2013). “Comparison of Predicted Embankment Settlement from Piezocone Penetration Test with Field Measurement and Laboratory Estimated”. *Geotechnical and Geophysical Site Characterization 4 – Proceedings of the 4th International Conference on Site Characterization 4, ISC-4*, 7(1), (pp. 349-355).
- Acquah, H. D. G. (2010). “Comparison of Akaike information criterion (AIC) and Bayesian Information Criterion (BIC) in Selection of an Asymmetric Price Relationship”. *Journal of Development and Agricultural Economics*, 2(1).
- Ahadiyan, J, Ebne, J.R., and Bajestan, M.S. (2008). “Prediction Determination of Soil Compression Index, Cc, in Ahwaz Region”. *J. Faculty Eng.*, 35(3), (pp. 75-80).
- Alam, M., Panagopoulos, A. A., Rogers, A., Jennings, N. R., & Scott, J. (2014). “Applying Extended Kalman Filters to Adaptive Thermal Modelling in Homes: Poster Abstract”. *Proceedings of the 1st ACM Conference on Embedded Systems for Energy-Efficient Buildings* (pp. 214-215). ACM. Chicago.
- Al Khafaji, A, & Andersland, O (1992). “Equations for Compression Index Approximation”. *Journal of Geotechnical Engineering, ASCE*, 118(1), (pp. 148-155).
- Anderson, JR, Krafft, PA, and Remington, C (1981). *Environmental Geology*. Florida State University Foundation, Inc.
- Arditi, D., & Pulket, T. (2005). “Predicting the Outcome of Construction Litigation Using Boosted Decision Trees”. *Journal of Computing in Civil Engineering*, 19(4), (pp. 387-393).

- Azzouz, AS, Krizek, RJ, and Corotis, RB (1976). "Regression Analysis of Soil Compressibility". *Soils and Foundations*. 16(2).
- Bishop, C. M. (2006). "Pattern Recognition". *Machine Learning*, 128, (pp. 1-58).
- Bowles, JE (1989). *Physical and Geotechnical Properties of Soils*. McGraw-Hill Book Company Inc. New York.
- Casper, J., & Sallam, A. (2013). "SR 46 Detour Surcharge Observations and Proposed Modifications Seminole County, Florida Financial Project No. 240216-5". Terracon Consultants Inc., Winter Park, FL.
- Chang, C. C., and Lin, C. J. (2011). "LIBSVM: A Library for Support Vector Machines". *ACM Transactions on Intelligent Systems and Technology (TIST)*, 2(3).
- Claeskens, G., and Hjort, N. L. (2008). "Model Selection and Model Averaging". Cambridge University Press.
- Cook, P.N. (1956). "Consolidation Characteristics of Organic Soils". *Proc., 9th Canadian Soil Mechanics Conf.*, Vol. 41, NRC, ACSSM, Technical Memorandum, Ottawa Canada, (pp. 82-87).
- Cozzolino, VM (1961). "Statistical Forecasting of Compression Index". *Proceedings of the Fifth International Conference on Soil Mechanics and Foundation Engineering*.
- Das, BM (2002). *Principles of Geotechnical Engineering*. Thomson Learning Inc.
- Dhowian, A.W., Erol A.O., and Sultan S (1987). "Settlement Predictions in Complex Sabkha Soil Profiles". *Bulletin of the International Association of Engineering Geology.*, 36(1), (pp. 11-21).

- Elnaggar, H.A., and Krizek R.J. (1970). "Statistical Approximation for Consolidation Settlement". *Highway Res. Rec.*, 323(1), (pp. 87-96).
- FDOT (2013). "Soils and Foundations Handbook". State Materials Office, Florida Department of Transportation. Gainesville, FL.
- Freud, R. J., & Littell, R. C. (2000). *SAS system for regression*. Sas Institute.
- Guide, M. U. S. (1998). *The Mathworks Inc.* Natick, MA.
- Gunduz, Z, and Arman, H (2007). "Possible Relationships between Compression and Recompression Indices of a Low Plasticity Clayey Soil". *The Arab Journal for Science and Engineering*. 32(2B).
- Gray, K (2016). Interviewed by Scott Kirts February 24, 2016.
- Herrero, AM (1983). "Universal Compression Index Equation". *Journal for Geotechnical Engineering ASCE*. 109(5).
- Hine, AC (2013). *Geologic History of Florida*. University Press of Florida.
- Hough, BK (1957). *Basic Soils Engineering*. The Ronald Press Company New York.
- Kalantary, F, and Kordnaeij, A. (2012). "Prediction of Compression Index Using and Artificial Neural Network". *Scientific Research and Essays*. 7(31).
- Kirts, S, Panagopoulos, O, Xanthopoulos, P, and Nam, B (2017). "Soil-Compressibility Prediction Models Using Machine Learning". *Journal of Computing in Civil Engineering*. 32(1).
- Kohavi, R. (1995). "A Study of Cross-Validation and Bootstrap for Accuracy Estimation and Model Selection". *In Ijcai*, 14(2).

- Koppula, SD (1981). "Statistical Estimation of Compression Index". *Geotechnical Testing Journal*. 4(2).
- Lambe, T.W., & Whitman, R.V. (1969). *Soil Mechanics*. John Wiley & Sons, Inc. New York.
- Lee Rodgers, J., & Nicewander, W. A. (1988). Thirteen ways to look at the correlation coefficient. *The American Statistician*, 42(1), (pp. 59-66).
- Leu, S. S., Chen, C. N., & Chang, S. L. (2001). "Data Mining for Tunnel Support Stability: Neural Network Approach". *Automation in Construction*, 10(4), (pp. 429-441).
- Levinson, N. (1946). "The Wiener (Root Mean Square) Error Criterion in Filter Design and Prediction". *Journal of Mathematics and Physics*, 25(1).
- Liu S, Cai G, Puppala A.J., and Tu Q (2011). "Prediction of Embankment Settlements over Marine Clay using Piezocone Penetration Tests". *Bulletin of Engineering Geology and the Environment*, 70(3), (pp. 401-409).
- Mayne, PW (1980). "Cam-Clay Predictions of Undrained Strength". *Journal of the Geotechnical Engineering Division ASCE*, 106(11).
- McClelland, B (1967). "Progress of Consolidation in Delta Front and Pro-Delta Clays on the Mississippi River." *Marine geotechnique*, Univ. of Illinois Press, Champaign, IL, (pp. 22-40).
- McVay, M, and Nugyen, D (2004). "Evaluation of Embankment Distress at Sander's Creek – SR 20". *Florida Department of Transportation*.
- Melhem, H. G., & Cheng, Y. (2003). "Prediction of Remaining Service Life of Bridge Decks Using Machine Learning". *Journal of Computing in Civil Engineering*, 17(1), (pp. 1-9).

- Miyakawa, I (1960). "Some Aspects of Road Construction in Peaty of Marshy Areas in Hokkaido". Hokkaido Development Bureau, Civil Engineering Research Institute, Sapporo, Japan (text in Japanese).
- NAVFAC (1982). "Design Manual: Soil Mechanics, Foundations, and Earth Structures". NAVFAC DM-7, Department of the Navy, Washington, D.C.
- Nagaraj, T, & Murthy, B (1985). "Prediction of the Preconsolidation Pressure and Recompression Index of Soils". *Geotechnical Testing Journal, ASTM*, 8(4), (pp. 199-202).
- Nagaraj, T, & Murthy, B (1986). "A Critical Reappraisal of Compression Index". *Geotechnique*, 36(1), (pp. 27-32).
- Nagelkerke, N. J. (1991). "A Note on a General Definition of the Coefficient of Determination". *Biometrika*, 78(3).
- Nishida, Y (1956). "A Brief Note on Compression Index of Soils". *Journal of the Soil Mechanics and Foundations Division ASCE*, 82(3).
- Ozer, M, Isik, NS, and Orhan, M (2008). "Statistical and Neural Network Assessment of the Compression Index of Clay-Bearing Soils". *Bull Engineering Geological Environment*. 67(4).
- Park, H.I., and Lee, S.R. (2011). "Evaluation of the Compression Index of Soils Using an Artificial Neural Network". *Computers and Geotechnics*, 38(4).
- Panagopoulos, A. A., Alam, M., Rogers, A., & Jennings, N. R. (2015a). "AdaHeat: A general Adaptive Intelligent Agent for Domestic Heating Control". *Proceedings of the 2015*

- International Conference on Autonomous Agents and Multiagent Systems* (pp. 1295-1303). International Foundation for Autonomous Agents and Multiagent Systems.
- Panagopoulos, A. A., Chalkiadakis, G., & Jennings, R. N. (2015b). "Towards Optimal Solar Tracking: A Dynamic Programming Approach". *Proceeding of the 29th AAAI Conference on Artificial Intelligence (AAAI-2015)*.
- Panagopoulos, A. A., Chalkiadakis, G., & Koutroulis, E. (2012). "Predicting the Power Output of Distributed Renewable Energy Resources within a Broad Geographical Region". *Proceedings of the 20th European Conference on Artificial Intelligence* (pp. 981-986). IOS Press.
- Panagopoulos, A. A., Jennings, A., Maleki, S., Rogers, A., & Venanzi, M. (2017). "Advanced Economic Control of Electricity-Based Space Heating Systems in Domestic Coalitions with Shared Intermittent Energy Resources". *Transactions on Intelligent Systems and Technology*.
- Panagopoulos, O. P., Pappu, V., Xanthopoulos, P., & Pardalos, P. M. (2016). "Constrained Subspace Classifier for High Dimensional Datasets". *Omega*, 59, (pp. 40-46).
- Pappu, V., Panagopoulos, O. P., Xanthopoulos, P., & Pardalos, P. M. (2015). "Sparse Proximal Support Vector Machines for Feature Selection in High Dimensional Datasets". *Expert Systems with Applications*. 42(23), 9183-9191.
- Peck, R.B., and Reed, W.C. (1954). "Engineering Properties of Chicago Subsoils". Engineering Experiment Station, Univ. of Illinois, Urbana, IL.
- Reich, Y. (1997). "Machine Learning Techniques for Civil Engineering Problems". *Microcomputers in Civil Engineering*, 12(4), (pp. 295-310).

- Sabatini PJ, Bachus RC, Mayne PW, Schneider JA, Zettler TE (2002). *Evaluation of Soil and Rock Properties*. Federal Highway Administration.
- Salem, M, and El-Sherbiny, R (2013). “Comparison of Measured and Calculated Consolidation Settlements of Thick under consolidated Clay”. *Alexandria Engineering Journal*, 53(1), (pp. 107-117).
- SAS Institute (2000). *JMP: Statistics and Graphics Guide*. SAS Inst.
- Sewell, J., & Abboud, M. (2012). “Final Plans Update Geotechnical Report for Roadways SR 415 Widening from the Seminole County Line to Reed Ellis Rd. Volusia County, Florida Financial Project ID 407355-3 Section 79120 PSI Project No. 0757570 (757-55293)”. PSI, Orlando.
- Sou-Sen, L., & Hsien-Chuang, L. (2004). “Neural-Network-Based Regression Model of Ground Surface Settlement Induced by Deep Excavation”. *Automation in Construction*, 13(3), (pp. 279-289).
- Sowers, GB (1970). *Introductory Soil Mechanics and Foundations*. 3rd Ed. London. The Macmillan Company of Collier-Macmillan Ltd.
- Teng, WC (1962). *Foundation Design*. Prentice-Hall, Inc. New Jersey.
- Terzaghi, K, and Peck, RB (1967). *Soil Mechanics in Engineering Practice*. 2nd edition. New York. Wiley.
- Theil, H. (1959). “Economic Forecasts and Policy”. *The American Economic Review*, (49)4.
- Vapnik, V. (2000). “The Nature of Statistical Learning Theory”. *Springer Science & Business Media*. New York, USA.

- Veropoulos, K., Campbell, C., & Cristianini, N. (1999). "Controlling the Sensitivity of Support Vector Machines". *Proceedings of the International Joint Conference on AI*, (pp. 55-60).
- Xanthopoulos, P., & Razzaghi, T. (2014). "A Weighted Support Vector Machine Method for Control Chart Pattern Recognition". *Computers & Industrial Engineering*, 70. (pp. 134-149).
- Yoon, GL, and Kim, BT (2006). "Regression Analysis of Compression Index for Kwangyang Marine Clay". *KSCE Journal of Civil Engineering*, 10(6).